The Physiology and Pathophysiology of a Fetal Splice Variant of the Cardiac Sodium Channel

by

Lisa Lynn Murphy

Dissertation submitted to the faculty of the Graduate School of Vanderbilt University

in partial fulfillment of the requirements for the degree of

DOCTOR OF PHILOSOPHY

in

Pharmacology

May, 2014

Nashville, Tennessee

Approved:

Alfred L. George, Jr. MD (mentor)

Ronald B. Emeson, PhD (chair)

Katherine T. Murray, MD

Dan M. Roden, MD

Jennifer A. Kearney, PhD

DEDICATION

To my amazing parents, Jim and Linda Murphy,

for always believing in me and inspiring me to be my best

&

To my wonderful future husband, Tom Scudder,

for all of his never-ending support and encouragement

ACKNOWLEDGEMENTS

This work would not have been possible without the financial support of the Vanderbilt Interdisciplinary Graduate Program (IGP), the Vanderbilt Ion Channels and Transporters Training Grant, and the American Heart Association's pre-doctoral fellowship. I am grateful to all those involved with the IGP that helped me in my earliest years of graduate school especially Dr. Roger Chalkley for providing excellent advice during those years. I would also like to thank the Department of Pharmacology, especially Dr. Heidi Hamm, Dr. Seva Gurevich, Dr. Joey Barnett, and Karen Geig for all of their hard work and dedication to the training program.

I would like to express my gratitude and appreciation to Dr. Alfred L. George and the members of my committee. Al has provided me with wonderful advice and suggestions throughout my time in his lab. His continuous support and guidance has prepared me for an enjoyable and promising career in cardiovascular research. I wish him all the best in his new appointment as the chair of Pharmacology at Northwestern University.

My career development would not have been possible without the help of my committee members- Dr. Ron Emeson (chair), Dr. Kathy Murray, Dr. Dan Roden, and Dr. Jennifer Kearney. Thank you for all of your expertise, encouragement, and support throughout my pre-doctoral years. I have been honored to have such an incredible group of scientists to guide me through this process. I send special thanks to Ron for being the chair of my committee and providing me with his expert advice. I would also like to thank Kathy for all of the letters of support that she has written for me over the years, for her continuing encouragement, thoughtful questions, and great advice. I would like to acknowledge Dan and Jennifer for their

thoughtful questions and suggestions during our meetings. I have been very fortunate to have all of you on my committee.

I am grateful for all those that I have had the pleasure of working with over the years in the George laboratory. Everyone was a joy to work with and a wonderful part of my life. The pleasure of great company has been the real reason why I came to work every day with a smile on my face. I would like to acknowledge Jennifer Kunic for helping me with aspects of this project such as the site-directed mutagenesis, cloning, and RT-PCR. This work would not have been possible without her molecular biology expertise. I would also like to thank Dr. Christopher Thompson for teaching me how to troubleshoot and fix everything that I managed to break or thought that I had broken. I would also like to acknowledge Chris for his helpful suggestions in the lab and at meetings. Furthermore, I would like to acknowledge Dr. Carlos Vanoye and Dr. Franck Potet for providing me with their wealth of knowledge on ion channels, electrophysiology, and data analysis. In addition, I would like to thank Rick Welch for all of his assistance with the rabbit cardiomyocyte isolations and helping me learn digest techniques for iPS-cardiomyocytes and cell culture.

I would also like to acknowledge my wonderful group of scientist friends and colleagues that I have made here at Vanderbilt through the IGP. We have had many fun and exciting times together and I am forever indebted to you all for your true friendship and support. I wish you all the best in your future careers. I can only hope that we are able to cross paths again soon.

Long before my time at Vanderbilt there were many people in my life that have encouraged me to pursue my passion for science. I would like to thank my entire family for their love and support. At a very young age, my parents and grandparents recognized my

enthusiasm for exploring the world around me. They were the reason I became interested in science and they taught me many valuable lessons about hard work, dedication, perseverance, and maintaining a positive attitude even in the face of adversity.

I will never forget my mom taking me to Rensselaer Polytech Institute to listen to a presentation by an astronaut about space travel and satellites. I was the only 10 year old girl at the conference but I remember taking notes and loving every second of that experience. I still have them today in a science journal that I kept when I was young. To some people this might seem like one insignificant event, but to a young girl interested in science that was one of many examples of my parents' support and encouragement. I am fortunate to have had parents that gave me opportunities to learn more than what was available at school.

Many years later, while I was attending college at Albany College of Pharmacy (ACP), my father was always keeping me informed of opportunities to expand my knowledge. One day he found an article in our local newspaper about the Masonic Medical Research Laboratory's (MMRL) summer fellowship program in Utica, New York. I applied for the program the following year and was accepted. It was a wonderful experience and a great summer job working alongside many well-known cardiac electrophysiologists and researchers such as Dr. Charles Antzelevitch. The summer fellowship gave me the opportunity to learn about cardiac electrophysiology and how to deliver a scientific presentation. I am so glad that my dad introduced me to scientific research and I am grateful for the people I have met along the way. I was very fortunate to have had numerous mentors and professors at the MMRL and ACP that prepared me so well for graduate school a Vanderbilt.

In the summer of 2005, a very important person came into my life- my best friend and partner, Tom Scudder. I have never known a more loving, loyal, kind, and fun person. Tom has provided me with many years of continuous support no matter what the cost. We were over 1000 miles apart for 3 years so that I could pursue my PhD at Vanderbilt University. There are very few relationships that I know of that could survive that distance. Instead of trying to hold me back, Tom has encouraged me to do what I needed to do for my career and he still continues to support my endeavors. During that time apart, Tom never seemed that far away because of our constant phone calls, frequent visits, and emails to cheer me on. I attribute all of my sanity during qualifying exams and writing this dissertation to Tom and our really cute dog, Oscar. They are the best guys to come home to after a long day in the lab. Thank you, Tom, for all of your never-ending love and support.

TABLE OF CONTENTS

PAGE

LIST OF FIGURES

FIGURE **PAGE**

LIST OF TABLES

TABLE **PAGE**

CHAPTER I

INTRODUCTION

The Perinatal Heart and the Cardiac Action Potential

The cardiac action potential is an essential physiological event that enables rapid changes in heart rate and is also a response to changes in autonomic tone. Propagation of an action potential by a single cardiac cell occurs through activation of multiple ionic currents mainly, sodium channels, potassium channels, and calcium channels in a specific sequence (Figure 1). The shape and duration of the action potential of the working myocardium is determined by multiple phases that correlate with specific ionic currents.[1] Phase 4 is the resting membrane potential of the cardiac cell that is stabilized by inward rectifying potassium channels. The inwardly rectifying potassium channel (Kir2.x) subfamily members primarily mediate cardiac I_{K1}, but other inward rectifiers may also be involved in cardiac excitability.[2,3] The resting membrane potential is typically -90 mV for healthy adult ventricular myocytes. The initial phase of the action potential, phase 0, is the rapid depolarization phase driven by an influx of sodium ions through voltage-gated sodium channels, primarily $Na_V1.5$. Phase 1 is a phase of rapid repolarization when sodium channels are inactivated and there is activation of transient outward potassium currents (I_{to}). Phase 2 is the plateau phase that is due to the influx of calcium ions by L-type calcium channels ($Ca_V1.2$) balanced with outward potassium currents.[1,4] The third phase of the action potential, phase 3, is the rapid repolarization that restores the membrane voltage back to resting potential.

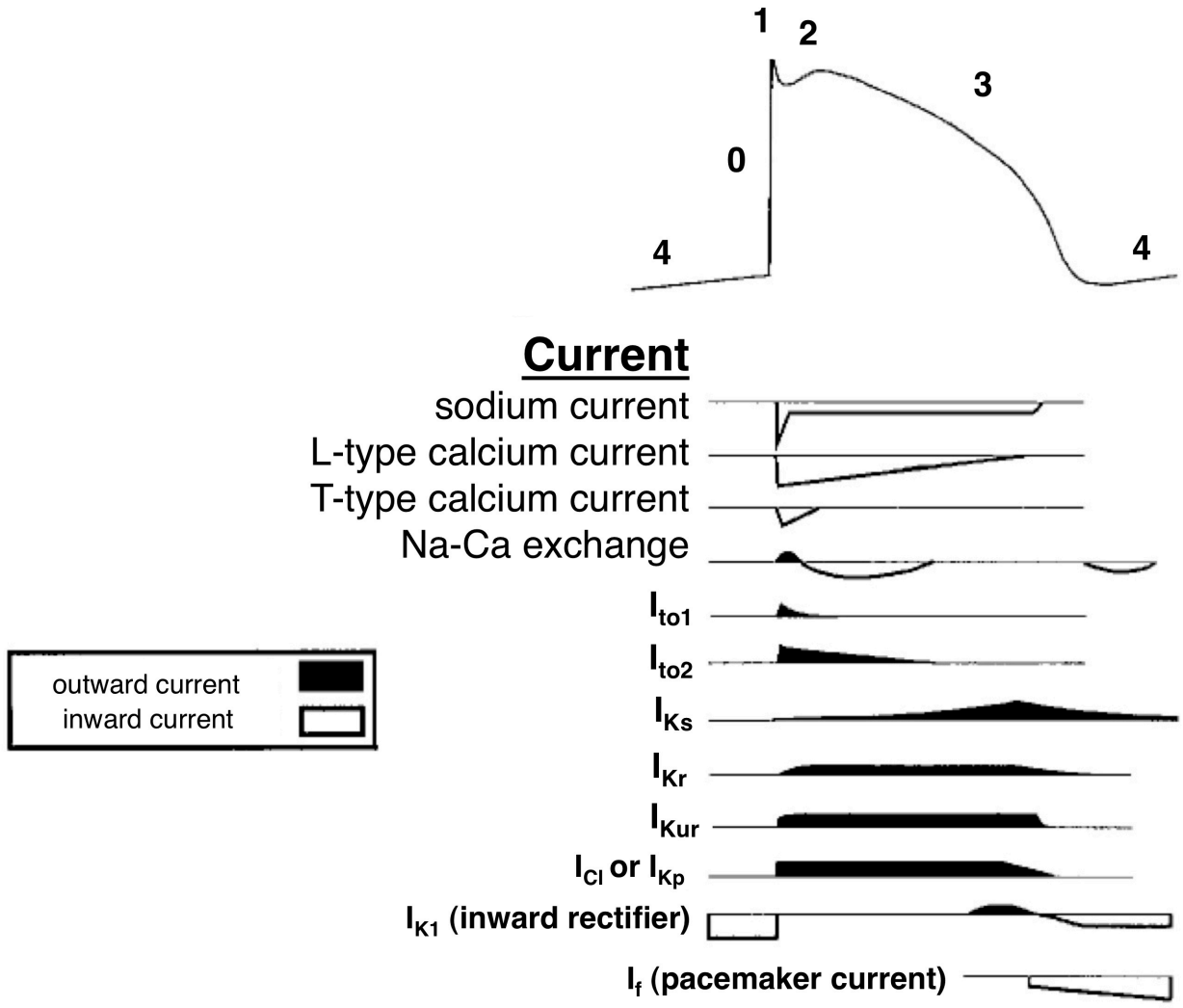

Figure 1: The cardiac action potential.

The phases of the action potential are labeled above as described in the text. The balance of inward and outward ionic currents is shown below the action potential. Currents are not drawn to scale. Figure adapted from Roden and George, *Annu. Rev. Med.* (1996).[1]

This phase is largely driven by voltage-gated potassium channels, $K_V11.1$, also known as KCNH2 or hERG (I_{Kr}), and $K_V7.1$, also known as KCNQ1 or KvLQT1 (I_{Ks}).[4]

Nodal “pacemaker” cells of the heart have a different action potential and resting membrane potential (-50 to -60 mV) compared to cardiac muscle cells. This is due to the rate of depolarization in phase 0 being much slower than that of working myocardial cells, resulting in slower propagation of the cardiac impulse in the nodal regions.[4,5] The cardiac action potential configuration of the atria, ventricles, and nodal cells are heterogeneous, which is reflected by the different types of action potentials and ionic currents measured in isolated cardiomyocytes by electrophysiological recordings.[1,5,6]

The depolarization and repolarization phases of the action potential are reflected in the electrocardiogram (ECG). The ECG measures the electrical activity of the heart over a period of time. The average atrial depolarization (P wave) and ventricular repolarization (QT interval) duration is determined by the ECG. Abnormalities in heart rhythm are detected by the ECG and can result in reduced pumping efficiency of the heart muscle. The ECG cannot measure the pumping efficiency of the heart. Therefore it is measured by echocardiography (see Chapter II).[4]

Throughout the course of perinatal heart development, ion channel expression patterns are constantly changing which in turn alters the cardiac action potentials responsible for the rapid activation and repolarization of cardiac cells.[7–10] It is important to understand some of the distinguishing features between the adult and fetal heart in order to determine the molecular mechanisms of perinatal cardiac arrhythmias. The fetal heart rate is significantly higher (120–160 beats/min) than the adult heart rate (60–100 beats/min). In addition, the fetal myocardium

is also less compliant than the infant or adult heart and the cell capacitance (size) is reduced in the much smaller fetal heart.[11]

In development, the cardiac action potential duration (APD) has been shown to vary among fetal, neonatal, and adult cardiomyocytes in several experimental animal models.[7–9,12] The timing of the APD is crucial because as long as the ventricular tissue is depolarized it cannot be re-excited due to the unavailability of the voltage-gated sodium channels as discussed further below. This mechanism is cardioprotective against premature excitation and is an essential process required to maintain the proper timing between diastolic filling and ejection intervals by the heart.[13] In the guinea pig, APDs at 50% and 90% repolarization have been shown to decrease between fetal and neonatal periods and later increase between the neonatal and adult periods. Additionally, there was no substantial age-related change in resting membrane potential or action potential overshoot reported.[9] In fetal and neonatal rat heart, the duration of the ventricular and atrial action potentials was also inversely related to heart rate, and their rate sensitivity decreased with age.[14] The changes observed for the APD between fetal and infant heart is due to developmental changes in the expression of ion channels.

In many animal model systems, changes in ion channel expression have been observed throughout development but there is very little evidence of those specific changes in human fetal and infant hearts.[12] A study of murine embryonic development and ion channel function showed that sodium channel current density increases during murine embryogenesis and L-type calcium activation plays a dominant role in depolarization at the earliest stages.[15] In a large-scale analysis of ion channel gene expression in the mouse heart during perinatal development, investigators confirmed that mRNA expression of $Na_V1.5$ was reduced in the

immature (fetal and neonatal) hearts compared to adult hearts. This study also found significant up-regulation of chloride channels in fetal and neonatal hearts compared to adult, especially chloride channels activated by intracellular calcium.[16]

A more recent study comparing neonatal and adult canine ventricular myocytes has shown that two major repolarizing potassium currents (I_{Ks} and I_{to}) are present in adult ventricular cells but these currents are absent in the 2-week-old neonate, which may contribute to the shortening of the APD after birth. They also showed that peak and late sodium currents are significantly smaller in the neonatal heart compared to adult.[12] Therefore, the immature heart exhibits some major differences in ionic currents compared to the adult heart. These observations may have important implications when elucidating a molecular mechanism for perinatal cardiac arrhythmias. Further investigation of the developmental regulation of ion channels is required for a better understanding of disease pathogenesis in the earliest stages of life.

Molecular Mechanisms of the Long-QT Syndrome

The long-QT syndrome (LQTS) occurs infrequently in the general population with a prevalence of approximately 1 in 2500 people.[13,17] Patients with LQTS exhibit two diagnostic features that include prolongation of the heart rate–corrected QT interval (QTc ≥ 450 ms) and, in some cases, stress-induced syncope.[13] In addition, severe life-threatening cardiac arrhythmias may occur such as ventricular fibrillation. Ventricular fibrillation can sometimes lead to a morphologically distinctive polymorphic tachycardia known as 'torsades de pointes.'[18] The genetic basis of LQTS was identified in the mid-nineties and all the LQTS genes identified

so far encode cardiac ion channel subunits or proteins involved in modulating the previously described ionic currents (Figure 1). Mutations in ion channel genes cause the disease by prolonging the APD and subsequently ventricular repolarization.[17]

There are multiple subtypes of congenital LQTS based on the disease-associated genes. Type-1 LQTS (LQT1), is the most prevalent subtype with over 50% of cases caused by mutations in the gene *KCNQ1* encoding the $K_V7.1$ potassium channel.[17] This channel is responsible for the slow component of the delayed rectifier repolarizing current (I_{Ks}) involved in phase 3 of the cardiac action potential.[19,20] Therefore, a loss of function of $K_V7.1$ results in a reduction in I_{Ks} and delays ventricular repolarization. Type-2 LQTS (LQT2) is prevalent in about 30% of genotyped patients and occurs as a result of mutations in *KCNH2.* The gene *KCNH2* encodes the major repolarizing voltage-gated potassium channel, $K_V11.1$, also known as human ether–a-go-go related gene (hERG). Loss of function mutations in hERG result in prolongation of APD and the QT interval.[21] LQT1 patients typically exhibit a progressive QTc prolongation at higher heart rates or during exercise. By contrast, LQT2 patients typically demonstrate maximum QTc prolongation at submaximal heart rates with subsequent QTc correction toward baseline values at higher heart rates.[22,23] Cardiac events in patients with LQT2 are predominately associated with sudden arousal.[24]

Mutations in the gene *KCNE1* encoding KCNE1 protein has been associated with type-5 LQTS (LQT5). KCNE1 is a potassium channel subunit that assembles with $K_V7.1$ (*KCNQ1*) to produce the slow delayed rectifier I_{Ks} and may also assemble with hERG to modulate the rapid delayed rectifier I_{Kr}.[25] In addition, mutations in the gene *KCNE2* that encodes another auxiliary subunit of voltage-gated potassium channels is associated with type-6 LQTS (LQT6). Some mutations in *KCNE1* or *KCNE2* modulate voltage-gated potassium channel function that

reduces potassium currents (I_{Ks} or I_{Kr}) and results in a prolongation of ventricular repolarization.[26,27]

The combination of β-adrenergic receptor antagonists such as propranolol and an implanted cardioverter defibrillator (ICD) is a safe and reliable form of therapy for managing high-risk LQTS.[28] The β_1-adrenergic receptors (β-ARs) are G-protein coupled receptors expressed in cardiac tissue that upon activation are responsible for an increase in heart rate and cardiac contractility by a calcium dependent mechanism.[29] In the case of LQT1 syndrome patients, β-blocker administration is thought to reduce incidence of cellular imbalance in response to stimulation of β-ARs, which occurs when one target of β-AR stimulation, the KCNQ1 channel, is eliminated from the cellular response.[13] However, this treatment is also effective for other subtypes of LQTS to control heart rate.

Mutations in an integral membrane protein, ankyrin-2, have been associated with type-4 LQTS (LQT4) likely because of the protein's association with ion channels.[17] A loss of function of ankyrin-2 results in disruption of the cellular organization of the sodium/potassium (Na^+/K^+) ATPase,[30] the sodium/calcium (Na^+/Ca^{2+}) exchanger, and inositol-1,4,5-trisphosphate receptors. All of which are ankyrin-2-binding proteins. Ankyrin-2 loss of function reduces targeting of these proteins to the transverse tubules and reduces the overall protein level in cardiomyocytes. Ankyrin-2 mutations may also lead to altered calcium signaling in adult cardiomyocytes which provides insight to the molecular mechanism of LQT4.[31]

Calcium signaling is essential for many of the cellular processes within cardiomyocytes and many other cell types. Mutations in the gene *CACNA1C* encoding the L-type calcium channel, $Ca_V1.2$, are associated with type-8 LQTS (LQT8 or Timothy syndrome).[17] Timothy

syndrome is a rare autosomal dominant disorder characterized by physical malformations, QT-prolongation and arrhythmias, as well as neurological and developmental defects. This syndrome is a result of a gain of function of L-type calcium channels that disrupts cellular calcium homeostasis.[32] The most common biophysical defect associated with LQT8 is loss of calcium-dependent inactivation (CDI) of the L-type calcium channels (see Chapter IV).[33,34]

An autosomal dominant disorder, Anderson-Tawil syndrome or LQT7, is associated with mutations in *KCNJ2* that encodes an inwardly rectifying potassium channel, Kir2.1.[13,17] Anderson-Tawil syndrome is characterized by QT prolongation as well as periodic paralysis and skeletal developmental abnormalities. Kir2.1 is responsible for maintenance of the resting membrane potential of cardiac and skeletal muscle cells. The mutations that were discovered in association with this disease have been shown to exhibit a loss of Kir2.1 function which may contribute to arrhythmogenesis.[35]

Another subtype of LQTS, LQT9, is associated with mutations in caveolin-3 encoded by the gene *CAV3*.[17] Caveolin-3 is the major scaffolding protein of cardiac caveolae and has been associated with skeletal muscle disease, cardiomyopathy, and LQT9. It is proposed that caveolin-3 co-immunoprecipitates with hERG channels.[36] However, caveolin may participate in the scaffolding and trafficking of other ion channels important for cardiac repolarization. Reduced trafficking of ion channel proteins such as hERG results in loss of function of the potassium channels and prolongs ventricular repolarization.

In recent years, mutations in the gene *SCN4B* that encodes the β4 subunit responsible for modulating cardiac sodium channel gating have been discovered. These mutations are associated with LQT10. Four different beta-subunits have been described and all are

detectable in cardiac tissue. A mutation in the β4 subunit may lead to a gain of function of $Na_V1.5$ that delays ventricular repolarization.[37] Type-3 long QT syndrome (LQT3), which will be discussed further in the next section, is associated with mutations in *SCN5A* encoding the voltage-gated cardiac sodium channel ($Na_V1.5$) and is prevalent among 10-15% of LQTS cases genotyped. Patients with LQT3 typically experience syncopal episodes during sleep or with slower heart rates. [24]

In summary, there are multiple subtypes of LQTS that correspond to the genotype-specific cause of the disease. Additionally, the molecular triggers for cardiac events in these patients also differ. There are many molecular mechanisms that may result in delayed ventricular repolarization, prolongation of the QT interval, and episodes of ventricular tachycardia. Investigations into the clinical aspects and molecular mechanisms of LQTS have provided novel and important insight into the electrical activity of the human heart and how small disturbances in ion flow can have significant consequences for human disease.[13]

Voltage-Gated Cardiac Sodium Channel Dysfunction and the Pathogenesis of LQT3

A variety of inherited human disorders affecting skeletal muscle contraction, heart rhythm, and nervous system function are caused by mutations in genes encoding voltage-gated sodium channels. The gene *SCN5A*, located on the short arm of chromosome 3 at position 21, encodes the alpha (α) subunit of the voltage-gated cardiac sodium channel, $Na_V1.5$ (Figure 2).[38] The sodium current conducted by $Na_V1.5$ is critical for the maintenance of impulse conduction in the heart and is responsible for the depolarizing phase of the cardiac action potential in the working myocardium (Figures 1 & 4).[39]

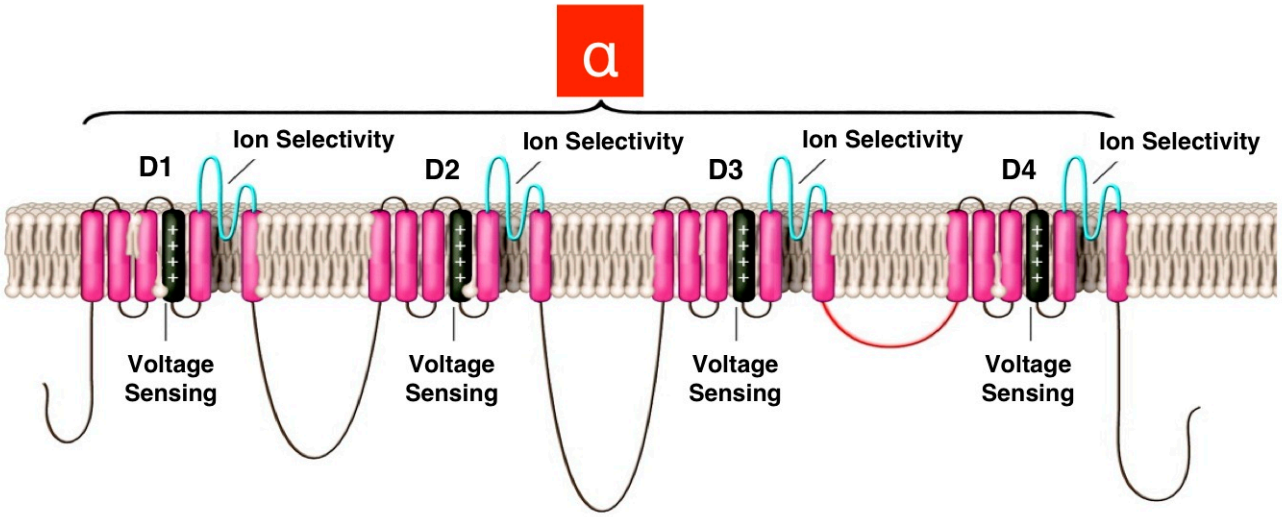

Figure 2: Topology diagram of the alpha subunit of the voltage-gated cardiac sodium channel.

$Na_V1.5$ consists of 4 domains with 6 trans-membrane regions. The S4 transmembrane region of each domain is a positively charged voltage sensor. The S5 and S6 transmembrane regions of each domain form an ion selective pore. The D3/D4 linker (shown in red) is required for the rapid inactivation of the sodium channel. Figure adapted from George, A. JCI (2005).[38]

The cardiac voltage-gated sodium channel consists of four domains with six transmembrane-spanning regions.[40] The S5 and S6 transmembrane regions form the ion selectivity pore while the S4 transmembrane region functions as the voltage sensor.[41] Voltage-gated sodium channel activation is elicited upon depolarization of membrane potential that leads to opening of the channel. Normally, activation of $Na_V1.5$ is transient, owing to fast inactivation that is mediated by structures located on the cytoplasmic face of the channel protein, mainly the D3/D4 linker. The channels cannot open again until the membrane is repolarized and they undergo voltage-dependent recovery from inactivation.[38] During the recovery from inactivation period, channels must deactivate or transition from the inactivated to the closed state.[42]

The three states of the ion channel (activation, inactivation, and closed) occur within a few milliseconds and are essential for the normal function and rapid gating of $Na_V1.5$ (Figure 3).[38] The cardiac sodium channel is a multi-protein complex in which auxiliary proteins interact with the α-subunit to regulate its gating, cellular localization, intracellular transport, and degradation. These proteins include beta (β) subunits (1-4), calmodulin, protein kinases, phosphatases, and many others. These proteins also play important roles in the normal function and gating of the sodium channel (also see Chapter IV).[43]

Mutations in *SCN5A* are associated with sodium channel dysfunction that can result in life-threatening cardiac arrhythmias such as in LQTS.[38] The major biophysical defect of $Na_V1.5$ that contributes to type-3 LQTS (LQT3) is persistent sodium current (I_{Na}) that is usually due to impaired inactivation of the channels (Figure 4).[38] Persistent sodium currents lead to delayed ventricular repolarization and torsades de pointes.[44]

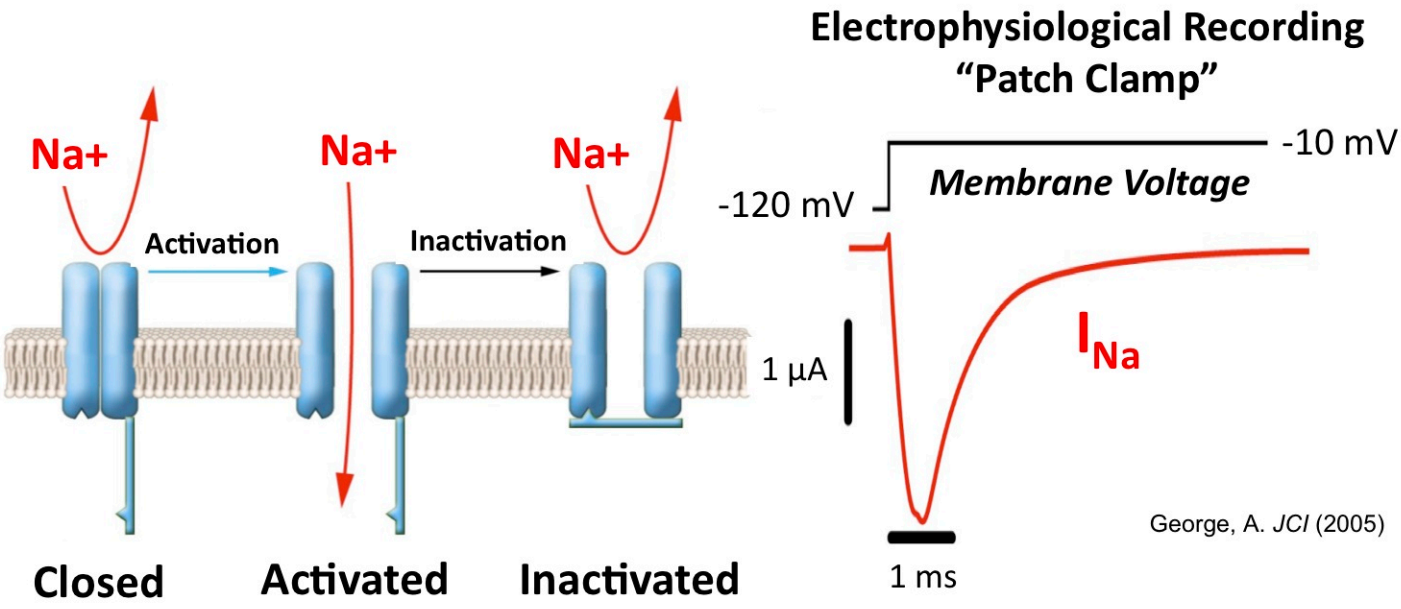

Figure 3: The three functional states of the voltage-gated cardiac sodium channel.

Depolarization of the cellular membrane results in activation of voltage-gated sodium channels. This allows the influx of sodium current followed by a rapid inactivation of the channels. Sodium channels will remain in the closed state when the cell membrane is hyperpolarized. Figure adapted from George, A. JCI (2005).[38]

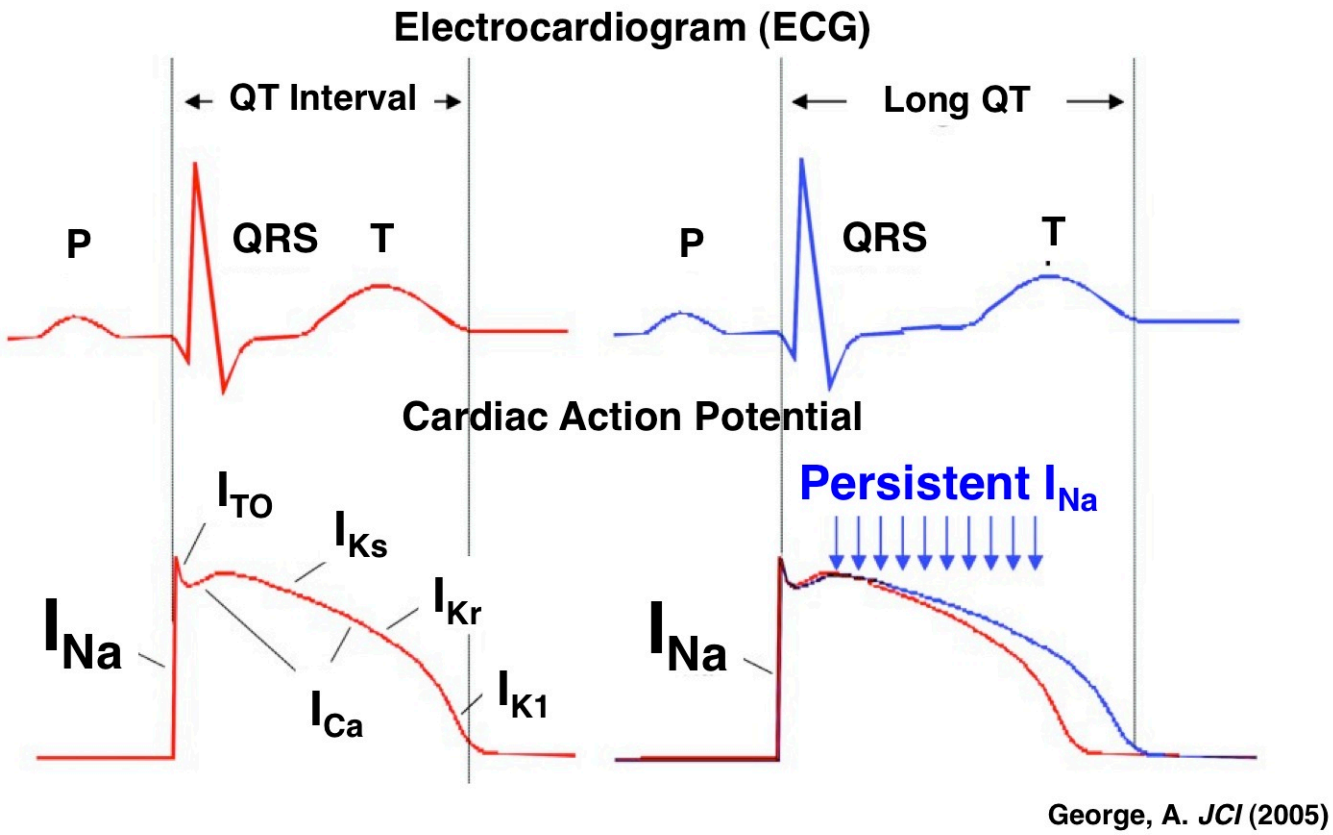

Figure 4: Persistent sodium current in the pathogenesis of LQTS.

Persistent sodium current (I_{Na}) is the most common functional defect of the cardiac sodium channel associated with type-3 LQTS. Persistent sodium current prolongs ventricular repolarization and results in prolongation of the QT interval on the ECG. Figure adapted from George, A JCI (2005).[38]

Severe arrhythmias, such as LQTS, typically present in early childhood or during adulthood, but in extreme cases may present during the perinatal period.[45–47] A number of *SCN5A* mutations, many of which are *de novo* (not inherited), present with earlier onset and more severe congenital arrhythmia syndromes than is typical for LQTS.[48–51] The reason for greater severity and lethality of certain genetic variants during early life is not well understood.

The major consequences of LQTS in fetal life include severe hydrops fetalis (edema) and intrauterine fetal demise.[11,52–54] Clinical signs suggestive of fetal LQTS include ventricular tachycardia, second-degree atrioventricular (AV) block and, most commonly, sinus bradycardia.[53] The term '2:1 AV block' is defined by two P waves preceding 1 QRS wave on the ECG.[60] This is due to the intermittent failure of AV conduction caused by sodium channel dysfunction.[61] Unfortunately, such findings may go undetected due to the lack of routine electrocardiographic testing of fetuses.[46]

In developed countries, sudden infant death syndrome (SIDS) is the leading cause of death in the first year of life. SIDS is a diagnosis of exclusion when rigorous efforts to identify the cause of death are not revealing.[46] The pathophysiological mechanisms of SIDS are poorly understood and current theories comprise a multitude of genetic and environmental factors that may contribute to its cause.[55]

An Italian study in which ECG-screening was performed on apparently healthy newborn infants revealed a prevalence of QTc prolongation (> 450 ms) of 1 in every 2534 live births.[56] Ion channel mutations have been discovered in approximately 10% of SIDS victims, implicating cardiac arrhythmias as a contributing factor to this tragic condition.[57] Furthermore, approximately 5% of these cases are associated with mutations in *SCN5A*.[58] Therefore, it is of

great importance to identify the preventable causes of sudden death in neonates for the effective diagnosis and preventative treatment.

Genetic Studies of *SCN5A* Mutations and LQTS

Genetic studies have revealed numerous *SCN5A* mutations that cause voltage-gated sodium channel dysfunction associated with LQTS. In addition, cardiac arrhythmias are implicated as a contributing factor to cases of intrauterine fetal demise and SIDS.[58] Previous studies of SIDS victims identified *SCN5A* rare variants F2004L and P2006A that are both located on the C-terminal tail of $Na_V1.5$.[56,59] These rare variants exhibited increased persistent sodium current resembling the biophysical defect observed for LQT3.[58] Although *SCN5A* mutations associated with SIDS have been well characterized in the canonical form of $Na_V1.5$,[56,59] there still remains little evidence of the molecular mechanisms and molecular context that predispose to severe forms of LQTS and sudden death in the earliest stages of life.

Here we present the clinical background and the known molecular mechanisms of several *SCN5A* mutations investigated in our laboratory. In addition to the previous *de novo* *SCN5A* rare variants described, a mutation of alanine-1330 to glutamic acid (A1330D) was discovered in an Italian boy with early-onset LQTS. The proband, a Caucasian male, was delivered by Caesarean section at 33 weeks' gestation because of oligohydramnios. On the second day of life, he exhibited bradycardia followed by an episode of ventricular fibrillation and he was successfully resuscitated (chest thump, defibrillation). The electrocardiogram revealed a prolonged QTc (500 msec) and 2:1 AV block. Echocardiography demonstrated

normal cardiac anatomy and function. Despite treatment with lidocaine, $MgSO_4$, propranolol, and mexiletine, the subject continued to have frequent episodes of ventricular tachycardia, including torsades de pointes, and ventricular fibrillation prompting repeated external defibrillations. He died at age 70 days following a final episode of cardiac arrest.

The *SCN5A*-A1330D mutation affects the same residue as another de novo mutation (A1330P) associated with sudden cardiac death at age 9 weeks.[45] These two mutations are located within D3 between S4 and S5 of $Na_V1.5$ (Figure 5). Biophysical studies on A1330D and A1330P have shown that they both evoke a greater persistent sodium current compared with wild-type channels.[45,62]

The most severe cases of LQTS in early life that are associated with sodium channel dysfunction are typically *de novo* mutations; another example is F1473C. This phenylalanine-1473 to cysteine mutation was discovered in a newborn infant with extreme QT prolongation of 800ms, 2:1 AV block, and differential responses to treatment such as lidocaine. This mutation occurs within the inactivation gate or the D3/D4 linker of $Na_V1.5$ (Figure 5). The D3/D4 linker is a highly conserved region of $Na_V1.5$ and is essential for fast inactivation of the channel.[63] Biophysical studies of F1473C revealed multiple changes to sodium channel gating that could contribute to delayed ventricular repolarization such as persistent sodium current and a shift in the voltage-dependence of inactivation.[48]

Another novel *de novo* missense *SCN5A* mutation, R1623Q, was discovered in a Japanese infant girl with episodes of sporadic LQTS. This arginine-1623 to glutamine mutation is located in the S4 of D4 within $Na_V1.5$ (Figure 5). In contrast to many other *SCN5A* mutations

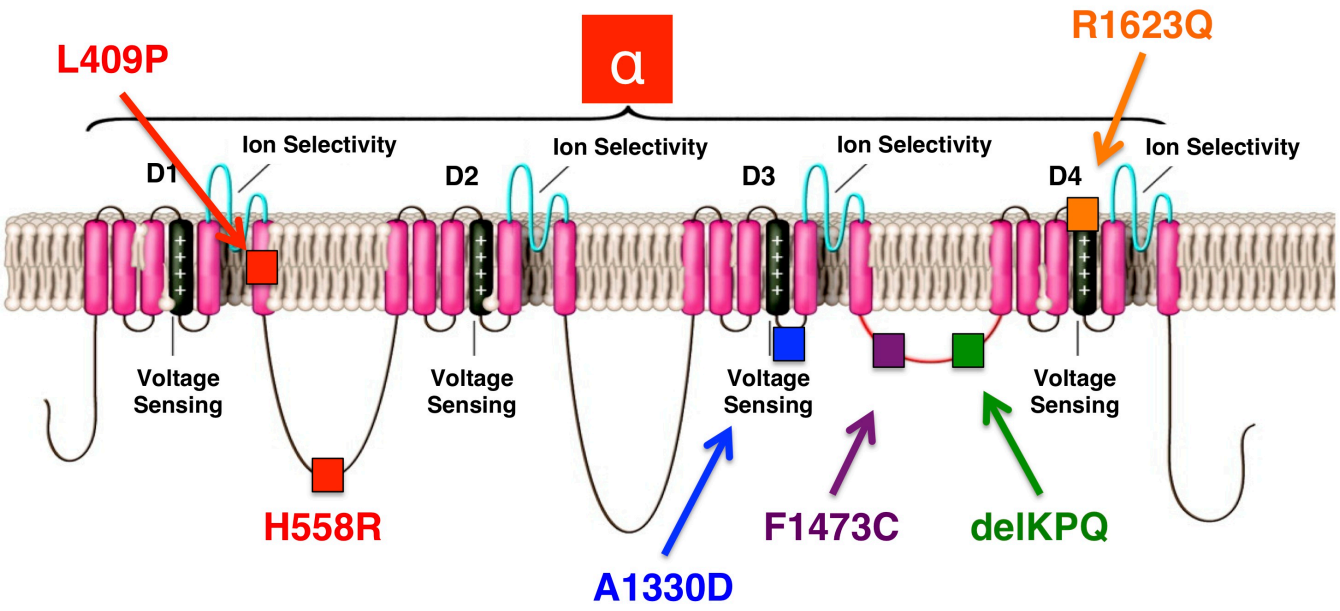

Figure 5: *SCN5A* mutations associated with perinatal and typical onset LQTS.

L409P and the common polymorphism R558 associated with LQTS of a 19-week fetus are shown in red. A1330D associated with perinatal LQTS and sudden death is shown in blue. F1473C associated with neonatal LQTS and fetal bradycardia is shown in purple. R1623Q associated with neonatal LQTS is shown in orange. Deletion of 1505-1507 of KPQ residues (delKPQ) is shown in green. Figure adapted from George, A. JCI (2005).[38]

associated with LQTS, R1623Q does not evoke persistent sodium current. However, R1623Q increased the probability of long openings as shown through single-channel recordings. This mutation also caused early re-openings and a prolongation of inactivation kinetics.[64] While these gating defects differ mechanistically from other *SCN5A* mutations associated with LQT3, slowed inactivation is another biophysical defect that also contributes to the pathogenesis of the disease.

In a rare case of an early-onset fetal arrhythmia, a *de novo SCN5A* mutation, L409P, was discovered. This leucine-409 to proline mutation was identified in a 19-week fetus with a severe case of LQTS, torsades de pointes, 2:1 AV block, and severe hydrops fetalis that resulted in termination of the pregnancy. This is the earliest known presentation of LQTS ever reported and the severity of the arrhythmia was profound. The fetus also demonstrated homozygosity for a common polymorphism H558R, also designated R558 (Figure 5).[52,65] The *SCN5A* polymorphism, R558, is present in 20% of the Caucasian population and is also found in other ethnic backgrounds.[66–70] In addition, R558 has been shown to potentiate dysfunction of other mutations in domain I of the sodium channel.[71] Therefore, it is important to consider the additional effects of a common variant (R558) in combination with the L409P mutation (see Chapter II).

In contrast to the previous mutations described, genetic studies on LQTS have also revealed numerous *SCN5A* mutations that cause voltage-gated sodium channel dysfunction associated with a later or more typical presentation of the disease in early childhood or early adulthood. A very well studied mutation associated with 'typical' onset of LQTS is a deletion mutation of nine bases that code for lysine-1505, proline-1506, and glutamine-1507 (ΔKPQ or delKPQ) in the inactivation gate between D3 and D4 of $Na_V1.5$ (Figure 5). $Na_V1.5$-delKPQ

exhibits sustained inward sodium current that contributes to prolongation of the cardiac action potential leading to LQTS.[72,73] However, this deletion is rarely reported in neonates and classically presents in adulthood[74] but the underlying molecular mechanism of this later onset is unknown. These characteristics make delKPQ an interesting candidate to study as a strong comparison with mutations discovered in early life arrhythmias (see Chapter III).

There are more than 450 mutations in *SCN5A* that have been identified in patients with arrhythmia predisposition syndromes.[75] In addition to mutations that result in LQT3, *SCN5A* mutations have been found to be associated with Brugada Syndrome,[43,76] atrial fibrillation,[68,77,78] conduction diseases,[61,66] and dilated cardiomyopathy.[79–81] Brugada Syndrome (BrS) is an inherited autosomal dominant arrhythmia characterized by right bundle branch block and prominent ST segment elevation on the ECG in addition to ventricular fibrillation.[60] It is estimated that 20-25% of patients affected with BrS have mutations in *SCN5A*. In contrast to the mechanism of LQTS, *SCN5A* mutations associated with BrS result in a loss of function of $Na_V1.5$. The biophysical defects associated with a loss of function of the cardiac sodium channel include a reduction in current density, defective trafficking of the channels, loss of channel availability, or faster channel inactivation.[76] Furthermore, some *SCN5A* mutations are associated with a phenotypic overlap of BrS and LQTS (e.g. E1784K). These *SCN5A* mutations may evoke a persistent sodium current of $Na_V1.5$ in addition to a reduction in current density or loss of channel availability.[82]

Although many *SCN5A* mutations associated with cardiac arrhythmias such as LQTS and BrS have been investigated, the molecular factors that predispose to sudden death during early life are still unknown. Therefore, we must also consider cellular processes that regulate gene expression such as alternative splicing. Variability in alternative splicing patterns of pre-

mRNA is a major source of protein diversity in higher eukaryotes. The most common form of alternative pre-mRNA splicing is called exon skipping. In exon skipping, a particular exon may be included in mRNAs under some conditions or in particular tissues, and may be absent from the mRNA in others.[83] Therefore we must consider the developmentally regulated alternative splicing mechanisms of ion channel genes that may contribute to the onset and severity of cardiac arrhythmias.

Alternative Splicing of $Na_V1.5$

The gene *SCN5A* that encodes the voltage-gated cardiac sodium channel consists of 28 exons spanning approximately 80 kb on chromosome 3p21. There have been 10 different alpha subunits of the cardiac sodium channel cloned from different mammalian tissues. The protein diversity of the cardiac sodium channel is due to alternative splicing.[84] In this cellular process, exons of a gene may be included or excluded from the final processed mRNA produced from that gene. When the protein is translated from different mRNAs, this results in changes in the amino acid sequence and subsequently alters the function of the protein.[83,85] Each splice variant of $Na_V1.5$ has its own tissue specificity and function.

Previous studies have shown the presence of two wild-type splice variants, one with a glutamine residue at position 1077 (Q1077) and one lacking this glutamine (Q1077del) in human hearts. Quantitative mRNA analysis from human hearts showed that a shorter 2015 amino acid splice variant lacking glutamine at position 1077 (Q1077del) made up ~65% of the transcript in every heart examined out of 200 samples. Age, sex, race, or structural heart disease did not affect the proportion of Q1077del. The only significant differences between Q1077 (hH1) and delQ1077 are that Q1077 exhibits a significantly hyperpolarized shift in the

voltage-dependence of inactivation and slower recovery from inactivation. In addition, the common polymorphism H558R (described previously) in combination with Q1077, results in a significant reduction in the sodium current density. A reduction in current density underlies the mechanism for BrS and conduction system disorders.[69] Therefore, alternative splicing of $Na_V1.5$ may contribute to cardiovascular disease risk in some individuals.

Heart failure has also shown to be associated with reductions in sodium current. Studies investigating the presence of $Na_V1.5$ splice variants in heart failure have revealed three new mRNA splice variants in exon 28 designated as E28B (27 bp), E28C (39 bp), and E28D (114 bp). Splice variants E28B, E28C, and E28D were shorter than the full-length mRNA transcript for $Na_V1.5$ and were predicted to result in prematurely truncated sodium channel proteins missing the segments from domain IV, S3 or S4 to the C terminus. Individually, E28C and E28D do not exhibit sodium currents when expressed in heterologous cells. Quantitative real-time RT-PCR experiments revealed that the relative abundances of each of the variants increased from fetal to adult heart, respectively. In addition, explanted ventricles from patients that suffered from heart failure exhibited a significant increase in E28C and E28D transcripts as well as a significant reduction in E28B and full-length transcripts. When E28C and E28D were co-expressed with WT $Na_V1.5$ in heterologous cells, the splice variants suppressed sodium current density of the functional channels compared to over-expression of $Na_V1.5$ alone. Therefore, abnormal *SCN5A* splicing may contribute to reductions in sodium current in heart failure and may contribute to regulation of the developing heart.[86,87]

Fetal $Na_V1.5$, previously known as $Na_V1.5e$ or neonatal $Na_V1.5$,[88] is another alternatively spliced voltage-gated sodium channel that contains an alternative exon 6 (designated here as exon 6A) in the mRNA transcript and results in translation of several residues within a voltage-

sensor domain (D1/S3-S4) that differ from adult $Na_V1.5$ (Figure 6). Exon 6A and exon 6 differ in 31 nucleotide substitutions that result in the following amino acid substitutions for the fetal $Na_V1.5$: T206V, T207S, F209N, V210I, D211K, V215L and S234P.[52,85,88] Alternative splicing of fetal $Na_V1.5$ is developmentally regulated (also see Chapter II).[88]

Fetal $Na_V1.5$ was first observed in two independent studies in a human neuroblastoma cell line and in a highly metastatic human breast cancer cell line.[89,90] Further investigation of fetal $Na_V1.5$ revealed that it is also expressed in human, rat, and mouse brain tissues.[88] In addition, fetal $Na_V1.5$ is strongly expressed in neonatal mouse heart but is down-regulated in later developmental stages.[90] The exon 6A alternative splicing mechanism is also conserved in 5 other sodium channel genes (*SCN1A*, *SCN2A, SCN3A*, *SCN8A*, *SCN9A).*[88]

It is important to consider that fetal $Na_V1.5$ exhibits differential biophysical properties compared with adult $Na_V1.5$ as demonstrated by whole-cell electrophysiological recordings of heterologously expressed channels. Most notably, fetal $Na_V1.5$ exhibits a more depolarized

conductance-voltage relationship (activation curve) compared with the adult isoform that is dependent on a single charged amino acid residue, a lysine (K) at position 211.[52,85] This suggests that the fetal $Na_V1.5$ may exert a unique effect on the electrical properties of the fetal heart.[88] Furthermore, fetal $Na_V1.5$ may also be important in the pathophysiology of perinatal forms of LQTS.

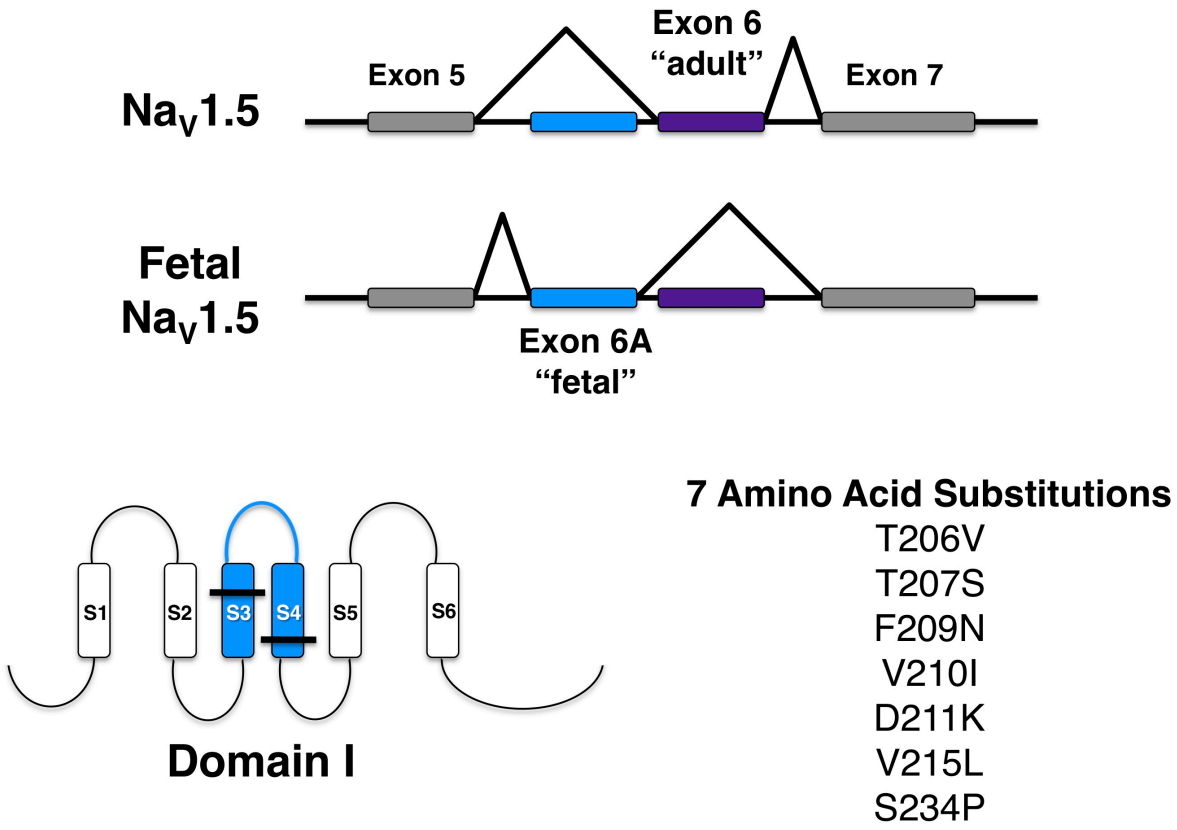

Figure 6: Alternative splicing of $Na_V1.5$.

Fetal $Na_V1.5$ is a result of developmentally regulated alternative splicing mechanism that includes exon 6A in the final mRNA transcript. This mechanism results in seven amino acid substitutions between S3 and S4 of DI of the cardiac sodium channel compared to the canonical adult isoform.

Therefore, we hypothesized that fetal $Na_V1.5$ will provide a more sensitive background for *SCN5A* mutations identified in early life (fetal through infancy) and will result in exacerbation of cardiac sodium channel dysfunction. Four early onset LQT3 mutations were compared to an *SCN5A* mutation that is associated with a later onset of the arrhythmia (Figure 5) in order to better understand the molecular mechanism of fetal $Na_V1.5$. To test this hypothesis, we transfected tsA201 cells with the wild-type (WT) or mutant fetal $Na_V1.5$ and WT or mutant adult $Na_V1.5$, then examined the effects of each mutation by whole-cell electrophysiological recording. Comparisons of the biophysical properties of these alleles in the two splice variants as well as a comparison of the two groups (early onset vs. adult onset arrhythmias) are shown in Chapters II & III. The goal of these studies was to elucidate the biophysical properties of $Na_V1.5$ mutations expressed in fetal $Na_V1.5$ giving important new insight into arrhythmia susceptibility manifested during perinatal life.

We also hypothesized that fetal $Na_V1.5$ alternative splicing alters the pharmacology of WT $Na_V1.5$ and mutant $Na_V1.5$-L409P/R558 especially in the mutant channels. Lidocaine, a class Ib anti-arrhythmic drug and sodium channel blocker, is a current experimental treatment for fetal LQTS. In addition, previous studies were preformed in our laboratory on the pharmacology of a splice variant of *SCN1A* (SCN1A-5N) which is the conserved splicing event exhibited for the fetal $Na_V1.5$.[90,91] The splice variant SCN1A-5N exhibited enhanced tonic block and use-dependent block by phenytoin and lamotrigine, across a range of stimulation frequencies and concentrations as well as induced shifts in steady-state inactivation and recovery from fast inactivation. These data suggest that the splice variant is more sensitive to commonly used anti-epileptic drugs. To test the hypothesis that mutant fetal $Na_V1.5$ may exhibit differential biophysical effects in the presence of lidocaine compared to WT fetal

channels, we transfected tsA201 cells with WT fetal $Na_V1.5$ or fetal $Na_V1.5$-L409P/R558, then examined the effects of lidocaine on each condition by whole-cell electrophysiological recording. The studies shown in Chapter II investigated the pharmacology of WT and mutant (L409P/R558) fetal $Na_V1.5$. The goal of these studies and proposed future work is to evaluate lidocaine as a current treatment for fetal ventricular arrhythmias.

Recent evidence from our laboratory has revealed that *de novo* calmodulin mutations are also associated with a severe neonatal LQTS causing recurrent cardiac arrest during infancy.[92] One plausible contributing molecular mechanism for LQTS in these cases may be $Na_V1.5$ dysfunction. We hypothesized that calmodulin mutations would result in more severe functional consequences when co-expressed with the fetal $Na_V1.5$ compared to the adult isoform of the channel. To test this hypothesis, we transfected tsA201 cells with either fetal or adult $Na_V1.5$ in combination with either the WT or mutant calmodulins (*CALM1*-D130G, *CALM1*-F142L, *CALM2*-D96V, *CALM2*-D134H, *CALM2*-D132E, *CALM1*-F90L). We ascertained the effects of each mutation by whole-cell electrophysiological recording and compared the biophysical properties of the two splice variants. The studies in Chapter IV will elucidate the molecular mechanism of calmodulin mutations on the functional effects of $Na_V1.5$. These experiments provide an important insight into arrhythmia susceptibility associated with “calmodulinopathies” in early life.

CHAPTER II

Developmentally Regulated *SCN5A* Splice Variant Potentiates Dysfunction of a Novel Mutation Associated With Severe Fetal Arrhythmia*

INTRODUCTION

Congenital long-QT syndrome (LQTS) refers to a group of disorders with primary impairment of myocardial repolarization predisposing to life-threatening cardiac arrhythmias especially torsades de pointes (TdP) that are caused by genetic mutations in cardiac ion channels or channel modulating proteins.[93] The disease is typically recognized in late childhood or early adolescence but extreme cases may present during infancy or in the perinatal period.[45,47,94] Clinical signs suggestive of fetal LQTS include ventricular tachycardia, second degree atrioventricular (AV) block, and most commonly, sinus bradycardia but such findings may go undetected owing to the lack of routine electrocardiographic testing of fetuses.[95,96]

Evidence for Mendelian inheritance is not always apparent in cases of fetal LQTS because of *de novo* mutations or germ line mosaicism.[53,54] Certain *SCN5A* mutations, many of which are *de novo* present with earlier onset and more severe congenital arrhythmia

* Modified from Murphy et al. *Heart Rhythm Journal*. (2012).

syndromes than is typical for LQTS.[45,47,49,50,94,97–99] The reason for greater severity and lethality of certain genetic variants during early life is unknown.

Here we describe the clinical, electrocardiographic, and genetic diagnosis of LQTS in a fetus at 19 weeks gestation presenting with ventricular tachycardia and severe hydrops fetalis.[52] To our knowledge, this is the earliest gestational age at which a diagnosis of LQTS has been made after being suspected on the basis of clinical presentation. A novel, *de novo* *SCN5A* mutation (L409P) combined with a common genetic variant (H558R) was discovered in the proband. The *SCN5A* polymorphism, H558R, is present in 20% of the Caucasian population and is also found in other ethnic backgrounds.[66–70] The proband was homozygous for H558R. Therefore, we chose to investigate the molecular consequences of this mutation and the common genetic variant (L409P/R558) on sodium channel function.

Our laboratory has demonstrated prominent expression of an alternatively spliced $Na_V1.5$ mRNA transcript in fetal and neonatal human heart that differs from the adult isoform by several residues within a voltage-sensor domain (Chapter I, Figure 6). Therefore, we hypothesized that mutations associated with sudden death in early life (fetal through early infancy) have more severe functional consequences when expressed in the context of fetal $Na_V1.5$ as compared with the adult splice variant. To elucidate the functional consequences of the mutation, we preformed *in vitro* electrophysiological experiments comparing WT and mutant (L409P/R558) human cardiac sodium channels in the canonical channel and in the alternatively spliced form of $Na_V1.5$ expressed in fetal heart. Additionally, we hypothesized that fetal $Na_V1.5$-L409P/R558 may exhibit differential pharmacological effects compared to WT in the presence of a sodium channel blocker. Therefore, we also investigated the

pharmacological effects of lidocaine, a treatment for fetal arrhythmias, on WT and mutant L409P/R558 fetal sodium channels.

METHODS

Testing for mosaicism

Parental DNA extracted from blood, saliva and buccal swabs was examined by direct sequence, restriction enzyme digest (EagI, MspI or NciII) and Taqman allelic discrimination assay.

Measurement of cardiac *SCN5A* expression

De-identified, frozen, postmortem heart tissues from white-American subjects were obtained from the Brain and Tissue Bank of the University of Maryland under an exemption for human subject research granted by the Vanderbilt University institutional review board. Total RNA was extracted from pulverized heart muscle using TRIzol reagent (Invitrogen, Carlsbad, CA) followed by DNase digestion and final purification with RNeasy MinElute (Qiagen, Valencia, CA). RNA quality was determined by spectrophotometry and gel electrophoresis, and samples exhibiting degradation were not used. Reverse transcription was performed using 3 µg RNA, 3.75 µM random hexamers (Applied Biosystems, Foster City, CA), 0.5 mM deoxynucleoside triphosphates (Roche, Basel, Switzerland), 1x M-MLV buffer (Promega, Madison, WI), 10 mM DTT, 40 units RNase inhibitor (Promega), and 200 units M-MLV reverse transcriptase (Promega). Reverse-transcription reactions were incubated sequentially for 5 min at 65°C, 2 min at 42°C, 10 min at 25°C, 50 min at 42°C, then 15 min at 70°C. Real-time quantitative RT-PCR using TaqMan probes specific for *SCN5A* exon 6 (VIC-

TTACGCACCTTCCGAGTC-MGB [MGB, minor groove binder]) or 6A (FAM-TTCGAACTTTCAGAGTCC-MGB) were used to measure relative levels of mRNA transcripts containing either of these alternate exons. Amplification primers (forward: CCATGGAACTGGCTGGACTT; reverse: GACCATCACATCAGCCAGCTT) used in the assay generated a 192 bp amplicon (nucleotides 574-765 based on the open reading frame of Genbank:NM_198056) with a two-temperature cycling protocol (95°C for 20 s followed by 45 cycles of 95°C, 1 s and 60°C, 30 s). Under these conditions, neither TaqMan probe exhibited cross-reactivity with the opposite allele. All reactions were performed in triplicate on a 7900HT Fast Real-Time PCR system (Applied Biosystems). Individual reactions (20 µl) contained 1x Fast Universal PCR Master Mix (Applied Biosystems), forward and reverse primers (3 µM), an allele-specific probe (10 µM), and 5 µl of cDNA (or 5 µl water for template-negative controls). The ability of the assay to quantitatively distinguish different proportions of the two alleles with high specificity was assessed using plasmid cDNA standards in the following mass ratios (exon 6:6A): 4:1, 2:1, 1:1, 1:2, and 1:4. The cDNA standards were diluted to a final concentration of 0.025 ng/µl after preliminary studies determined that this concentration produced cycle threshold values similar to heart tissue RNA. Assays were performed in triplicate and each RNA sample was assayed from 2-3 independent preparations of cDNA. Initial data analysis was performed using Applied Biosystems Sequence Detection System software (version 2.2.2). Cycle threshold (CT) values were used to generate a $\log_2$-based standard curve from cDNA standards and then sample CT values were used to interpolate expression levels for each splice isoform. Finally, ratios of mRNA transcripts containing *SCN5A* exon 6A compared with exon 6 were calculated.

Mutagenesis and heterologous expression of human cardiac sodium channel

Mutagenesis of recombinant human cardiac sodium channel ($Na_V1.5$) was performed as described previously, except that a rare variant present in the original cDNA (glutamine-1027; Genbank accession number M77235) was reverted to the common allele (arginine-1027).[47,100] The common variant R558 was engineered in some constructs to match the genotype of the study subject. Wild-type (WT), R558 variant, or L409P/R558 mutant channel cDNA (0.5 μg) were transiently transfected into tsA201 cells using FuGene 6 (Roche Diagnostics, Indianapolis, IN) combined with a plasmid encoding enhanced green fluorescent protein (IRES2-eGFP, 0.5 μg). Initial experiments co-expressed the β1 subunit cDNA (IRES2-eGFP-hβ1, 0.5 μg) with $Na_V1.5$ in place of IRES-eGFP. Transiently transfected cells were incubated for 48 hours at 37°C prior to electrophysiological measurements. Cells exhibiting green fluorescence were selected for patch-clamp recordings. A fetal $Na_V1.5$ cDNA was engineered by making the following amino acid substitutions encoded by the alternate exon 6 (designated exon 6A): T206V, T207S, F209N, V210I, D211K, V215L, S234P.

*In vitro el*ectrophysiology

Sodium currents were recorded at room temperature using the whole-cell patch clamp technique as described previously.[47,58] The extracellular bath solution contained the following (in mmol/L): 140 NaCl, 4 KCl, 1.8 $CaCl_2$, 1 $MgCl_2$, 10 HEPES, and 10 glucose, pH 7.35 (adjusted with NaOH). Osmolality of the bath solution was adjusted to 300mOsm/L with sucrose. The intracellular pipette solution contained the following (in mmol/L): 10 NaF, 105 CsF, 20 CsCl, 2 EGTA, 10 HEPES, 10 glucose, pH 7.35 (adjusted with CsOH). Osmolality of the intracellular solution was adjusted to 310mOsm/L with sucrose. Data were acquired with an

Axopatch 200B patch-clamp amplifier and pClamp 10.2 software. Electrode resistance ranged from 1.0 to 1.5 MΩ. Pipette resistance and junction potential were corrected and whole-cell capacitance and series resistance were 90% compensated (voltage error ≤ 2 mV). Voltage-clamp pulse protocols assessing channel activation, steady-state inactivation, recovery from inactivation, and RAMP current are depicted in figure insets. TTX-sensitive persistent current was determined with a 200-ms depolarization to -30 mV as the average current recorded between 190 and 200 ms and reported as a percentage of peak current following digital subtraction of currents recorded in the presence and absence of 30 μmol/L tetrodotoxin (Tocris Biosciences, Ellisville, MO). For pulse train experiments, cells were pulsed at frequencies of 1 and 2 Hz with 400ms pulses to -20 mV with a holding potential of -90 mV at room temperature. Sodium current was normalized to the level of current at the first pulse. All data were analyzed with pClamp 10.2 (Axon Instruments, Inc, Sunnyvale, CA) and plotted using Sigmaplot 10.0 (SPSS, Inc, Chicago, IL) software. Results are presented as mean ± SEM. Unless otherwise noted, statistical comparisons were made by using an unpaired Student *t* test in reference to WT $Na_V1.5$. Statistical significance was assumed for $P < 0.05$.

Lidocaine pharmacology

Pulse train experiments were performed at room temperature on heterologous cells expressing WT or mutant $Na_V1.5$ in the absence and presence of 100 μM lidocaine HCL (Sigma Aldrich, St. Louis, MO). Cells were pulsed at a frequency of 2 and 5 Hz with 50 ms pulses to -20 mV with a holding potential of -120 mV. Recordings were performed at room temperature. Sodium current was normalized to the level of current at the first pulse.

RESULTS

Identification of a novel *SCN5A* mutation in a fetus with torsades de pointes

A 29-year-old primiparous woman was referred for evaluation of an irregular fetal heart rhythm at 19-6/7 weeks gestation (by last menstrual period and an 11 week ultrasound). There was no family history of pregnancy loss, syncope, seizures, sudden cardiac death at any age, accidental death or drowning. An initial fetal echocardiogram at 20 weeks gestation disclosed normal cardiac anatomy with decreased ventricular function, mild tricuspid valve insufficiency and a very small pericardial effusion. The atrial rate was regular at 130-160 beats per minute (bpm) but the ventricular rate was variable. There were frequent premature ventricular contractions and couplets, and short (3-4 beat) runs of tachycardia (Figure 7A). During non-sustained tachycardia, the atrial rate was slower than the ventricular rate, leading to a presumptive diagnosis of ventricular tachycardia. There was no evidence of AV block. Maternal electrolytes were normal, and serum testing for maternal SSA/SSB antibodies, IgG to cytomegalovirus and Toxoplasma gondii were negative. The QTc intervals determined from 12- lead ECG recordings were in the normal range for the patient and fetus' father (424 ms and 383 ms, respectively). At 20-6/7 weeks, a fetal magnetocardiogram (fMCG) revealed frequent short episodes of polymorphic ventricular tachycardia consistent with TdP and a QTc interval of 604 msec (Figure 7B & 7C). During 2 hours of data recording, AV block was not observed. An ultrasound the same day showed interval accumulation of pleural fluid and ascites consistent with hydrops fetalis.

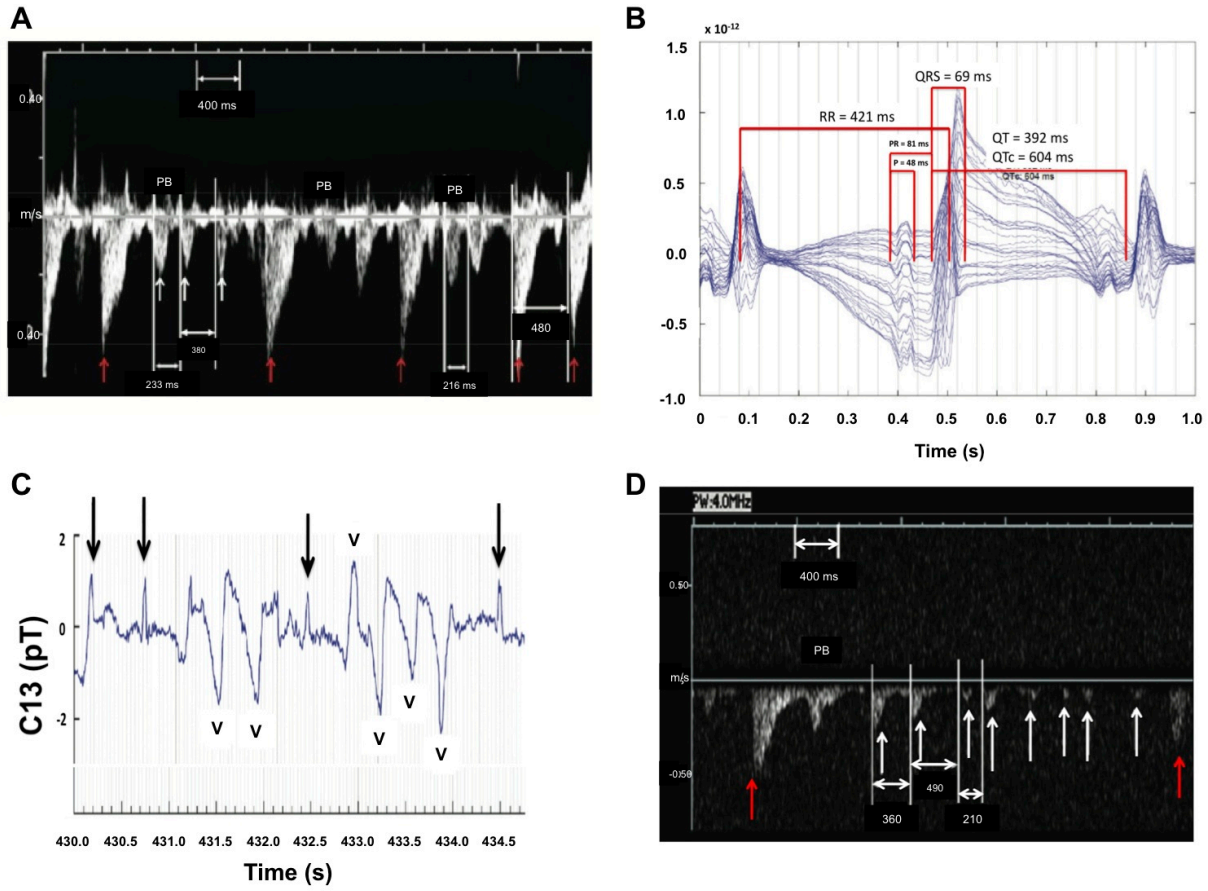

Figure 7: Fetal Doppler echocardiogram and magnetocardiogram. (A) Pulsed wave Doppler of the fetal aorta at 20 weeks gestation. Normal conducted beats (red arrows) are interrupted by frequent premature beats (PBs), and 2-3 beat runs of tachycardia with variable cycle length (white arrows). The flow velocity is maintained during the short runs of tachycardia, suggesting stroke volume is only slightly diminished. (B) Signal averaged 'butterfly plot' determined by fetal magnetocardiography during sinus rhythm at 20-6/7 weeks gestation illustrating T-wave alternans, a QTc interval of 604 msec, normal PR interval and a QRS duration that was slightly prolonged for age (0.69 msec). (C) Representative rhythm trace obtained by fetal magnetocardiography at 20-6/7 weeks gestation. Arrows indicate sinus beats interrupted by two episodes of non-sustained polymorphic ventricular (V) tachycardia (torsades de pointes) with varying cycle length (400 to 200 msec). (D) Pulsed wave Doppler of the middle cerebral artery at 22 weeks gestation illustrating fetal arrhythmia. At this time, the fetus was severely hydropic with very poor systolic function (not shown). The tracing shows the onset of a sustained period (> 3500 msec) of ventricular tachycardia (white arrows), initiating by a premature beat (PB). During the tachycardia, there is decreased stroke volume as evidenced by the extremely low velocity Doppler signals. The tachycardia cycle length was 480 to 210 ms.

Treatment of the fetal arrhythmia was discussed with the family, however, because of the dire clinical status, the parents elected not to pursue treatment.

Echocardiography at 22 weeks gestation revealed severe cardiac dysfunction, more frequent and more prolonged episodes of ventricular tachycardia (Figure 7D), and worsening hydrops fetalis. Although tachycardia cycle length was similar to that observed 2 weeks prior (Figure 7A), the velocity of the Doppler signals were extremely low, suggesting that the stroke volume was greatly decreased during tachycardia episodes. At this time, tachycardia episodes had a longer duration, and the intervals between tachycardia episodes were shorter (not shown) implicating increased tachycardia burden as a factor for the progression of cardiac dysfunction.

Based on the extent of clinical deterioration, the pregnancy was terminated at the request of the family. Postmortem genetic testing (Familion, New Haven, CT, USA) of the fetus identified a novel heterozygous *SCN5A* transition mutation (T1226C) predicting a missense change in codon 409 from leucine to proline (designated *SCN5A*-L409P). The fetal proband was also homozygous for a common nonsynonymous variant, R558. However, extensive analysis of parental DNA identified no evidence of germline mosaicism suggesting that *SCN5A*-L409P occurred on a *de novo* basis in the fetus.

Functional Consequences of *SCN5A*-L409P

We determined the functional consequences of *SCN5A*-L409P by *in vitro* electrophysiological recording of heterologously expressed recombinant human cardiac sodium channels ($Na_V1.5$). To recapitulate the genotype of the fetus, we engineered the L409P mutation along with the R558 variant (combination allele designated as L409P/R558). Expression of mutant channels in tsA201 cells generated voltage-dependent sodium currents that exhibited several differences compared to WT $Na_V1.5$ including a trend toward reduced peak current density (Figure 8A & B), significant depolarized shifts in the voltage-dependence of steady-state inactivation and conductance-voltage relationships (Figure 8C; Table 2), and markedly accelerated recovery from inactivation (Figure 8D). Additionally, as compared to WT channels, L409P/R558 exhibited a 7-fold greater level of persistent sodium current measured as a percentage of peak current (1.4 ± 0.2%, Figure 9A; Table 1). Increased persistent current is the most frequently observed functional disturbance exhibited by *SCN5A* mutations associated with LQTS,[101] and can also explain abnormal inward current evoked by a slow depolarizing voltage ramp (Figure 9B & C). The overall findings indicate that L409P/R558 causes dysfunction of cardiac sodium channels consistent with cardiac arrhythmia predisposition. However, these findings do not provide an explanation for the severe intrauterine presentation of ventricular arrhythmia.

We also repeated these experiments with co-expression of the auxiliary β1 subunit with $Na_V1.5$ (Figure 10). In the presence of β1, the current density of both WT and mutant channels increased. However this was not significant compared to channels in the absence of β1 subunits. Overall, L409P/R558 exhibited similar effects in the presence and absence of β1 compared to respective WT channels.

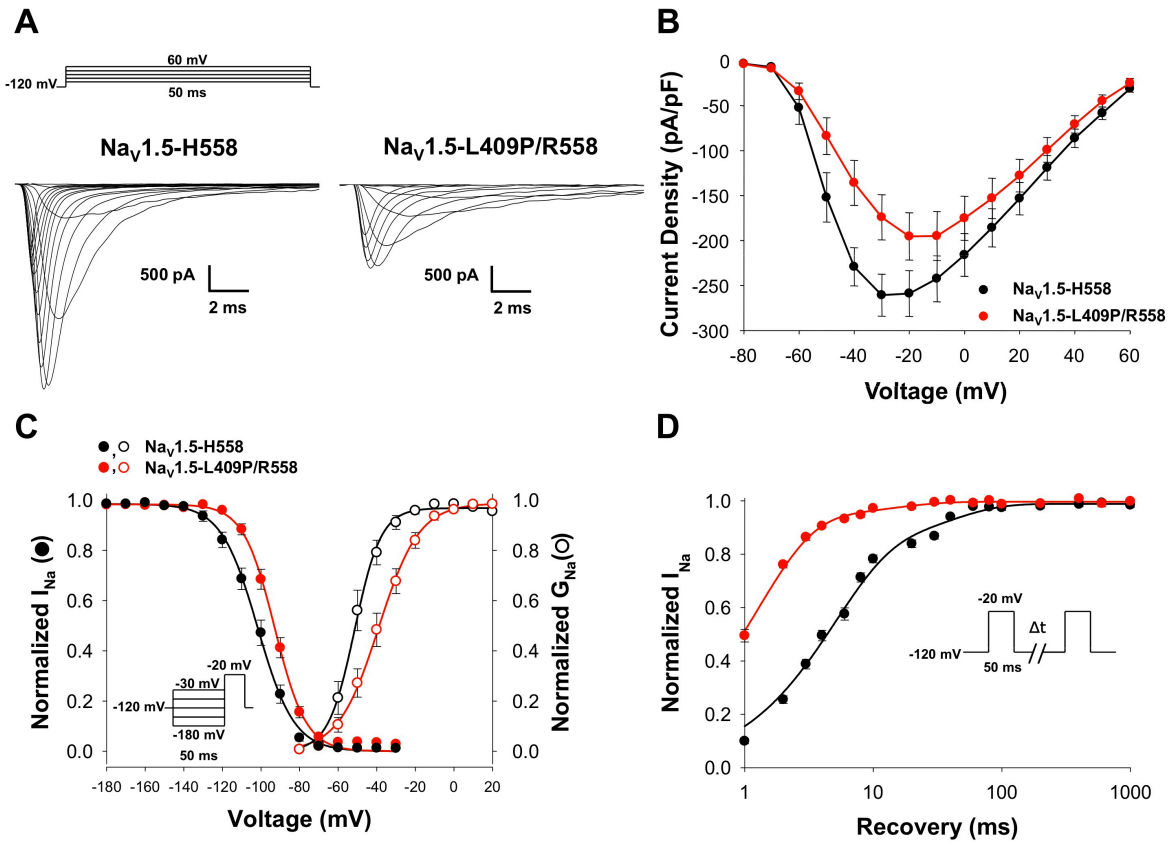

Figure 8: Biophysical properties of WT and mutant sodium channels.
(A) Representative whole-cell current recordings from cells expressing either WT (adult $Na_V1.5$- H558) or mutant (adult $Na_V1.5$-L409P/R558) channels (voltage protocol shown as inset). (B) Current-voltage relationships for WT (n = 10) and mutant (n = 10) channels. Current was normalized to cell capacitance to give a measure of current density. (C) Superimposed curves representing the voltage dependence of steady-state inactivation (left y-axis) and conductance- voltage (right y-axis) relationships for WT and mutant channels. Lines represent average fits of the data with Boltzmann functions. (D) Time course of recovery from inactivation recorded using the illustrated voltage protocol. Biophysical fit parameters for all experiments are provided in Table 2.

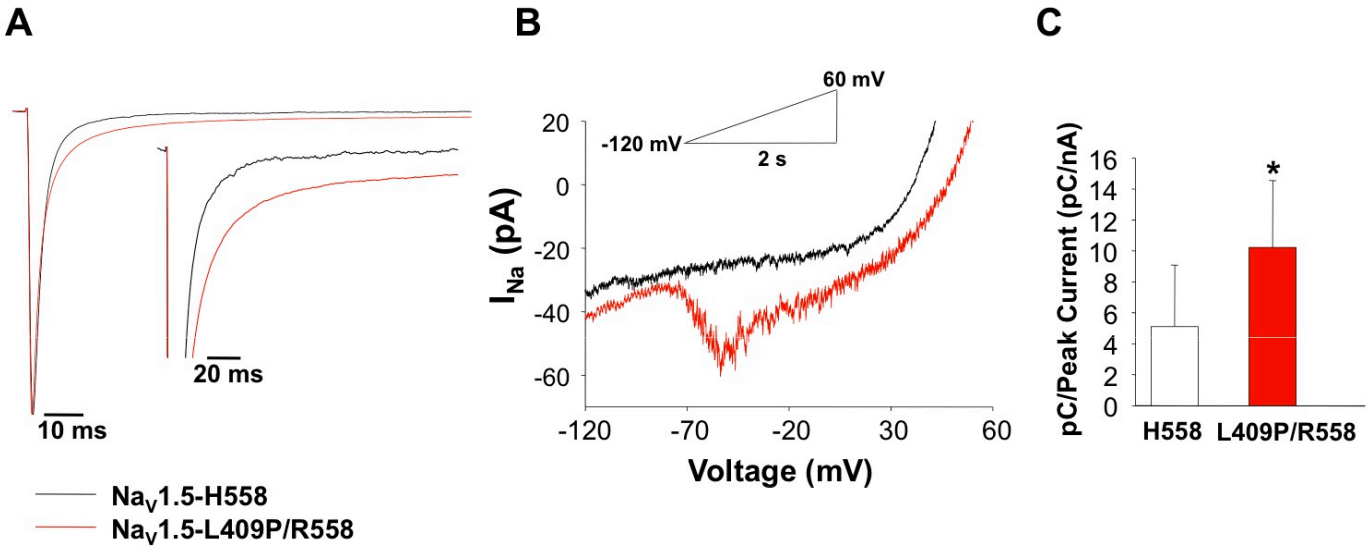

Figure 9: *SCN5A*-L409P/R558 exhibits increased persistent current.

(A) Representative tetrodotoxin (TTX)-sensitive currents were normalized to the peak current measured at -30mV during a 200 ms depolarization to illustrate persistent current. The inset represents the same data plotted on an expanded vertical scale. Summary data are provided in Table 1. (B) WT and mutant currents elicited by voltage ramps defined by the inset. (C) Amount of charge moved between -70 and -30mV normalized to peak current and quantified. Charge movement was significantly ($p < 0.02$) greater for mutant (10.2 ± 4.3 pC/nA, n = 9) than for WT (5.1 ± 4.0 pC/nA, n = 9) channels.

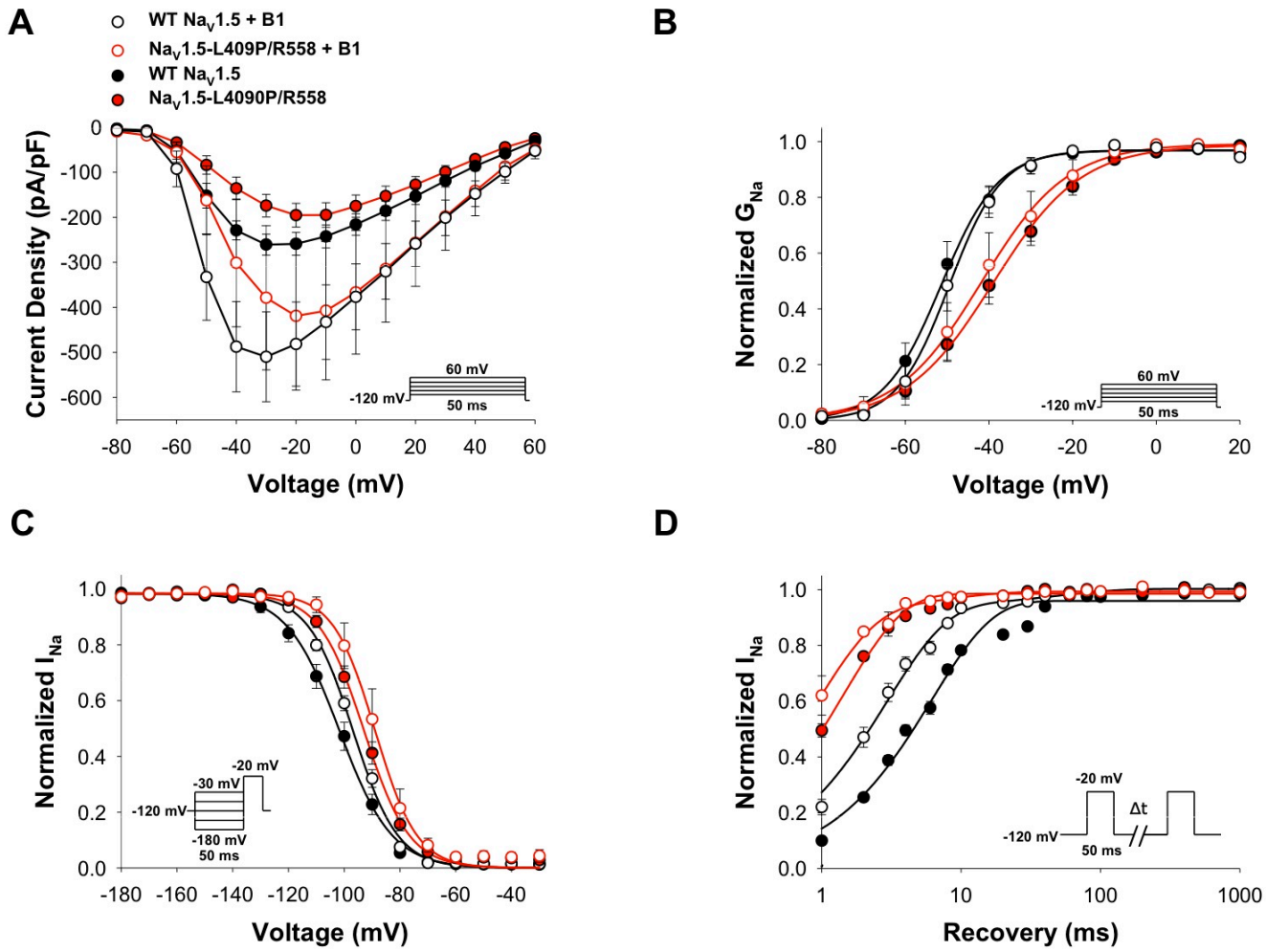

Figure 10: β1 subunit does not significantly affect L409P/R558 channel function.

(A) Current density-voltage relationships recorded from cells expressing either WT Na$_V$1.5 (n = 10), Na$_V$1.5-L409P/R558 (n = 10), WT Na$_V$1.5 + β1 (n = 9), or Na$_V$1.5-L409P/R558 + β1 (n = 4) channels (voltage protocol in the inset). (B) Conductance-voltage relationships for WT and mutant channels in the presence of absence of β1 subunits. (C) Steady-state voltage dependence of inactivation for WT and mutant channels (n = 4-10). In (B) and (C) lines represent average fits of the data with Boltzmann functions. (D) Time course of recovery from inactivation recorded using the illustrated voltage protocol.

Recovery from inactivation of WT channels co-expressing β1 was significantly faster than WT channels without β1. However, this was not consistent with previous studies investigating β1 effects on channel function. Previous studies in CHO cells over-expressing β1 have shown that β1 has no effect on recovery from inactivation, shifts the voltage-dependence of activation and inactivation to more hyperpolarized potentials, and significantly increases current density compared to $Na_V1.5$ without β1.[102–104] Therefore we concluded that β1 does not have additional effects on the mutant $Na_V1.5$ channels despite differences in WT channel function in the presence of β1.

Developmental regulation of *SCN5A* exon 6 splicing

We hypothesized that the severity of LQTS presentation in this fetus was due to more severe functional consequences conferred by the mutant genotype in the background of a fetal-expressed alternatively spliced *SCN5A* transcript. We focused on the developmentally timed alternative splicing of exon 6 that generates two splice isoforms differing by seven amino acid residues within a voltage-sensing domain (D3/S3-S4) originally described in neuroblastoma cells.[105] We determined the relative levels of *SCN5A* mRNA transcripts containing the canonical exon 6 or the alternative exon 6A in human heart samples representing various developmental stages including the fetal period (28-33 weeks gestation), infancy (2-6 months of age) and adulthood (> 18 years of age).

In fetal human heart, we observed ~1.5-fold greater levels of *SCN5A* mRNA transcript containing exon 6A, encoding what we designated as fetal $Na_V1.5$, as compared with transcripts containing the canonical exon 6, encoding the adult splice variant of $Na_V1.5$ (Figure 11). In hearts from infants, the relative abundance of adult and fetal $Na_V1.5$ mRNA was

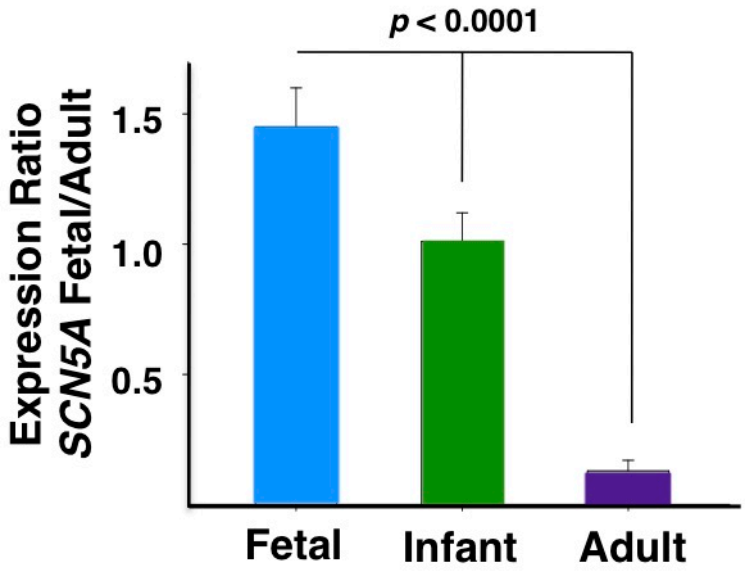

Figure 11: Developmental timing of *SCN5A* exon alternative splicing.

Expression ratio (exon 6A / exon 6) of *SCN5A* mRNA transcripts expressed in human fetal (n = 4), infant (n = 4) and adult (n = 24) hearts determined by quantitative real-time RT-PCR. Differences among groups was significant at $p < 0.0001$ (one-way ANOVA with Tukey test).

approximately equal, while in adult heart there was a 7.5-fold higher level of adult $Na_V1.5$ mRNA as compared to the fetal splice variant. The fetal (exon 6A) to adult (exon 6) $Na_V1.5$ expression ratio in adult heart was significantly different from both infant and fetal heart ($p < 0.0001$) whereas differences between fetal and infant heart expression ratios were not significant ($p = 0.06$). We conclude that *SCN5A* exhibits a developmental switch in exon 6/6A alternative splicing in human heart during early postnatal life.

Functional properties of WT and mutant fetal $Na_V1.5$

To test whether the functional consequences of L409P/R558 are different in fetal $Na_V1.5$, we engineered a recombinant human fetal $Na_V1.5$ cDNA and compared its electrophysiological properties to adult $Na_V1.5$. We demonstrated that fetal $Na_V1.5$ exhibits a significantly more positive midpoint (+9 mV shift in $V_{1/2}$) in the conductance-voltage relationship as compared with the adult splice variant, but no significant differences in peak current density, voltage- dependence of steady-state inactivation curve or recovery from inactivation (Figure 12; Table 2). These data demonstrate intrinsic differences in biophysical properties between human fetal and adult $Na_V1.5$ splice isoforms.

We investigated the consequences of the common *SCN5A* variant R558 on the functional properties of fetal $Na_V1.5$ and compared these to the effect of the variant on the adult splice isoform. Whereas, R558 has minimal functional impact on adult $Na_V1.5$ (Table 2), the expression of this variant in fetal $Na_V1.5$ demonstrates substantial effects including lower whole cell current density and a large persistent sodium current (Figure 13; Table 1). These findings demonstrate a considerable functional defect for the non-mutant allele, R558.

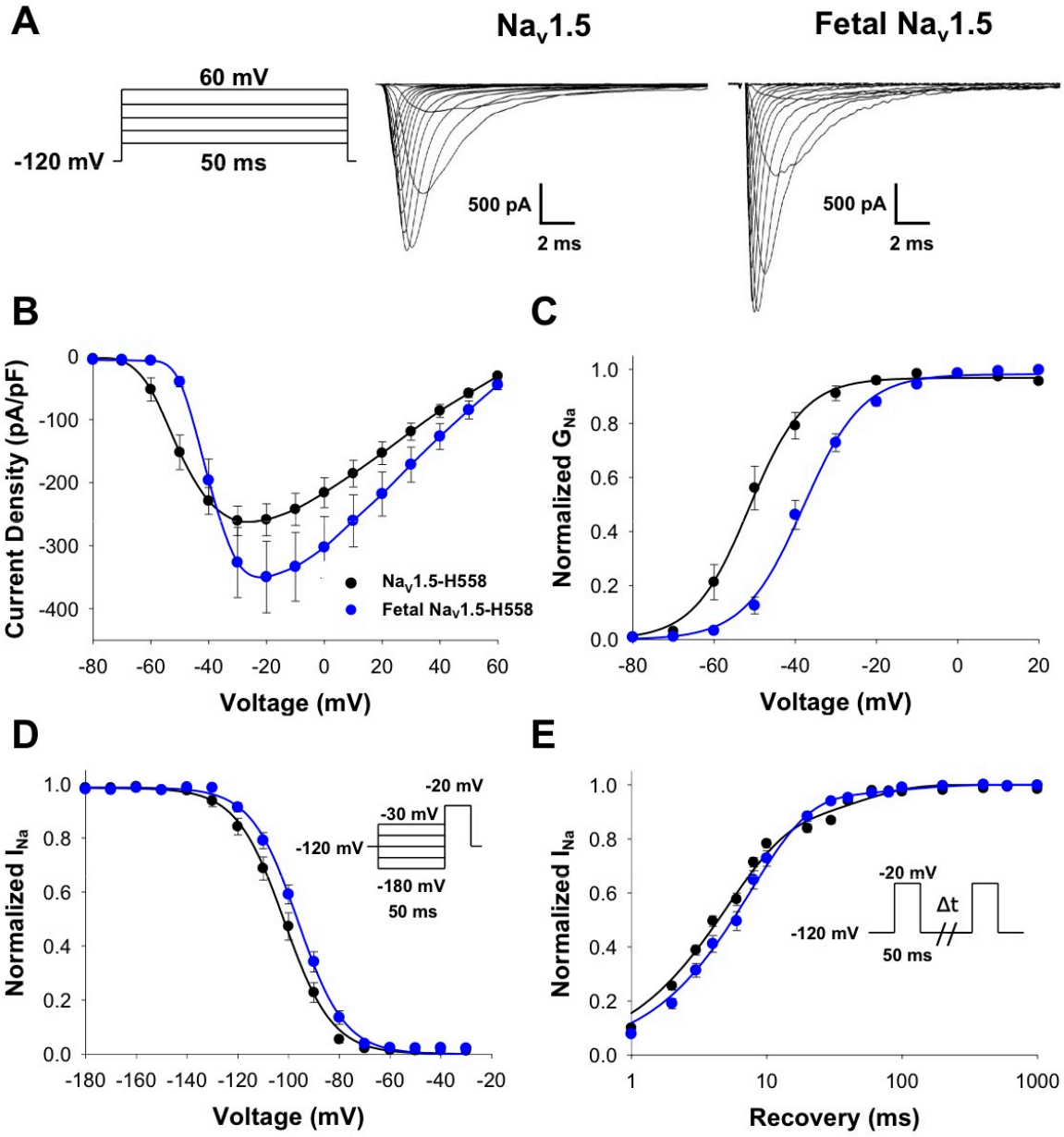

Figure 12: Comparison of biophysical properties for adult and fetal Na$_V$1.5 channels.

(A) Representative whole-cell current recordings from cells expressing either adult Na$_V$1.5 or fetal Na$_V$1.5 obtained using the illustrated voltage-clamp protocol. Both channel isoforms included the common allele at position 558 (H558). (B). Current-voltage relationships for adult Na$_V$1.5 and fetal Na$_V$1.5. Current was normalized to cell capacitance to give a measure of current density. (C) Conductance-voltage relationships for adult Na$_V$1.5 and fetal Na$_V$1.5. (D) Steady-state voltage dependence of inactivation for adult Na$_V$1.5 and fetal Na$_V$1.5. In (C) and (D) lines represent average fits of the data with Boltzmann functions. (E) Time course of recovery from inactivation recorded using the illustrated voltage protocol. Biophysical fit parameters for all experiments are provided in Table 2. Data were collected from 10-11 cells.

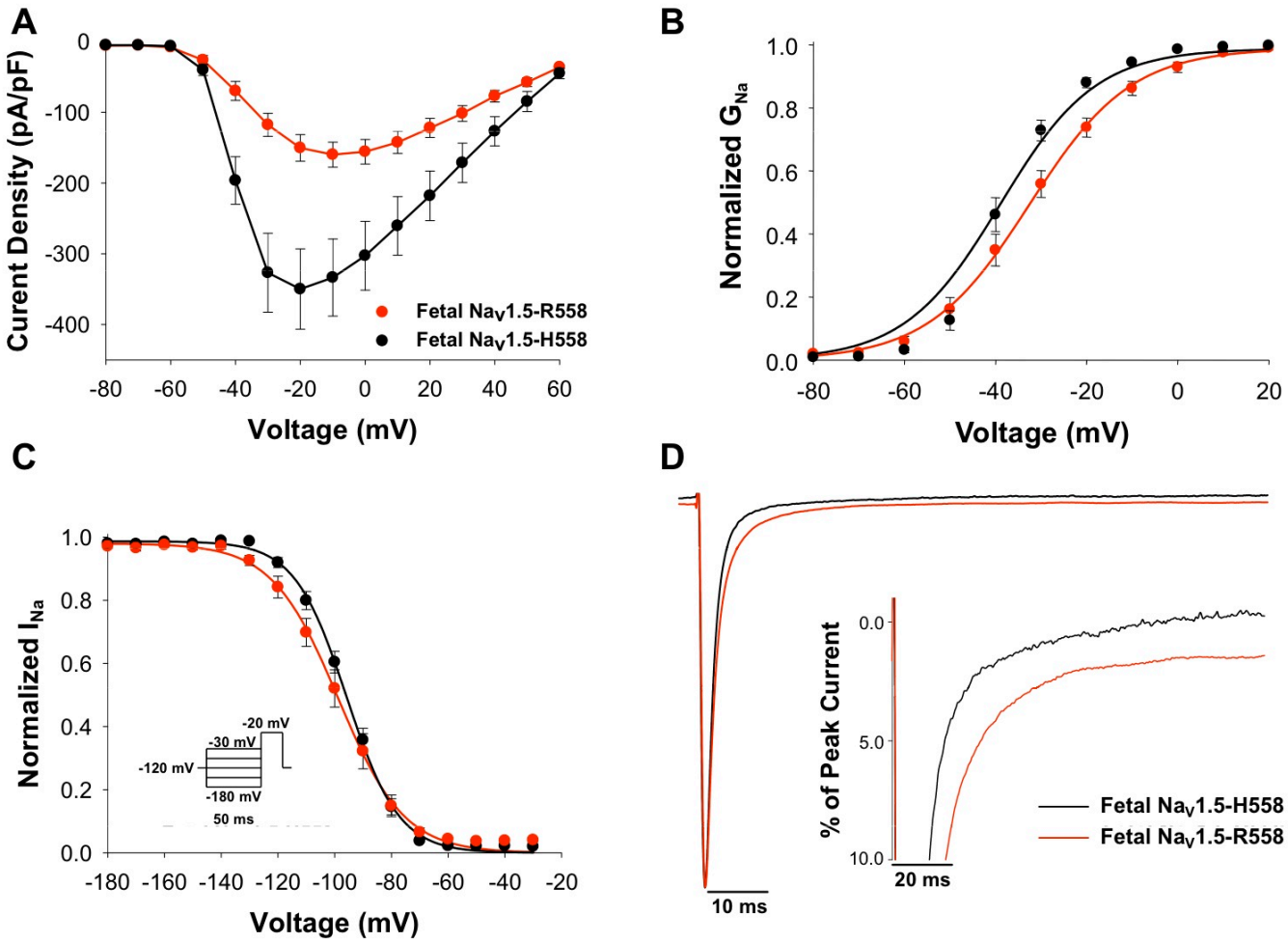

Figure 13: Functional consequences of R558 variant on fetal-Na$_V$1.5.

(A) Current density-voltage relationships recorded from cells expressing either WT (labeled fetal-Na$_V$1.5-H558; n = 11) or variant (fetal Na$_V$1.5-R558; n = 14) channels (voltage protocol same as in Figure 8A). (B) Conductance-voltage relationships for WT and variant channels. (C) Steady-state voltage dependence of inactivation for WT (n = 10) and variant channels (n = 10). In (B) and (C) lines represent average fits of the data with Boltzmann functions. (D) Averaged TTX-sensitive persistent currents measured at -30mV during a 200 ms depolarization and normalized to peak current (n = 7). The inset represents the same data plotted on an expanded vertical scale. Biophysical fit parameters for all experiments are provided in Table 2, and magnitude of persistent current is provided in Table 1.

Finally, we determined the functional consequences of L409P/R558 in fetal $Na_V1.5$. Compared with biophysical properties of this mutation in the adult isoform, L409P/R558 in fetal $Na_V1.5$ exhibited greater depolarizing shifts in steady-state inactivation and in conductance-voltage relationships (Figure 14; Table 2), and greater persistent current (Figure 14; Table 1). Superimposed, normalized current traces (Figure 14D) and quantitative analysis also illustrate slower activation rise time and slower kinetics of inactivation for fetal $Na_V1.5$-L409P/R558 as compared with WT fetal $Na_V1.5$, functional defects that were not as prominent in the adult splice isoform (Figure 15). Collectively, these observations indicate that both *SCN5A* alleles carried by this fetus, one with R558 alone and the other with L409P/R558, cause much more profound sodium channel dysfunction in the background of fetal $Na_V1.5$ splice isoform providing a plausible explanation for severe presentation of intrauterine LQTS.

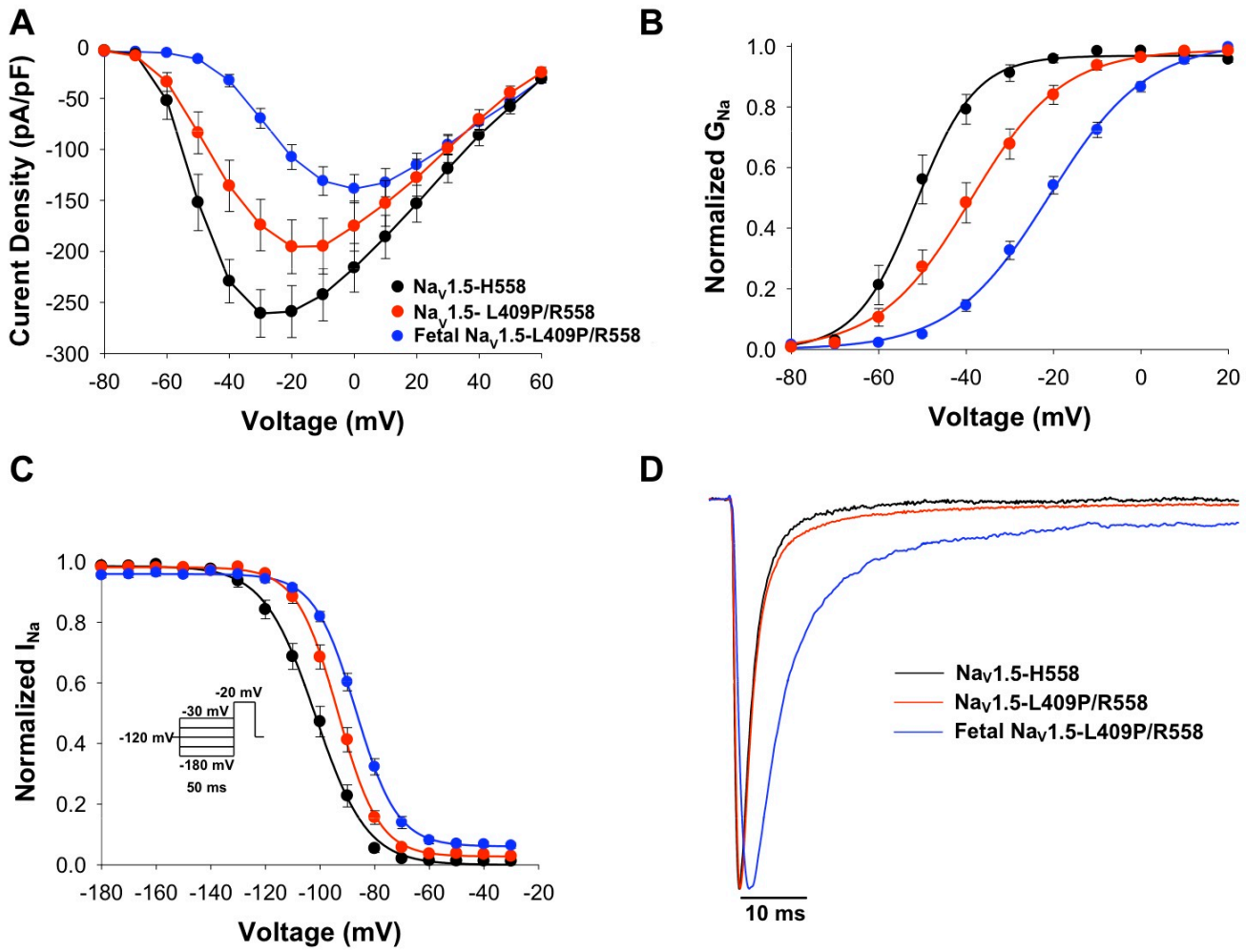

Figure 14: Expression in fetal Na$_V$1.5 potentiates effect of *SCN5A*-L409P/R558.

(A) Current density-voltage relationships comparing WT and mutant channels expressed in either adult or fetal Na$_V$1.5 channels (voltage protocol same as in Figure 8A; n = 10 for all groups). (B) Conductance-voltage relationships for WT and mutant channels. (C) Steady-state voltage dependence of inactivation for WT and mutant channels (n = 10-12). In (B) and (C) lines represent average fits of the data with Boltzmann functions. (D) Representative TTX-sensitive persistent currents measured at -30mV during a 200 ms depolarization and normalized to peak current. Biophysical fit parameters for all experiments are provided in Table 2 and magnitude of persistent current is provided in Table 1.

Table 1: Persistent TTX- sensitive sodium current measured at -30mV.

	Persistent Current (% of peak I_{Na})	Current Density (pA/pF)	n
$Na_v1.5$-H558	0.2 ± 0.4	0.4 ± 0.1	8
$Na_v1.5$-R558	0.4 + 0.2	0.4 ± 0.2	3
$Na_v1.5$- L409P/R558	1.4 ± 0.2 [b]	2.5 ± 0.9 [a]	7
Fetal $Na_v1.5$-H558	0.7 + 0.3 [a]	1.3 ± 0.9	4
Fetal $Na_v1.5$-R558	3.7 ± 0.9 [bc]	3.5 ± 1.2 [a]	7
Fetal $Na_v1.5$-L409P/R558	11.1 ± 1.5 [bc]	4.4 ± 1.2 [a]	10

[a] P < 0.05 compared to Adult $Na_v1.5$-H558 [b] P < 0.005 compared to Adult $Na_v1.5$-H558
[c] P < 0.05 compared to Fetal $Na_v1.5$ -H558 [d] P < 0.005 compared to Fetal $Na_v1.5$-H558
ANOVA and Dunn's Test

Table 2: Biophysical parameters for WT, variant, and mutant $Na_V1.5$ channels expressed in either adult or fetal splice isoform.

	Voltage-Dependence of Activation			Steady-State Availability			Recovery From Inactivation	
	$V_{1/2}$ (mV)	k (mV)	n	$V_{1/2}$ (mV)	k (mV)	n	τ (msec)	n
$Na_v1.5$-H558	-50.9 ± 2.3	5.7 ± 0.7	10	-102.0 + 2.0	-9.0 + 0.3	10	6.0 ± 0.4	10
$Na_v1.5$-R558	-45.8 ± 2.9	6.5 ± 0.8	5	-102.8 + 1.8	-9.2 + 0.8	5	13.4 ± 2.0 [a]	4
$Na_v1.5$-L409P/R558	-39.7 ± 2.9 [a]	8.9 ± 0.3 [b]	10	-93.9 + 1.6 [b]	-7.6 + 0.2 [b]	11	1.4 ± 0.1 [a]	8
Fetal $Na_v1.5$-H558	-38.2 + 1.5 [b]	6.9 + 0.4	11	-96.9 + 1.8	-8.9 +0.3	10	6.8 ± 0.3	7
Fetal $Na_v1.5$-R558	-32.9 ± 2.1 [b]	10.0 ± 0.5 [bc]	14	-98.5 + 2.7	-10.4 + 0.3 [ac]	10	8.8 ± 3.0	6
Fetal $Na_v1.5$-L409P/R558	-20.8 ± 1.5 [bce]	11.0 ± 0.5 [bce]	10	-85.3 + 1.1 [bce]	-9.0 + 0.5 [d]	12	1.2 ± 0.1 [cd]	4

[a] P < 0.05 compared to Adult $Na_v1.5$-H558 [b] P < 0.005 compared to Adult $Na_v1.5$-H558
[c] P < 0.05 compared to Fetal $Na_v1.5$ -H558 [d] P < 0.05 compared to Fetal $Na_v1.5$-R558
[e] P < 0.005 compared to Fetal $Na_v1.5$-R558 ANOVA and Dunn's Test

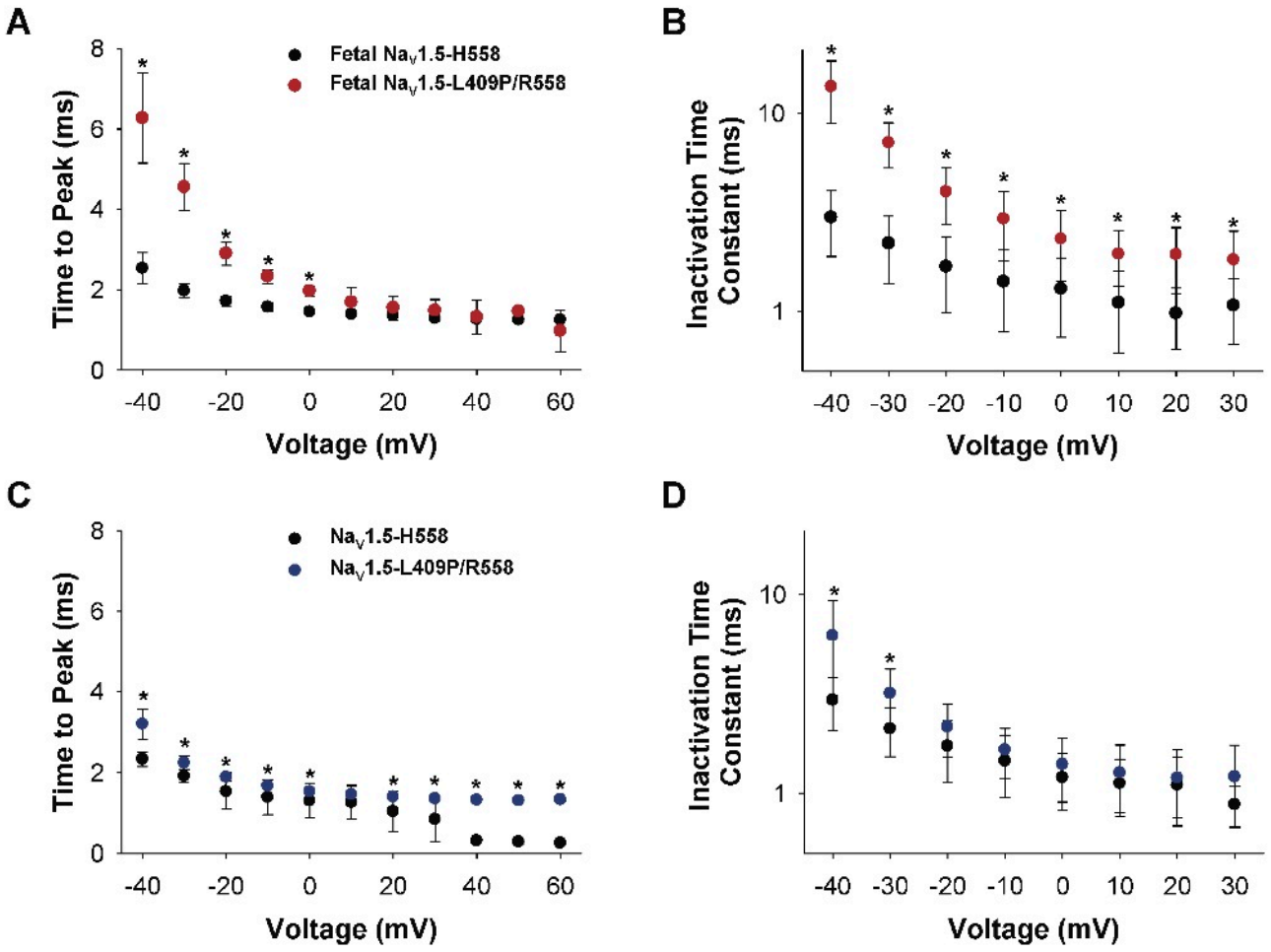

Figure 15: Activation and inactivation kinetics for WT and mutant channels.

(A) Time to peak current activation is compared for WT (fetal $Na_V1.5$-H558; n = 7) and mutant (fetal $Na_V1.5$-L409P/R558; n = 6) channels expressed in the fetal splice isoform (exon 6A). (B) Time constants of inactivation for WT (n = 7) and mutant (n = 9) fetal $Na_V1.5$ channels. Values were derived from single exponential fits to the decay phase of the current. (C) Time to peak current activation is compared for WT ($Na_V1.5$-H558; n = 8) and mutant ($Na_V1.5$-L409P/R558; n = 7) channels expressed in the adult splice isoform (exon 6). (D) Time constants of inactivation for WT (n = 10) and mutant (n = 10) adult $Na_V1.5$ splice variant. Values were derived from single exponential fits to the decay phase of the current. In each panel, asterisks mark values statistically different at the $p < 0.05$ level (Student t-test) for a given voltage.

Ultra-fast recovery from inactivation and repeated stimulation of mutant adult and fetal $Na_V1.5$

We initially observed that L409P/R558 expressed in both the canonical adult and fetal $Na_V1.5$ backgrounds elicited an ultra-fast recovery from inactivation at -120 mV. A faster recovery from inactivation compared to WT channels is consistent with a destabilization of inactivation. Therefore we investigated whether L409P/R558 would also exhibit ultra-fast recovery when channels were inactivated at more extreme voltages of -140 or -90 mV using a similar 50ms recovery protocol as shown in the Figure 12E inset. $Na_V1.5$-L409P/R558 channels exhibited an ultra-fast recovery from inactivation at -90 mV (17.4 ± 3.4 ms) compared to WT $Na_V1.5$ (68.7 ± 3.2 ms) but not at -140 mV (Figure 16A). Fetal $Na_V1.5$-L409P/R558 channels exhibited a significantly faster recovery from inactivation with smaller time constants at -140 mV (1.3 ± 0.2 ms) and -90 mV (9.0 ± 0.6 ms) compared to WT fetal $Na_V1.5$ (-140 mV: 3.3 ± 0.4 ms, -90 mV: 49.7 ± 5.9 ms) (Figure 16B). These results demonstrate that L409P/R558 channels exhibit an ultra-rapid recovery mechanism compared to WT channels.

We also investigated whether repeated stimulation of mutant sodium channels would result in attenuated or enhanced loss of channel availability compared to WT channels. WT and mutant sodium channels were pulsed at a frequency of 1 or 2 Hz and currents were normalized to the first pulse. It is important to note that the frequency of 2 Hz is similar to the fetal heart rate (~120 bpm) while a frequency of 1 Hz is similar to an adult heart rate (~60 bpm).[106,107] $Na_V1.5$-L409P/R558 and fetal $Na_V1.5$-L409P/R558 both exhibited a significantly attenuated loss of channel availability at both frequencies of 1 and 2 Hz (Figure 17).

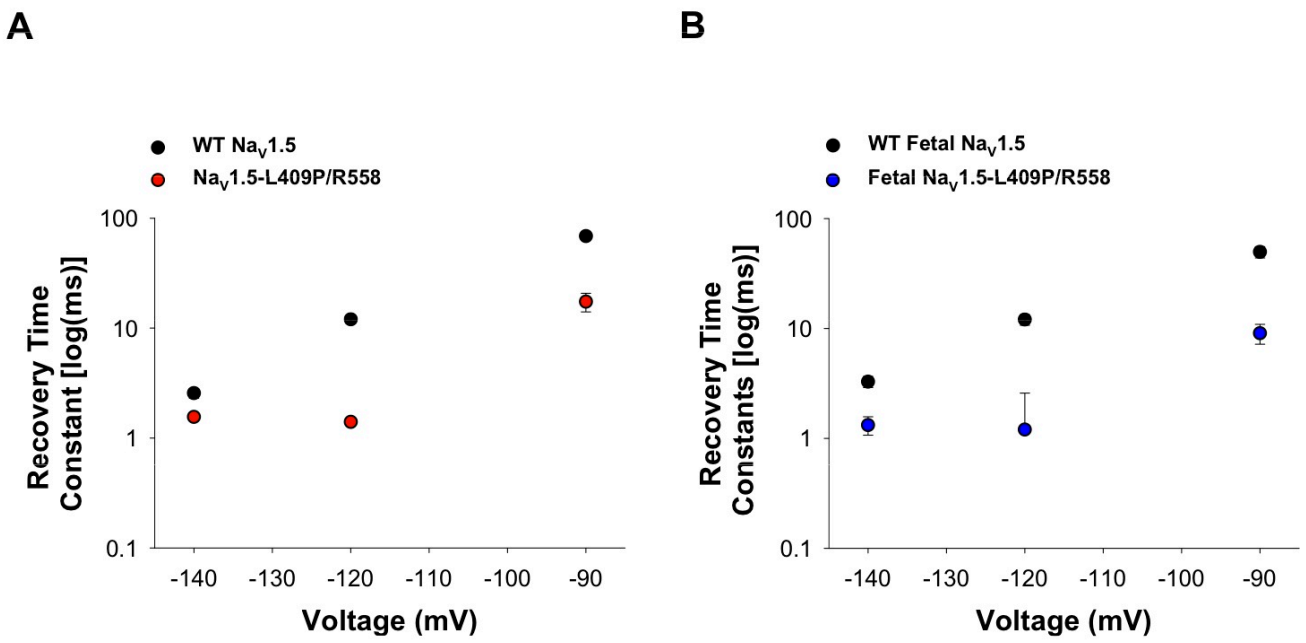

Figure 16: L409P/R558 channels exhibit ultra-fast recovery from inactivation.

(A) Recovery time constants at -140, -120, and -90 mV of WT $Na_V1.5$ (n = 5) and $Na_V1.5$-L409P/R558 channels (n = 5). (B) Recovery time constants of WT fetal $Na_V1.5$ (n = 5) and fetal $Na_V1.5$-L409P/R558 channels (n = 5). Recovery time constants are shown on a common log scale. See Table 2 for recovery time constant values at -120 mV. Also see Chapter III, Table 5 for statistical comparisons. Statistical significance was assumed for $P < 0.05$.

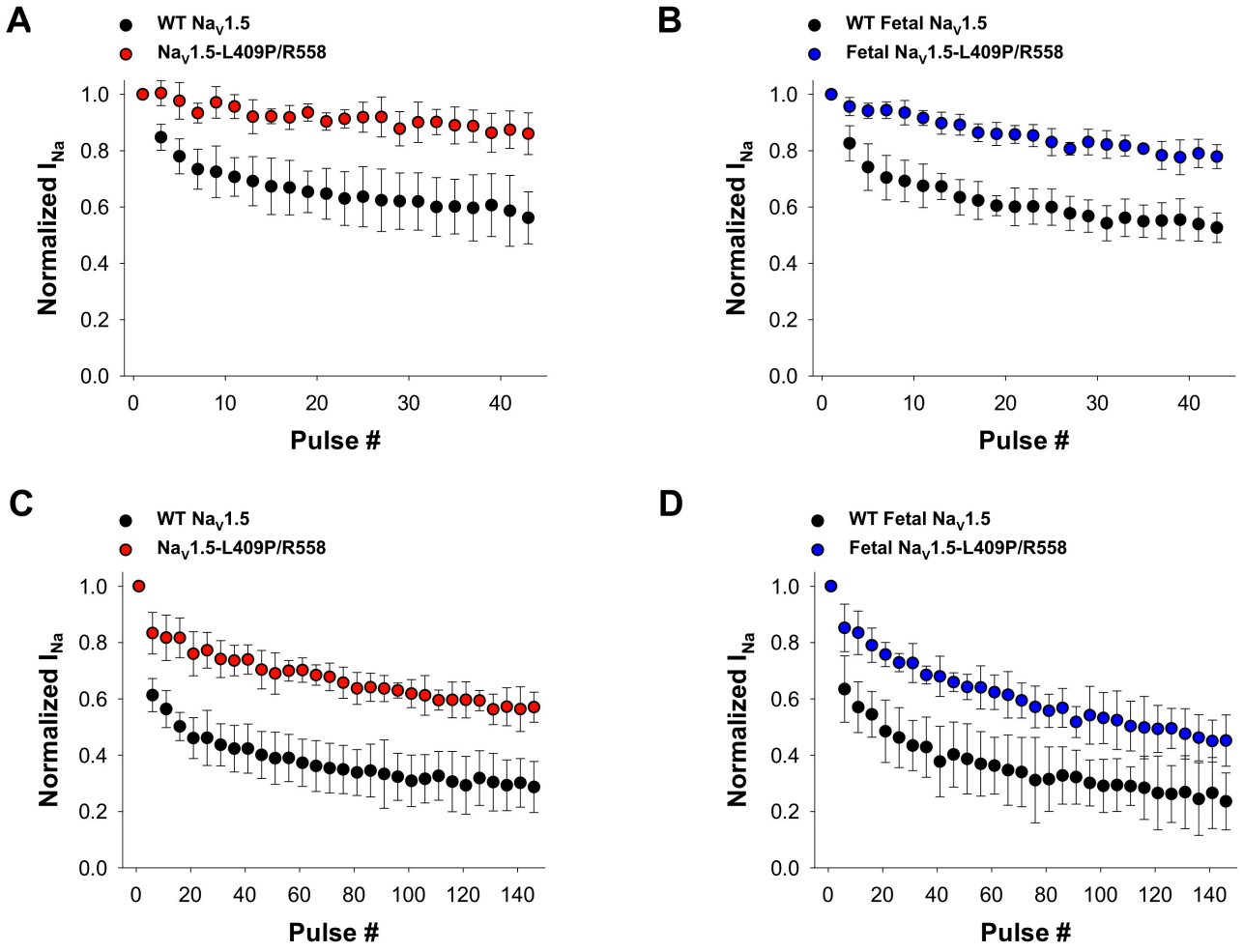

Figure 17: L409P/R558 channels have attenuated loss of channel availability upon repeated stimulation at frequencies of 1 and 2 Hz.

(A) Normalized current of WT Na$_V$1.5 (n = 6) and Na$_V$1.5-L409P/R558 (n = 5) during 1 Hz pulse trains. (B) Normalized current of WT fetal Na$_V$1.5 (n = 5) and fetal Na$_V$1.5-L409P/R558 (n = 5) during 1 Hz pulse trains. (C) Normalized current of WT Na$_V$1.5 (n = 6) and Na$_V$1.5-L409P/R558 (n = 5) during 1 Hz pulse trains. (D) Normalized current of WT fetal Na$_V$1.5 (n = 5) and fetal Na$_V$1.5-L409P/R558 (n = 5) during 2 Hz pulse trains. All data points shown are at every 5 pulses. Pulses were 50 ms long with a holding potential of -90 mV.

This suggests that mutant L409P/R558 channels exhibit impaired inactivation in response to repeat stimulation compared to WT. This observation is consistent with previous findings that L409P/R558 channels exhibit an ultra-fast recovery from inactivation and altered inactivation kinetics.

Lidocaine pharmacology of WT fetal $Na_V1.5$ and fetal $Na_V1.5$-L409P/R558 channels

Lidocaine is a sodium channel blocker often administered IV to pregnant women whose fetuses exhibit ventricular rhythm disturbances including those with suspected fetal LQTS. The efficacy of this treatment strategy is variable and may depend on the genotype of the fetus. Other factors such as developmentally regulated *SCN5A* alternative splicing may also be critical. However, the effects of lidocaine on the fetal isoform of $Na_V1.5$ are unknown. We hypothesized that certain *SCN5A* mutations such as L409P/R558 associated with severe perinatal LQTS will exhibit variable responses to lidocaine when expressed in either fetal or adult $Na_V1.5$ channel isoforms.

We performed pulse train experiments in heterologous cells expressing WT or L409P/R558 fetal sodium channels in the absence and presence of 100 μM lidocaine to determine if the fetal $Na_V1.5$-L409P/R558 exhibited altered pharmacology compared to WT channels. In the presence of lidocaine, WT fetal channels exhibited use-dependent loss of channel availability compared WT channels in the absence of lidocaine at 2 and 5 Hz (Figure 18). However, fetal $Na_V1.5$-L409P/R558 channels in the presence of lidocaine were resistant to lidocaine block at 2 and 5 Hz (Figure 18A & B).

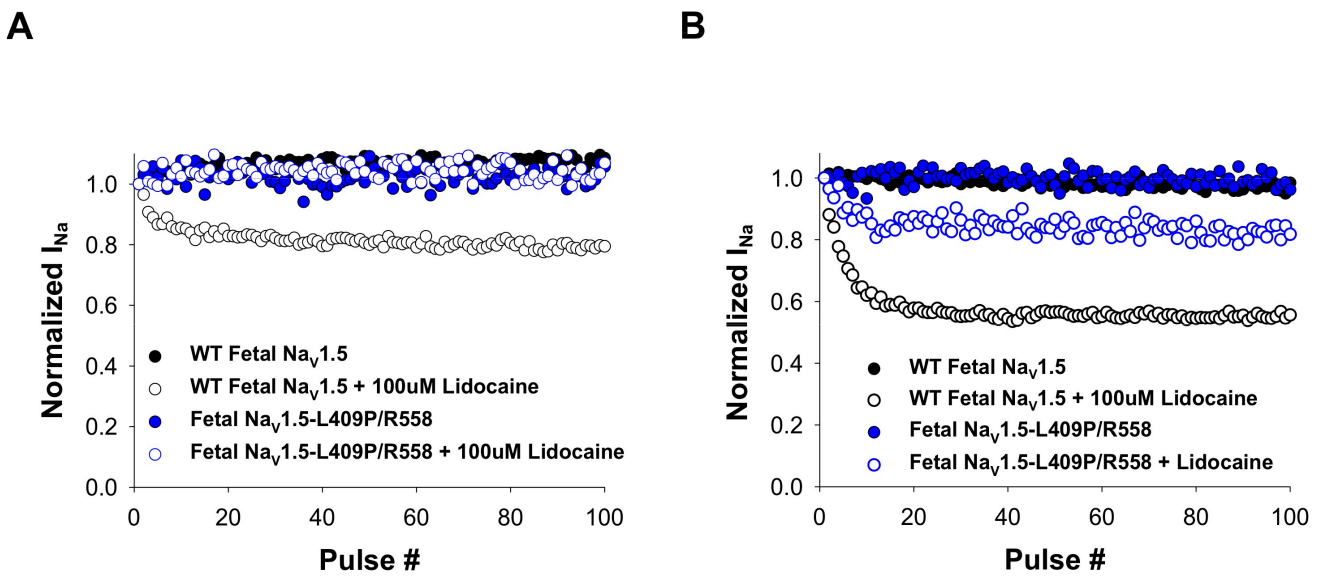

Figure 18: Fetal $Na_V1.5$-L409P/R558 is resistant to lidocaine upon repeated stimulation.

(A) Normalized current of WT fetal $Na_V1.5$ (n = 1) and fetal $Na_V1.5$-L409P/R558 (n = 2) in the absence of lidocaine or WT fetal $Na_V1.5$ (n = 1), fetal $Na_V1.5$-L409P/R558 in the presence of lidocaine (n = 2) during 2 Hz pulse trains. (B) Normalized current of WT fetal $Na_V1.5$ (n = 1) and fetal $Na_V1.5$-L409P/R558 (n = 2) in the absence of lidocaine, or WT fetal $Na_V1.5$ (n = 1), fetal $Na_V1.5$-L409P/R558 (n = 2) in the presence of lidocaine during 5 Hz pulse trains. These experiments were not performed with the adult $Na_V1.5$. Pulses were 50 ms long with a holding potential of -120 mV (see Methods).

This suggests that some *SCN5A* mutations such as L409P/R558 that are associated with fetal LQTS may be resistant to lidocaine treatment.

Discussion

The novel *SCN5A* mutation we identified in this study encodes a dysfunctional cardiac sodium channel, but the degree of channel dysfunction determined in the context of the canonical adult $Na_V1.5$ splice product did not explain the unusual severity and early onset of fetal arrhythmia. We considered that using the adult $Na_V1.5$ splice isoform to evaluate the functional consequences of a mutation associated with an intrauterine arrhythmia might be misleading if another molecular form of the channel was predominant in fetal heart. *SCN5A* undergoes alternative mRNA splicing to generate multiple isoforms of the protein.[88]

Although many described splicing events have uncertain physiological significance, at least one major alternative splicing event could have implications for understanding severe fetal LQTS. Specifically, a developmentally regulated *SCN5A* splicing event involving selection between two alternative forms of exon 6 generates $Na_V1.5$ isoforms that differ at several amino acid residues within a voltage-sensor domain (D1/S3-S4).[88,105] This alternative $Na_V1.5$ splice variant is strongly expressed in neonatal mouse heart but is down-regulated later in development.[90] Evidence for developmentally regulated expression in humans was not previously demonstrated. Here we show prominent expression of alternatively spliced $Na_V1.5$ mRNA incorporating exon 6A in fetal and infant heart. Previous studies have referred to this product of alternative splicing as a 'neonatal' *SCN5A*,[85,88] but given the high level of expression

we observed in fetal human heart (Figure 11), we suggest that fetal $Na_V1.5$ is a more appropriate designation.

Hence, we investigated the functional consequences of the mutation in the fetal $Na_V1.5$ splice isoform. These experiments indicated that the common variant (R558) and the compound mutant genotype (L409P/R558), the two alleles carried by the proband, each conferred much greater functional defects on fetal $Na_V1.5$ than on adult $Na_V1.5$. In particular, the proportion of persistent current was substantial for channels with L409P/R558 (11% of peak current) as well as with the R558 common variant alone (3.7% of peak current, Table 1), and was also abnormal for mutant adult $Na_V1.5$. Therefore, this fetus expressed mostly dysfunctional *SCN5A* alleles at the time of the presenting arrhythmia syndrome. However we cannot fully explain why the common variant alone does not result in a higher prevalence of fetal LQTS or SIDS.

Previous studies investigating the effects of R558 on sodium channel function have shown that the common variant may modulate the biophysical defects of a rare variant associated with SIDS such as P2006A.[108] It has also been shown that small peptides, spanning the H558R polymorphism, are sufficient to restore trafficking defects of Brugada syndrome-associated *SCN5A* mutations.[109] However, another study investigating the effects of R558 discovered that the variant expressed in combination with a mutation associated with LQTS, *SCN5A*-A572D, evokes an increase in persistent sodium current compared with *SCN5A*-A572D alone.[71] One possibility is that the position of the mutation (e.g. domain I) in combination with the R558 may be an important factor in determining whether the common variant will result in a pathogenic effect on $Na_V1.5$. Additionally, these studies highlight the

importance of investigating the effects of R558 on other *SCN5A* mutations associated with severe cardiac arrhythmias that occur during early life.

In addition to our previous findings, we also demonstrated that L409P/R558 channels exhibited an ultra-fast recovery from inactivation at -140, -120, and -90 mV. Fetal $Na_V1.5$-L409P/R558 exhibited an even faster recovery than L409P/R558 in the adult background suggesting a more severe destabilization of the inactivated state. Furthermore, L409P/R558 channels exhibited an attenuated loss of channel availability suggesting mutant $Na_V1.5$ channels may not fully inactivate during periods of frequent stimulation. Sodium channels with an ultra-rapid recovery mechanism may prime the cardiomyocyte for re-activation during ventricular repolarization. Therefore, recovery from inactivation may be an important biophysical property in the fetal heart under pathophysiological conditions such as re-entrant arrhythmias. However, further investigation of the molecular mechanism of mutant fetal $Na_V1.5$ in native cardiomyocytes or induced pluripotent cardiomyocytes (iPS-CMs) is required to determine if ultra-fast recovery from inactivation is pathological.

The profound defects observed for mutant fetal $Na_V1.5$ channels explains both the malignant character of the arrhythmia syndrome and the early onset of this condition in utero. We further speculate that impaired ventricular contractility was also the result of severe sodium channel dysfunction and related to either tachycardia as suggested by fetal Doppler studies (Figure 7) or disturbances in intracellular ionic homeostasis proposed for familial dilated cardiomyopathy associated with *SCN5A* variants.[79]

Another interesting finding of these studies was that mutant fetal $Na_V1.5$ channels are resistant to lidocaine treatment compared to WT when stimulated at 2 Hz and 5 Hz. Although

the sample size is small, the results are profound and suggest that some *SCN5A* mutations may be resistant to the current method of treatment for fetal LQTS. Further investigation is required to determine if the fetal $Na_V1.5$ exhibits differential pharmacological properties compared to adult channels and if other *SCN5A* mutations associated with fetal LQTS are also resistant to lidocaine. Specifically, dose-response analyses would provide valuable insight on the pharmacology of WT and mutant fetal $Na_V1.5$.

CONCLUSIONS

In summary, we present a case of fetal LQTS identified early in mid-gestation due to a novel, *de novo SCN5A* mutation. Fetal LQTS may be an under-recognized cause of early fetal hydrops and unexplained fetal loss, and should be considered in the differential diagnosis of the fetus with rapidly progressive heart failure and complex arrhythmia even if family history is negative. The unusual severity and early onset of arrhythmia in this case were explained by profound dysfunction of the mutant sodium channel carried by the fetus that was revealed only by considering the correct molecular context, a fetal-expressed alternatively spliced *SCN5A* transcript. Our findings demonstrate an important contribution of developmentally regulated alternative *SCN5A* splicing to the genetic risk for prenatal life-threatening cardiac arrhythmias. In addition, we show that mutant L409P/R558 fetal sodium channels exhibit resistance to lidocaine treatment, the current therapy for fetal LQTS.

CHAPTER III

Dysfunction of a Fetal-Expressed Sodium Channel Splice Isoform is a Distinguishing Factor for Early Onset Type-3 Long QT-Syndrome

INTRODUCTION

Mutations in the gene *SCN5A* encoding the cardiac voltage-gated sodium channel ($Na_V1.5$) can result in severe life-threatening cardiac arrhythmias such as the long QT syndrome (LQTS). Severe arrhythmias such as LQTS typically present in childhood or early adulthood but in some extreme cases may present during the perinatal period (fetal – infancy).[45–47] Although many *SCN5A* mutations associated with SIDS,[45,46,58] neonatal LQTS,[48,49,110] and fetal arrhythmias[52,53,111,54,112] have been investigated, the molecular basis for arrhythmia susceptibility in early developmental stages remains unclear.

The major biophysical defect of $Na_V1.5$ that contributes to type-3 LQTS (LQT3) is persistent sodium current that is typically due to impaired inactivation of the channels.[38] Persistent sodium current leads to a delayed ventricular repolarization and torsades de pointes.[44] We previously reported that developmentally regulated alternative splicing of *SCN5A* contributes to the genetic risk for prenatal life-threatening cardiac arrhythmias. We have demonstrated that a *SCN5A* mutation (L409P) associated with fetal LQTS exhibits more severe functional consequences when expressed in the context of a fetal-expressed

alternative splice variant of $Na_V1.5$.[52] Specifically, we have shown that L409P exhibited a greater persistent sodium current, impaired inactivation, and ultra-fast recovery kinetics in fetal $Na_V1.5$ compared to wild-type (WT) channels (Chapter II).[113]

Therefore, we hypothesized that other *SCN5A* mutations associated with perinatal forms of LQTS would also exhibit more severe functional consequences such as a greater persistent sodium current when expressed in fetal $Na_V1.5$. Here we demonstrate that one of three early-onset LQT3 mutations studied, A1330D, exhibits more severe functional consequences when expressed in fetal $Na_V1.5$ such as a greater persistent sodium current, a greater late current density, ultra-rapid recovery from inactivation, and shifts in the voltage-dependence of inactivation compared to WT channels. We also demonstrate that two other early-onset LQT3 mutations, F1473C and R1623Q, exhibit similar functional effects when expressed in the fetal splice variant as in the adult isoform of $Na_V1.5$.

Additionally, we considered the possibility that later onset (childhood-adulthood) LQT3 mutations such as delKPQ may exhibit 'protective' or masked effects when expressed in the fetal splice variant. Here we show that delKPQ exhibits a loss of function when expressed in fetal $Na_V1.5$ with a dramatic reduction in current density and late current density compared to the mutation expressed in the adult background. Our findings implicate dysfunction of a fetal-expressed sodium channel splice isoform as a distinguishing factor for the early onset of LQT3 compared to later onset arrhythmias. In clinical settings, these results may have relevance to sudden cardiac death in the earliest stages of life.

METHODS

Mutagenesis and heterologous expression of human cardiac sodium channel

Plasmids encoding recombinant human cardiac sodium channel isoforms ($Na_V1.5$) were described previously.[52] Site directed mutagenesis was performed using the QuikChange system (Stratagene) and primer sequences are available upon request. Wild-type (WT) or mutant channel cDNAs (0.5 μg) were transiently transfected into tsA201 cells using FuGene HD (Roche Diagnostics, Indianapolis, IN) combined with a separate plasmid encoding enhanced green fluorescent protein (pIRES2-EGFP, 0.5 μg). Transiently transfected cells were incubated for 48 hours at 37°C prior to electrophysiological measurements. Cells exhibiting green fluorescence were selected for patch-clamp recordings.

*In vitro el*ectrophysiology

Sodium currents were recorded at room temperature using the whole-cell patch clamp technique as described previously.[47,58] The extracellular bath solution contained the following (in mM): 140 NaCl, 4 KCl, 1.8 $CaCl_2$, 1 $MgCl_2$, 10 HEPES, and 10 glucose, pH 7.35 (adjusted with NaOH). The intracellular pipette solution contained the following (in mM): 10 NaF, 105 CsF, 20 CsCl, 2 EGTA, 10 HEPES, 10 glucose, pH 7.35 (adjusted with CsOH). Data were acquired with an Axopatch 200B patch-clamp amplifier and pClamp 10.2 software (Molecular Devices, Inc., Sunnyvale, CA). Electrode resistance ranged from 1.0 to 1.5 MΩ. Pipette resistance and junction potential were corrected and whole-cell capacitance and series resistance were 90% compensated (voltage error ≤ 2 mV). Cells with <500pA of current were

not included in the data analysis. Voltage-clamp pulse protocols assessing channel activation, steady-state inactivation, and recovery from inactivation are depicted in figure insets. TTX-sensitive persistent current was determined with a 200-ms depolarization to −30 mV as the average current recorded between 190 and 200 ms and reported as a percentage of peak current following digital subtraction of currents recorded in the presence and absence of 30 μM tetrodotoxin (Tocris Biosciences, Ellisville, MO). Time constants for recovery from inactivation were determined from single exponential fits. Unless otherwise noted, all fit amplitudes (A) were equal to 1.0 ± 0.1. For pulse train experiments, cells were pulsed at frequencies of 1 or 2 Hz with 400 ms pulses to −20 mV from a holding potential of −90 mV at room temperature. Sodium currents were normalized to the level of current at the first pulse. All data were analyzed with pClamp 10.2 and plotted using SigmaPlot 10.0 (SPSS, Inc, Chicago, IL) software. Results are presented as mean ± SEM. Unless otherwise noted, statistical comparisons were made by using one-way ANOVA with Bonferroni correction. Statistical significance was assumed for $p < 0.05$.

RESULTS

We previously demonstrated that a novel *SCN5A* mutation (L409P) associated with an intrauterine presentation of LQTS exhibited a greater degree of dysfunction when expressed in a fetal splice isoform of $Na_V1.5$ (Chapter II). We concluded from these observations that the pathogenesis of certain mutations may be potentiated in the fetal $Na_V1.5$ channel. Here we compared the functional effects of three additional *SCN5A* mutations associated with severe and early-onset LQTS with that of a mutation associated with typical onset LQTS (delKPQ). Additionally, we investigated whether channel dysfunction was potentiated in fetal $Na_V1.5$ as compared with the canonical splice isoform to determine if this was a common mechanism explaining the more severe and early onset nature of LQTS associated with certain *SCN5A* mutations. All mutant channels studied generated sodium currents in transiently transfected tsA201 cells with some notable differences between canonical and fetal $Na_V1.5$ (Figure 19).

Functional consequences of early onset LQT3 mutation A1330D in fetal $Na_V1.5$

Mutation *SCN5A*-A1330D was discovered in an Italian boy with early-onset LQTS. The proband, a Caucasian male, was delivered by Caesarean section at 33 weeks' gestation because of oligohydramnios. Birth weight was 2.3 kg and APGAR score was 9. On the second day of life, he exhibited bradycardia followed by an episode of ventricular fibrillation and he was successfully resuscitated (chest thump, defibrillation). Electrocardiogram revealed a prolonged QTc (500 msec) and 2:1 atrioventricular block. Echocardiography demonstrated normal cardiac anatomy and function. Despite treatment with lidocaine, $MgSO_4$, propranolol

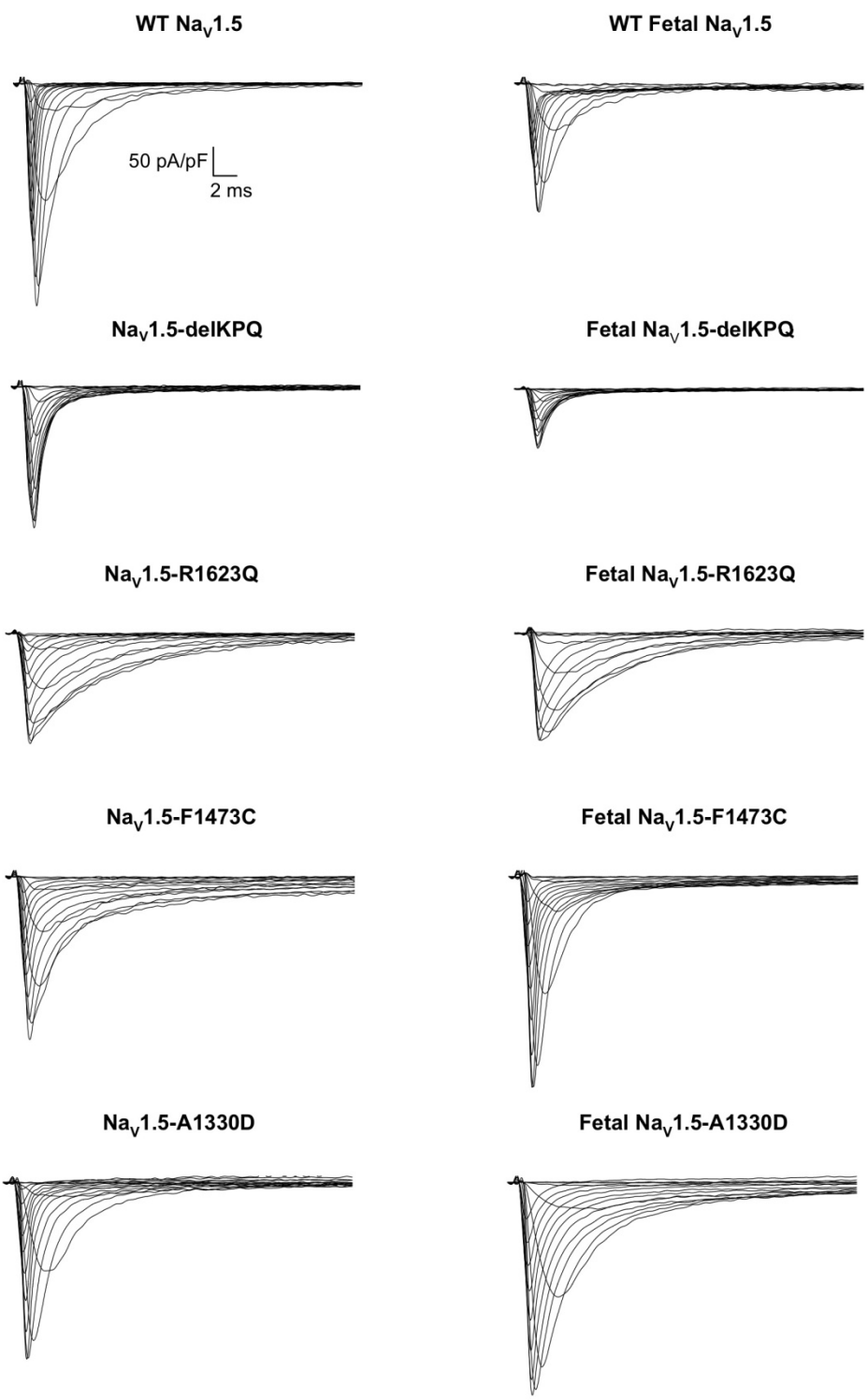

Figure 19: Representative traces of WT and mutant sodium currents.

The left side shows WT and mutant adult $Na_V1.5$ representative traces. The right side shows WT and mutant fetal $Na_V1.5$ representative traces.

and mexiletine, the subject continued to have frequent episodes of ventricular tachycardia, including torsades de pointes and ventricular fibrillation prompting repeated external defibrillations. He died at age 70 days following a final episode of cardiac arrest. Genetic testing revealed a novel *SCN5A* mutation (A1330D) in the proband but not in the parents or two siblings consistent with a *de novo* mutation. This mutation affects the same residue as another *de novo* mutation (A1330P) associated with sudden cardiac death at age 9 weeks.[45]

Mutation *SCN5A*-A1330D has previously been characterized expressed in the canonical adult isoform of $Na_V1.5$ and has been shown to evoke a significant increase in persistent sodium current compared to WT channels that is typical of LQT3 mutations.[62] We determined the functional consequences of A1330D expressed in the fetal splice isoform of $Na_V1.5$ by *in vitro* electrophysiological recording of heterologously expressed recombinant human cardiac sodium channels. We have confirmed that adult $Na_V1.5$-A1330D evokes a 4.5-fold greater level of persistent sodium current measured as a percent of peak current (0.9 ± 0.1%) and a 8.2-fold greater late current density (4.9 ± 0.8 pA/pF) compared to WT $Na_V1.5$. By contrast, when A1330D is expressed in the fetal splice variant, fetal $Na_V1.5$-A1330D evoked a 5.7-fold greater persistent sodium current (1.7 ± 0.2%) and a 14.5-fold greater late current density (5.8 ± 1.2 pA/pF) vs WT fetal $Na_V1.5$ (Figure 20, Table 3). Fetal $Na_V1.5$-A1330D exhibits a significantly larger persistent current and late current density compared to adult $Na_V1.5$-A1330D. Therefore the functional consequences of A1330D expressed in the fetal $Na_V1.5$ are more severe and channel dysfunction is consistent with cardiac arrhythmia predisposition.

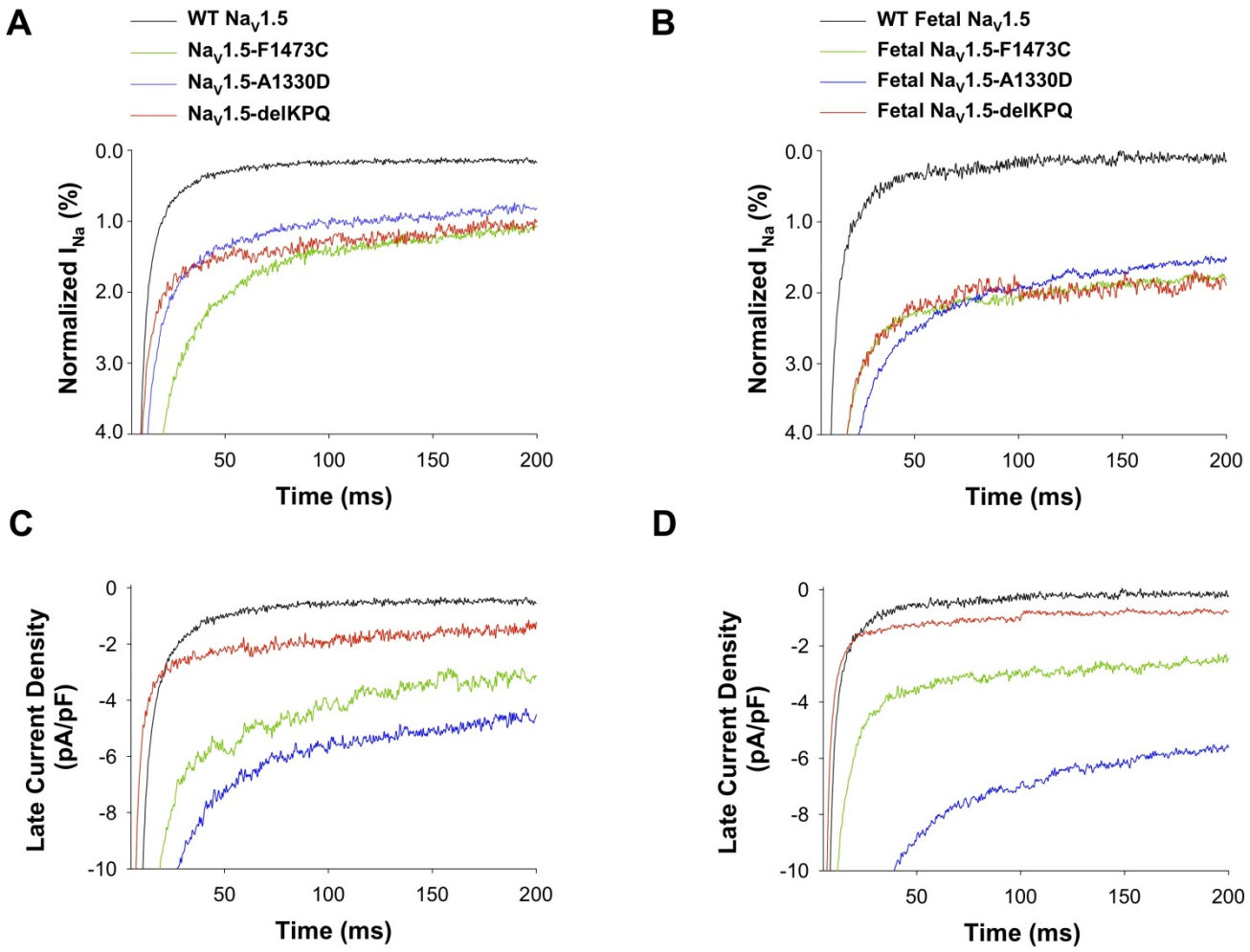

Figure 20: *SCN5A* mutations associated with early and later onset of LQTS exhibit differential late current densities in the canonical and fetal Na$_V$1.5.

(A) Averaged tetrodotoxin (TTX)-sensitive currents for WT and mutant canonical Na$_V$1.5 channels were normalized to the peak current measured at -30 mV during a 200 ms depolarization to illustrate persistent current. (B) Averaged tetrodotoxin (TTX)-sensitive currents for WT and mutant fetal Na$_V$1.5 channels. (C) Averaged tetrodotoxin (TTX)-sensitive late current densities for WT and mutant canonical Na$_V$1.5 channels were normalized to the capacitance measured for each cell at -30 mV during a 200 ms depolarization. (D) Averaged tetrodotoxin (TTX)-sensitive late current densities for WT and mutant fetal Na$_V$1.5 channels. Summary data are provided in Table 3.

Table 3: Persistent TTX- sensitive sodium current measured at -30mV for WT and *SCN5A* mutations

	Persistent Current %	Current Density (pA/pF)	n		Persistent Current %	Current Density (pA/pF)	n
WT $Na_V1.5$	0.2 ± 0.04	0.6 ± 0.1	10	**Fetal $Na_V1.5$**	0.3 ± 0.1	0.4 ± 0.2	10
$Na_V1.5$-L409P/R558	1.4 ± 0.2 [b]	2.5 ± 0.9 [b]	7	**Fetal $Na_V1.5$-L409P/R558**	11.1 ± 1.5 [bde]	4.4 ± 1.2 [bde]	10
$Na_V1.5$-F1473C	1.5 ± 0.3 [b]	3.4 ± 0.5 [b]	7	**Fetal $Na_V1.5$-F1473C**	1.9 ± 0.6 [bd]	3.2 ± 1.0 [bd]	7
$Na_V1.5$-A1330D	0.9 ± 0.1 [b]	4.9 ± 0.8 [b]	8	**Fetal $Na_V1.5$-A1330D**	1.7 ± 0.2 [bde]	5.8 ± 1.2 [bd]	10
$Na_V1.5$-R1623Q	0.5 ± 0.1	0.8 ± 0.1	6	**Fetal $Na_V1.5$-R1623Q**	0.4 ± 0.04	0.9 ± 0.4	8
$Na_V1.5$-delKPQ	1.2 ± 0.2 [b]	1.7 ± 0.4 [b]	6	**Fetal $Na_V1.5$-delKPQ**	2.1 ± 0.4 [bde]	1.0 ± 0.3	9

[a] P< 0.05 compared to WT $Na_V1.5$
[b] P < 0.01 compared to WT $Na_V1.5$
[c] P< 0.05 compared to WT Fetal $Na_V1.5$
[d] P < 0.01 compared to WT Fetal $Na_V1.5$
[e] P < 0.05 compared to $Na_V1.5$-mutant
(One Way ANOVA & Bonferroni)

We also compared current density, voltage-dependence of activation, and inactivation of A1330D expressed in the adult and fetal $Na_V1.5$ (Figure 21, Table 4). Compared to WT channels, we observed that fetal $Na_V1.5$-A1330D exhibited a significant +14 mV shift in the $V_{1/2}$ of the voltage-dependence of inactivation (Figure 21C) and significantly slower inactivation kinetics vs WT channels (Figure 22). No significant effects on current density or voltage-dependence of activation were observed (Figure 21A & B).

We also measured recovery from inactivation of WT and A1330D channels. Adult $Na_V1.5$-A1330D exhibits a significantly faster recovery from inactivation compared to WT channels with 22% recovery at 1 ms. However, A1330D expressed in fetal $Na_V1.5$ also resulted in ultra-rapid recovery from inactivation with 34% recovery at 1 ms vs WT (Figure 21D, Table 4). This is consistent with the observation that A1330D expressed in the fetal splice isoform exhibits destabilization of the inactivated state and resembles functional consequences observed for fetal $Na_V1.5$-L409P (Chapter II).

Functional consequences of early onset LQT3 mutations F1473C and R1623Q in fetal $Na_V1.5$

We have shown previously that two early-onset LQTS-associated *de novo SCN5A* mutations (L409P and A1330D) exhibited more severe functional consequences in the fetal isoform of $Na_V1.5$. Therefore we chose to investigate the effects of two other *SCN5A* mutations, R1623Q and F1473C. The clinical presentations of these two mutations have been previously reported.[48,49,64] The *SCN5A* mutation, R1623Q, was initially discovered in a Japanese infant with severe, sporadic LQTS, but has also been described in other reports.[49,64]

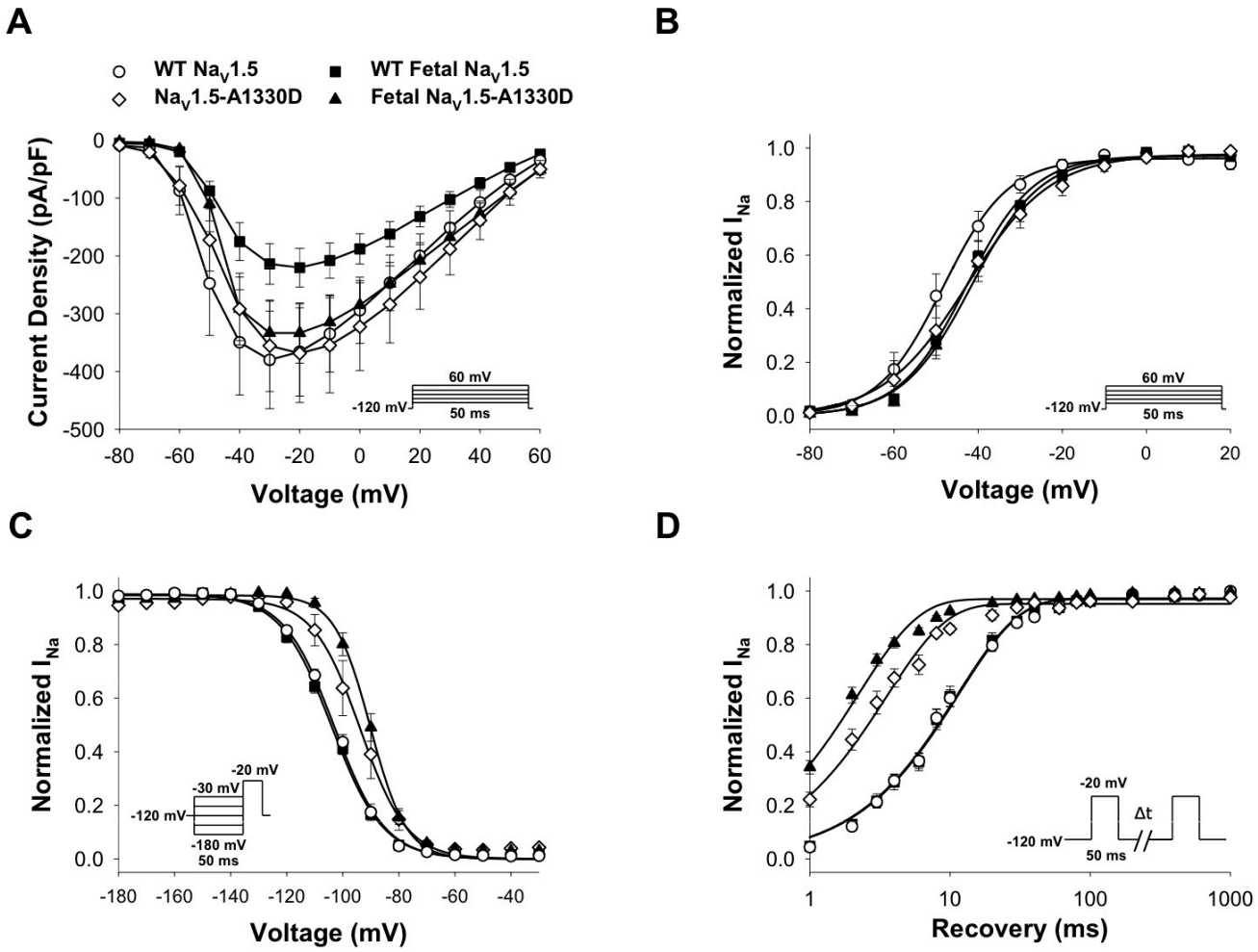

Figure 21: Fetal Na$_V$1.5-A1330D and Na$_V$1.5-A1330D exhibit a more depolarized voltage-dependence of inactivation and a faster recovery from inactivation vs WT.

(A) Current density-voltage relationships recorded from cells expressing either WT Na$_V$1.5 (n = 10), Na$_V$1.5-A1330D (n = 8), WT fetal Na$_V$1.5 (n = 10), or fetal Na$_V$1.5-A1330D (n = 14) channels (voltage protocol in the inset). (B) Conductance-voltage relationships for WT and mutant channels. (C) Steady-state voltage dependence of inactivation for WT and mutant channels (n = 9-12). In (B) and (C) lines represent average fits of the data with Boltzmann functions. (D) Time course of recovery from inactivation recorded using the illustrated voltage protocol. Biophysical fit parameters for all experiments are provided in Table 4.

Table 4: Biophysical parameters for WT and mutant $Na_V1.5$ channels expressed in either adult or fetal splice isoform

	Voltage-Dependence of Activation						
	$V_{1/2}$ (mV)	k (mV)	n		$V_{1/2}$ (mV)	k (mV)	n
WT $Na_V1.5$	-46.2 ± 2.3	6.6 ± 0.5	10	**WT Fetal $Na_V1.5$**	-40.5 ± 1.1 [a]	7.9 ± 0.3 [a]	10
$Na_V1.5$-L409P/R558	-39.7 ± 2.9 [a]	8.9 ± 0.3 [b]	10	**Fetal $Na_V1.5$-L409P/R558**	-20.8 ± 1.5 [bde]	11.0 ± 0.5 [bde]	10
$Na_V1.5$-R1623Q	-44.7 ± 1.7	8.0 ± 0.5 [a]	9	**Fetal $Na_V1.5$-R1623Q**	-41.0 ± 2.7	7.6 ± 0.5 [a]	10
$Na_V1.5$-F1473C	-33.8 ± 3.2 [b]	9.9 ± 0.7 [b]	6	**Fetal $Na_V1.5$-F1473C**	-33.3 ± 1.2	9.1 ± 0.3 [b]	10
$Na_V1.5$-A1330D	-41.9 ± 3.0	7.9 ± 0.6 [a]	8	**Fetal $Na_V1.5$-A1330D**	-41.0 ± 1.5	7.4 ± 0.6 [a]	14
$Na_V1.5$-delKPQ	-25.1 ± 1.2 [b]	10.9 ± 0.4 [b]	12	**Fetal $Na_V1.5$-delKPQ**	-22.2 ± 1.6 [bd]	11.7 ± 0.2 [bd]	9
	Voltage-Dependence of Inactivation						
	$V_{1/2}$ (mV)	k (mV)	n		$V_{1/2}$ (mV)	k (mV)	n
WT $Na_V1.5$	-102.7 ± 1.1	-8.5 ± 0.2	12	**WT Fetal $Na_V1.5$**	-104.1 ± 1.0	-9.0 ± 0.2	10
$Na_V1.5$-L409P/R558	-93.9 ± 1.6 [b]	-7.6 ± 0.2	11	**Fetal $Na_V1.5$-L409P/R558**	-85.3 ± 1.1 [bde]	-9.0 ± 0.5	12
$Na_V1.5$-R1623Q	-124.3 ± 1.9 [b]	-11.8 ± 0.9 [b]	9	**Fetal $Na_V1.5$-R1623Q**	-119.7 ± 1.3 [bd]	-11.0 ± 0.4 [bd]	12
$Na_V1.5$-F1473C	-99.0 ± 0.9	-7.9 ± 0.9	6	**Fetal $Na_V1.5$-F1473C**	-99.9 ± 0.9	-6.6 ± 0.2 [bd]	9
$Na_V1.5$-A1330D	-94.6 ± 3.3 [b]	-6.0 ± 0.3 [a]	9	**Fetal $Na_V1.5$-A1330D**	-89.6 ± 1.6 [bd]	-6.0 ± 0.3 [bd]	10
$Na_V1.5$-delKPQ	-116.7 ± 1.4 [b]	-8.3 ± 0.6	9	**Fetal $Na_V1.5$-delKPQ**	-112.8 ± 3.0 [bd]	-10.4 ± 0.8 [bd]	10
	Recovery from Inactivation (-120mV)						
	τ (msec)		n		τ (msec)		n
WT $Na_V1.5$	12.0 ± 1.0		10	**WT Fetal $Na_V1.5$**	12.0 ± 1.4		10
$Na_V1.5$-L409P/R558	1.4 ± 0.1 [b]		8	**Fetal $Na_V1.5$-L409P/R558**	1.2 ± 0.1 [bd]		4
$Na_V1.5$-R1623Q	12.1 ± 1.0		9	**Fetal $Na_V1.5$-R1623Q**	8.3 ± 0.6 [ace]		7
$Na_V1.5$-F1473C	3.0 ± 0.3 [b]		6	**Fetal $Na_V1.5$-F1473C**	3.0 ± 0.2 [bd]		9
$Na_V1.5$-A1330D	3.6 ± 0.4 [b]		7	**Fetal $Na_V1.5$-A1330D**	2.2 ± 0.2 [bd]		7
$Na_V1.5$-delKPQ	6.5 ± 0.4 [b]		11	**Fetal $Na_V1.5$-delKPQ**	10.0 ± 1.4 [e]		8

[a] P< 0.05 compared to WT $Na_V1.5$
[b] P < 0.01 compared to WT $Na_V1.5$
[c] P< 0.05 compared to WT Fetal $Na_V1.5$
[d] P < 0.01 compared to WT Fetal $Na_V1.5$
[e] P < 0.05 compared to $Na_V1.5$-mutant
(One Way ANOVA & Bonferroni)

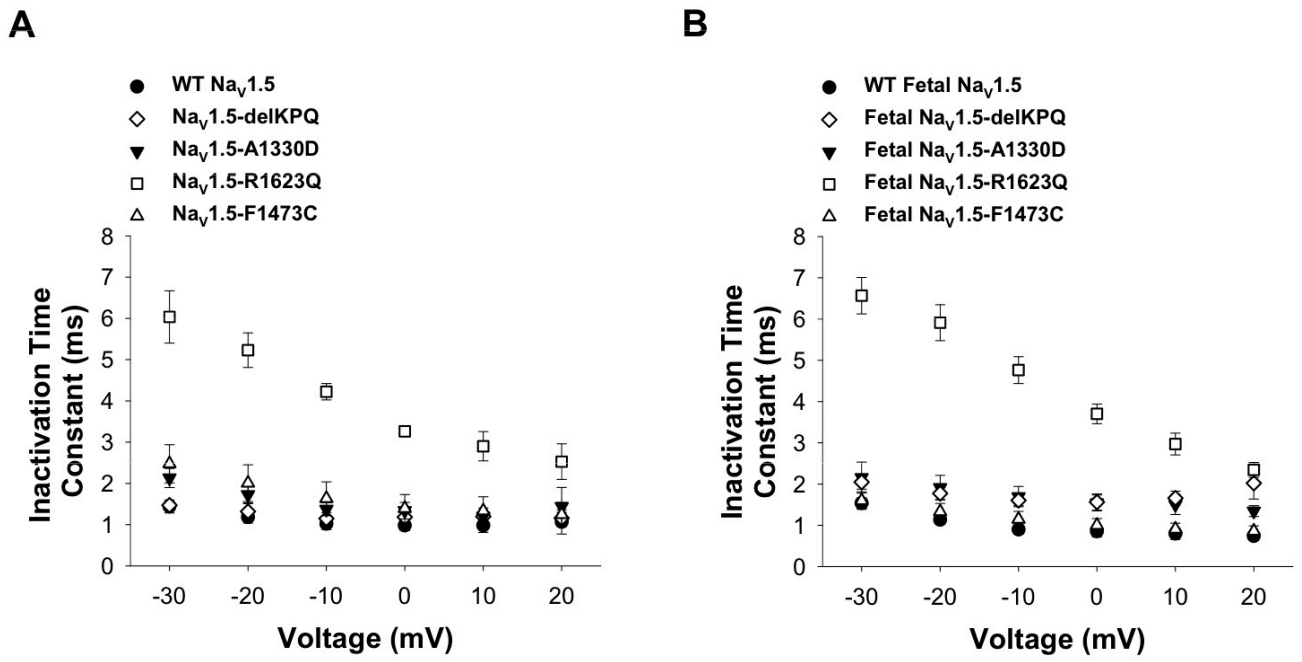

Figure 22: Inactivation kinetics of WT and mutant sodium channels.

(A) Time constants of inactivation for WT and mutant sodium channels in the adult NaV1.5 splice variant (n = 6-8). Na$_V$1.5-R1623Q exhibits significantly slower inactivation vs WT at all voltages (-30 to +20 mV). Na$_V$1.5-A1330D exhibits significantly slower inactivation vs WT at -30 mV. (B) Time constants of inactivation for WT and mutant sodium channels in the fetal NaV1.5 splice variant (n = 6-8). Fetal Na$_V$1.5-R1623Q exhibits significantly slower inactivation vs WT fetal Na$_V$1.5 at all voltages (-30 to +20 mV). Fetal Na$_V$1.5-A1330D exhibits significantly slower inactivation vs WT from -20 to +20 mV. Fetal Na$_V$1.5-delKPQ exhibits significantly slower inactivation vs WT fetal Na$_V$1.5 at all voltages (-30 to +20 mV). Values were derived from single exponential fits to the decay phase of the current. Statistical significance was determined at the $p < 0.05$ level by Student t-test for a given voltage.

Mutation *SCN5A*-F1473C was discovered in a newborn of Italian and Portuguese ancestry who presented with fetal bradycardia followed by extreme QT prolongation, 2:1 AV block, and recurrent episodes of torsades de pointes in early infancy.[48] Mutation *SCN5A*-F1473C has been shown to evoke a significant increase in persistent sodium current compared to WT channels when expressed in the adult isoform of $Na_V1.5$.[48] We have investigated the effects of F1473C on the fetal splice variant of $Na_V1.5$ and compared these effects to F1473C expressed in adult $Na_V1.5$. Adult $Na_V1.5$-F1473C evoked a 7.5-fold greater persistent sodium current (1.5 ± 0.3%) and a 5.7-fold greater late current density (3.4 ± 0.5 pA/pF) vs WT. However, fetal $Na_V1.5$-F1473C also evoked a 6.3-fold increase in the level of persistent sodium current (1.9 ± 0.6%) and an 8-fold greater late current density (3.2 ± 1.0 pA/pF) compared to WT fetal $Na_V1.5$ (Figure 20, Table 3). Therefore the functional consequences F1473C in the fetal splice variant are similar to those observed in the adult background.

We also compared current density, voltage-dependence of activation, inactivation, and recovery from inactivation of F1473C expressed in the adult and fetal $Na_V1.5$ (Figure 23, Table 4). Fetal $Na_V1.5$-F1473C significantly shifted the $V_{1/2}$ of voltage-dependence of activation +8 mV compared to WT fetal $Na_V1.5$. No significant effects on current density, voltage-dependence of inactivation, or inactivation kinetics were observed (Figure 23A & 3C, Figure 22, Table 4). Furthermore, both adult and fetal $Na_V1.5$-F1473C exhibited a significantly faster recovery from inactivation with 23% recovery at 1 ms compared to WT channels (Figure 23D, Table 4). Here we have shown that *SCN5A*-F1473C has the same functional effects when expressed in either the adult or fetal isoform of $Na_V1.5$.

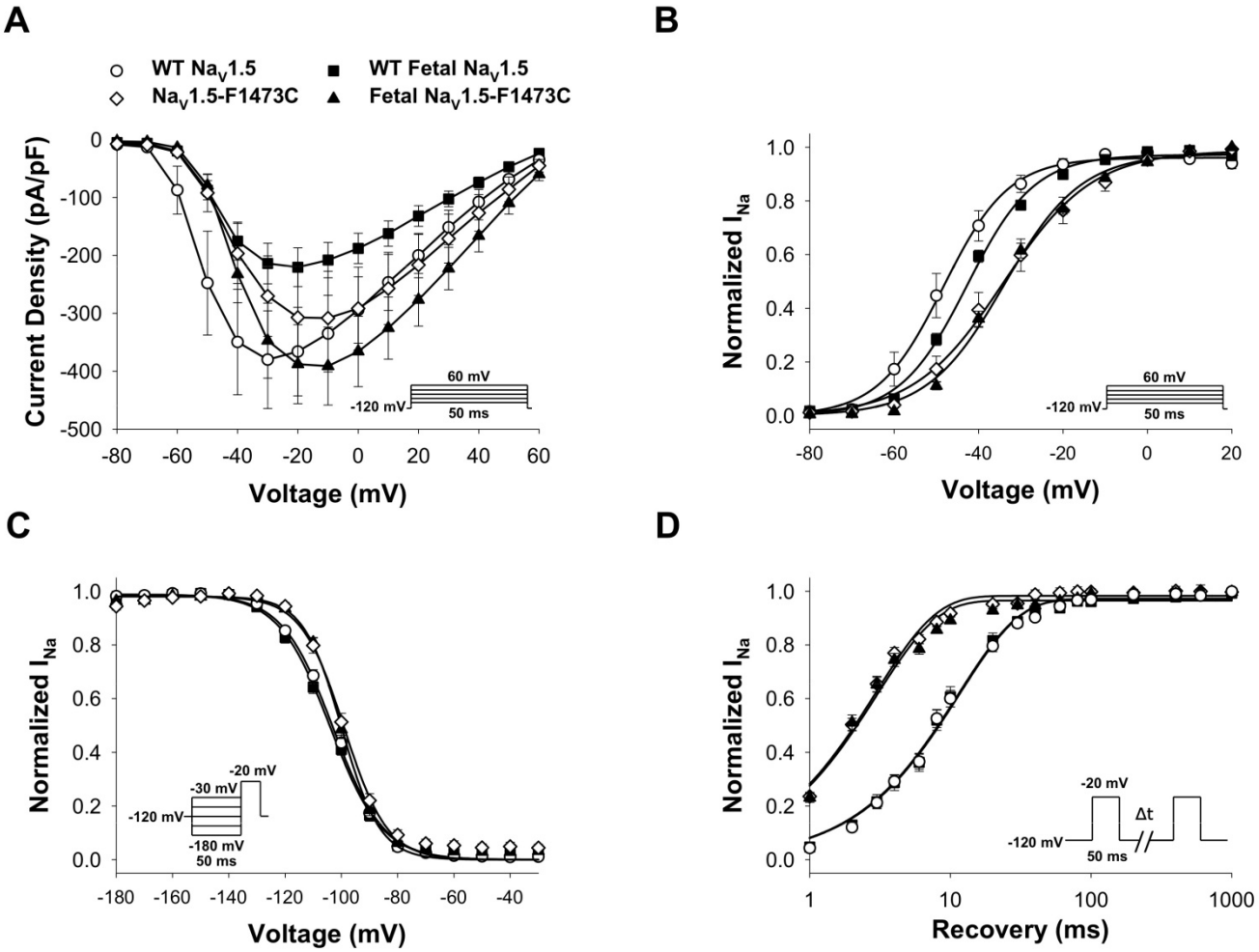

Figure 23: Fetal Na$_V$1.5-F1473C and Na$_V$1.5-F1473C exhibit a more depolarized voltage-dependence of activation and a faster recovery from inactivation vs WT.

(A) Current density-voltage relationships recorded from cells expressing either WT Na$_V$1.5 (n = 10), Na$_V$1.5-F1473C (n = 6), WT fetal Na$_V$1.5 (n = 10), or fetal Na$_V$1.5-F1473C (n = 10) channels (voltage protocol in the inset). (B) Conductance-voltage relationships for WT and mutant channels. (C) Steady-state voltage dependence of inactivation for WT and mutant channels (n = 6-12). In (B) and (C) lines represent average fits of the data with Boltzmann functions. (D) Time course of recovery from inactivation recorded using the illustrated voltage protocol. Biophysical fit parameters for all experiments are provided in Table 4. All wild-type data is the same as in Figure 21.

Additionally, we compared the functional effects of *SCN5A*-R1623Q expressed in canonical and fetal $Na_V1.5$ (Figure 24). Previous reports have shown that $Na_V1.5$-R1623Q does not evoke a significant increase in persistent current typical of most LQT3 mutations. Rather, $Na_V1.5$-R1623Q exhibits slowed activation and inactivation kinetics.[64] We have confirmed these observations in the adult isoform. However, fetal $Na_V1.5$-R1623Q also exhibited significantly slower activation rise times and significantly slower inactivation kinetics vs WT fetal channels. Although not statistically significant, fetal $Na_V1.5$-R1623Q exhibited even slower activation rise times and inactivation kinetics compared to R1623Q expressed in the adult isoform of $Na_V1.5$ (Figure 22 & 25).

We also compared current density, voltage-dependence of activation, inactivation, and recovery from inactivation of R1623Q expressed in the adult and fetal $Na_V1.5$. Fetal $Na_V1.5$-R1623Q exhibited a -15 mV shift in the $V_{1/2}$ of voltage-dependence of inactivation vs WT (Figure 24C, Table 4). Fetal $Na_V1.5$-R1623Q exhibits a significantly faster recovery from inactivation compared to WT and canonical $Na_V1.5$ mutant channels (Figure 24D, Table 4). However, this effect was not observed for adult $Na_V1.5$-R1623Q and was not as ultra-rapid as the other early-onset LQT3 mutations. No significant effects on current density or voltage-dependence of activation were observed (Figure 24A & B). Mutation *SCN5A*-R1623Q also exhibited similar functional effects when expressed in either isoform of $Na_V1.5$.

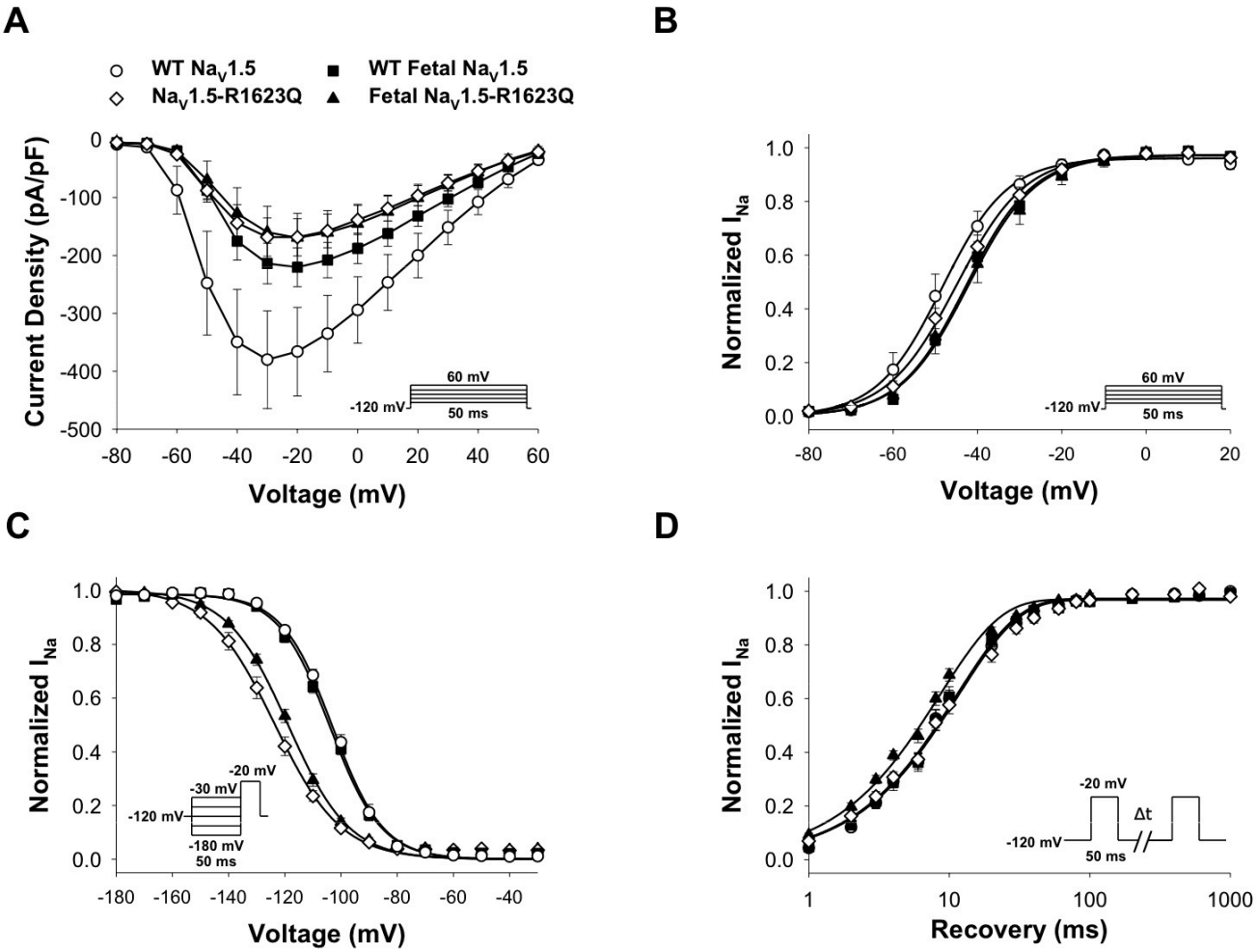

Figure 24: Fetal Na$_V$1.5-R1623Q exhibits a faster recovery from inactivation compared to Na$_V$1.5-R1623Q and WT channels.

(A) Current density-voltage relationships recorded from cells expressing either WT Na$_V$1.5 (n = 10), Na$_V$1.5-R1623Q (n = 9), WT fetal Na$_V$1.5 (n = 10), or fetal Na$_V$1.5-R1623Q (n = 10) channels (voltage protocol in the inset). (B) Conductance-voltage relationships for WT and mutant channels. (C) Steady-state voltage dependence of inactivation for WT and mutant channels (n = 9-12). In (B) and (C) lines represent average fits of the data with Boltzmann functions. (D) Time course of recovery from inactivation recorded using the illustrated voltage protocol. Biophysical fit parameters for all experiments are provided in Table 4. All wild-type data is the same as in Figure 21.

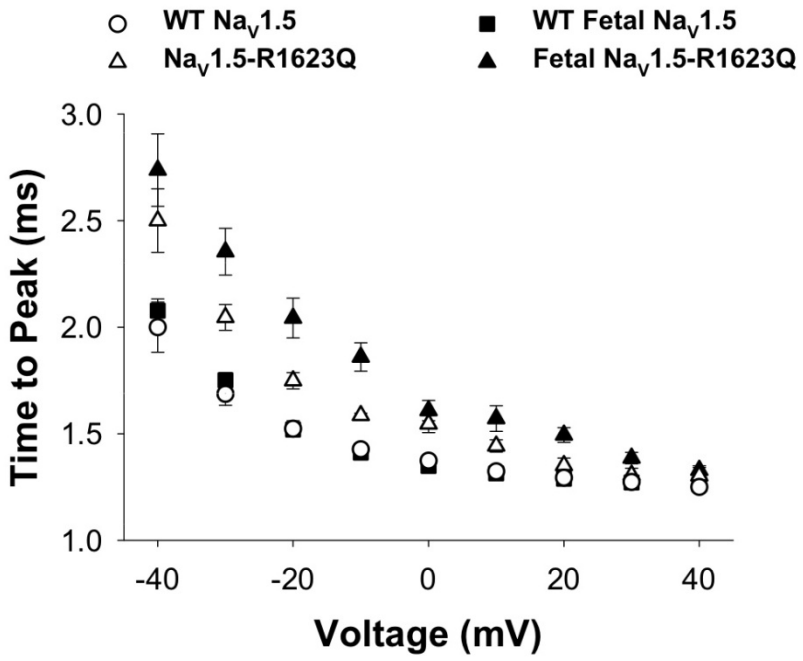

Figure 25: R1623Q channels exhibit slower time to peak vs WT.

Time to peak for WT and mutant R1623Q sodium channels in the adult and fetal $Na_V1.5$ splice variant (n = 6-8). $Na_V1.5$-R1623Q exhibited significantly slower time to peak vs WT at all voltages (-40 to +20 mV). Fetal $Na_V1.5$-R1623Q exhibited significantly slower time to peak vs WT at all voltages (-40 to +40 mV). Statistical significance was determined at the $p < 0.05$ level by Student t-test for a given voltage.

Functional consequences of a typical LQT3 mutation delKPQ expressed in fetal $Na_V1.5$

Some *SCN5A* mutations associated with LQT3 are rarely observed in early life and are associated with a more typical onset of QT prolongation in early adolescence to adulthood.[72,111,114–116] We hypothesized that fetal $Na_V1.5$ may exhibit protective or mask the effects for *SCN5A* mutations associated with a more typical age of onset such as delKPQ. To test this hypothesis, we expressed delKPQ in the fetal $Na_V1.5$ in heterologous cells and compared the functional effects to adult $Na_V1.5$-delKPQ.

We compared current density, voltage-dependence of activation, inactivation, and recovery from inactivation of delKPQ expressed in the adult and fetal $Na_V1.5$ (Figure 26, Table 4). Fetal $Na_V1.5$-delKPQ exhibited a greater reduction in current density vs WT channels and shifted peak current density +20 mV (Figure 26A). Additionally, fetal $Na_V1.5$-delKPQ exhibited depolarized shifts in the $V_{1/2}$ of the voltage-dependence of activation. $Na_V1.5$-delKPQ exhibited a significantly faster recovery from inactivation than fetal $Na_V1.5$-delKPQ and WT channels (Figure 26D, Table 4). Furthermore, adult and fetal $Na_V1.5$-delKPQ exhibited hyperpolarized shifts in the $V_{1/2}$ of the voltage-dependence of inactivation compared to WT channels.

$Na_V1.5$-delKPQ evoked a 6-fold greater persistent sodium current (1.2 ± 0.2%) and a 2.8-fold greater late current density (1.7 ± 0.4 pA/pF) vs WT (Figure 20, Table 3). Although fetal $Na_V1.5$-delKPQ exhibited a 7-fold greater persistent sodium current (2.1 ± 0.4%) compared to WT channels, late current density was not significantly increased (Figure 20, Table 3). The dramatic reduction in current density and the late current density of fetal $Na_V1.5$-delKPQ suggests an overall loss of function by fetal $Na_V1.5$-delKPQ channels compared to

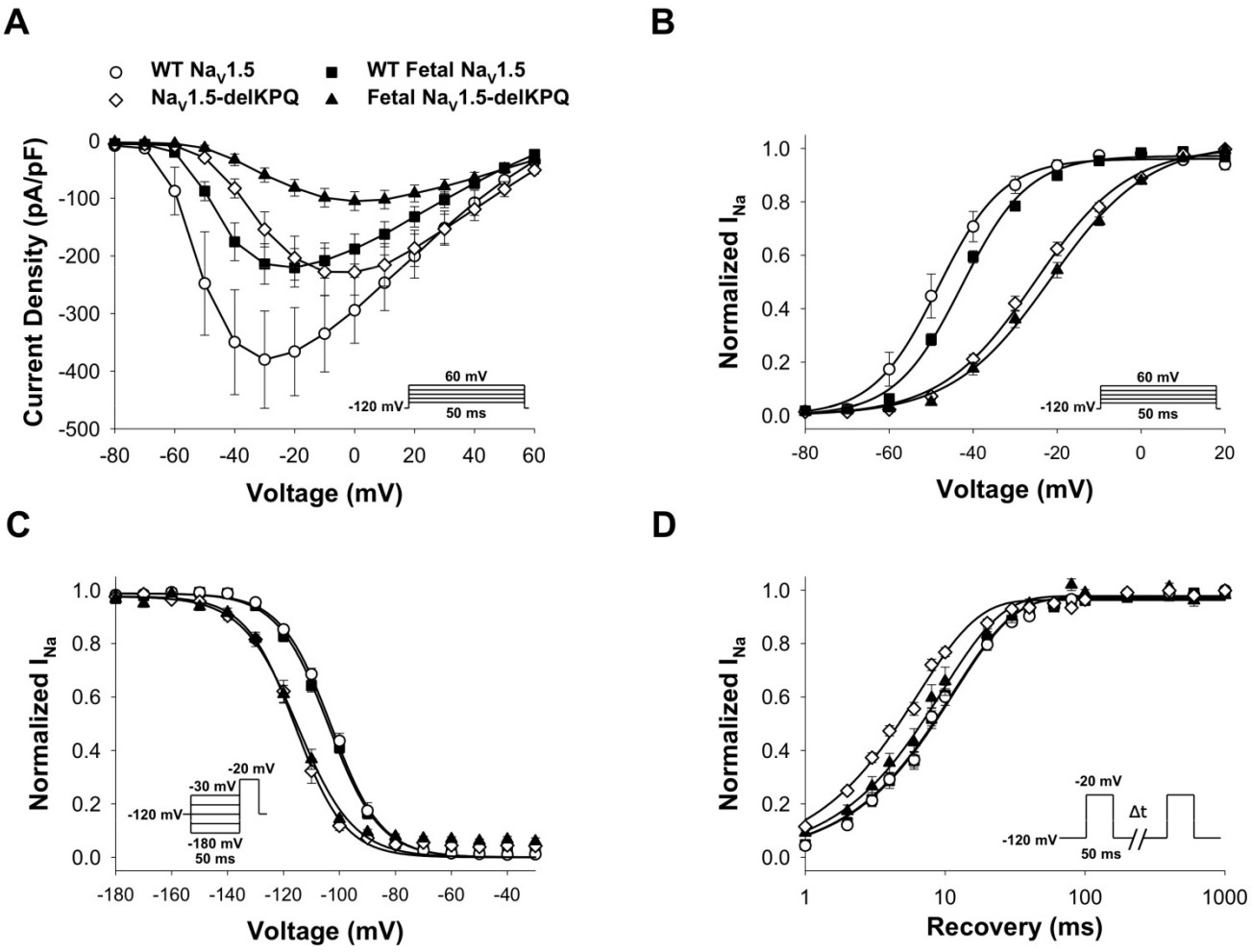

Figure 26: Fetal Na$_V$1.5-delKPQ exhibits a dramatic reduction in current density and slower recovery from inactivation compared to Na$_V$1.5-delKPQ.

(A) Current-voltage relationships for WT, Na$_V$1.5-delKPQ, and fetal Na$_V$1.5-delKPQ channels (n = 9-12). Current was normalized to cell capacitance to give a measure of current density. (B) Conductance-voltage (right y-axis) relationships for WT and mutant channels. Lines represent average fits of the data with Boltzmann functions. (C) Superimposed curves representing the voltage-dependence of steady-state inactivation. (D) Time course of recovery from inactivation recorded using the illustrated voltage protocol. Biophysical fit parameters for all experiments are provided in Table 4. All wild-type data is the same as in Figure 21.

adult $Na_V1.5$-delKPQ. These functional effects may be responsible for the later onset of LQT3 as expression of canonical $Na_V1.5$ increases after birth in human heart.[52]

SCN5A mutations exhibit ultra-fast recovery from inactivation and sodium channel dysfunction during pulse trains

The early onset LQT3 mutations, A1330D and F1473C, elicited ultra-fast recovery from inactivation that was similar to that observed for L409P/R558 previously described in Chapter II. Therefore, we investigated whether the early onset LQT3 mutations would also exhibit ultra-fast recovery when channels were inactivated at more extreme voltages of -140 or -90 mV using a similar 50 ms recovery protocol as shown in the Figure 26D inset (Figure 27, Table 5). $Na_V1.5$-A1330D channels exhibited an ultra-fast recovery from inactivation at -140 mV (1.4 ± 0.1 ms) and -90 mV (15.8 ± 2.1 ms) compared to WT $Na_V1.5$ (-140 mV: 2.6 ± 0.3 ms, -90mV: 68.7 ± 3.2 ms) (Figure 27A). Fetal $Na_V1.5$-A1330D channels exhibited a significantly faster recovery from inactivation with smaller time constants at -140 mV (1.3 ± 0.1 ms) and -90 mV (17.9 ± 6.3 ms) compared to WT fetal $Na_V1.5$ (-140 mV: 3.3 ± 0.4 ms, -90 mV: 49.7 ± 5.9 ms) (Figure 27B). These results demonstrate that A1330D channels exhibit an ultra-rapid recovery mechanism compared to WT channels in the fetal or adult $Na_V1.5$ at the more extreme voltages.

In addition, $Na_V1.5$-F1473C channels exhibited an ultra-fast recovery from inactivation at -140 mV (1.6 ± 0.1 ms) and -90 mV (16.2 ± 2.3 ms) compared to WT $Na_V1.5$ (-140 mV: 2.6 ± 0.3 ms, -90mV: 68.7 ± 3.2 ms) (Figure 27A). Fetal $Na_V1.5$-F1473C channels exhibited a

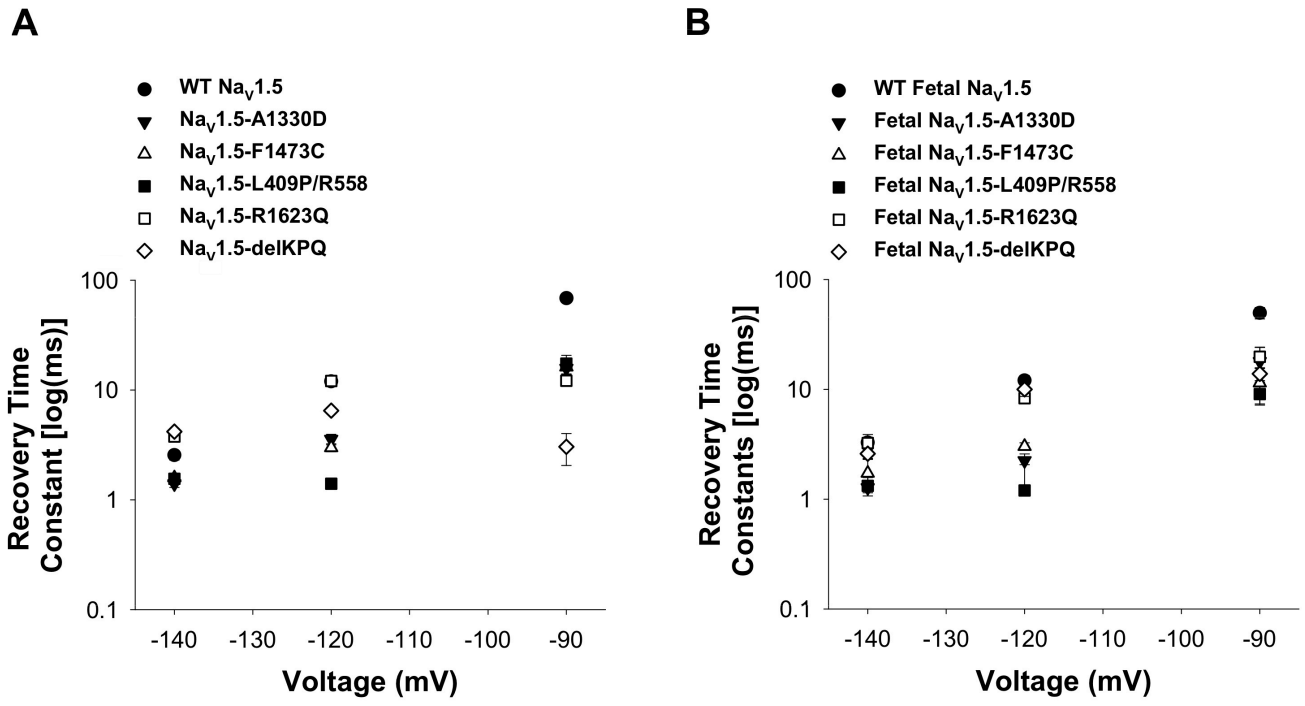

Figure 27: Recovery time constants for WT and mutant Na$_V$1.5 channels.

(A) Recovery time constants for WT and mutant adult Na$_V$1.5 channels shown at -140, -120, and -90 mV. (B) Recovery time constants for WT and mutant fetal Na$_V$1.5 channels shown at -140, -120, and -90 mV. The recovery time constant values and statistical comparisons for WT and mutant channels at -140 and -90 mV are shown in Table 5.

Table 5: Recovery time constants for WT and mutant $Na_V1.5$.

	Recovery from Inactivation (-140 mV)				
	τ (msec)	n		τ (msec)	n
WT $Na_V1.5$	2.6 ± 0.3	5	**WT Fetal $Na_V1.5$**	3.3 ± 0.4	5
$Na_V1.5$-L409P/R558	1.6 ± 0.1	5	**Fetal $Na_V1.5$-L409P/R558**	1.3 ± 0.2 [ac]	5
$Na_V1.5$-R1623Q	3.8 ± 0.3	5	**Fetal $Na_V1.5$-R1623Q**	3.2 ± 0.6	5
$Na_V1.5$-F1473C	1.6 ± 0.1	5	**Fetal $Na_V1.5$-F1473C**	1.7 ± 0.6 [c]	5
$Na_V1.5$-A1330D	1.4 ± 0.1 [a]	5	**Fetal $Na_V1.5$-A1330D**	1.3 ± 0.1 [ad]	5
$Na_V1.5$-delKPQ	4.2 ± 0.3	5	**Fetal $Na_V1.5$-delKPQ**	2.6 ± 0.3	5
	Recovery from Inactivation (-90 mV)				
	τ (msec)	n		τ (msec)	n
WT $Na_V1.5$	68.7 ± 3.2	5	**WT Fetal $Na_V1.5$**	49.7 ± 5.9	5
$Na_V1.5$-L409P/R558	17.4 ± 3.4 [b]	5	**Fetal $Na_V1.5$-L409P/R558**	9.0 ± 0.6 [bd]	5
$Na_V1.5$-R1623Q	12.2 ± 1.2 [b]	5	**Fetal $Na_V1.5$-R1623Q**	19.8 ± 4.3 [bd]	5
$Na_V1.5$-F1473C	16.2 ± 2.3 [b]	5	**Fetal $Na_V1.5$-F1473C**	11.5 ± 4.1 [bd]	5
$Na_V1.5$-A1330D	15.8 ± 2.1 [b]	5	**Fetal $Na_V1.5$-A1330D**	17.9 ± 6.3 [bd]	5
$Na_V1.5$-delKPQ	3.0 ± 1.0 [b]	3	**Fetal $Na_V1.5$-delKPQ**	13.9 ± 1.9 [bde]	5

[a] $P < 0.05$ compared to WT $Na_V1.5$
[b] $P < 0.01$ compared to WT $Na_V1.5$
[c] $P < 0.05$ compared to WT Fetal $Na_V1.5$
[d] $P < 0.01$ compared to WT Fetal $Na_V1.5$
[e] $P < 0.05$ compared to $Na_V1.5$-mutant
(One Way ANOVA & Bonferroni)

significantly faster recovery from inactivation with smaller time constants at -140 mV (1.7 ± 0.5 ms) and -90 mV (11.5 ± 4.1 ms) compared to WT fetal $Na_V1.5$ (-140 mV: 3.3 ± 0.4 ms, -90 mV: 49.7 ± 5.9 ms) (Figure 27B). These results demonstrate that F1473C channels exhibit an ultra-rapid recovery mechanism compared to WT channels in the fetal or adult $Na_V1.5$ as well. Typical onset LQT3 mutation delKPQ, exhibits a significantly faster recovery from inactivation but only at -90 mV in the adult $Na_V1.5$ (3.0 ± 1.0 ms) and fetal $Na_V1.5$ (13.9 ± 1.9 ms). However, the acceleration was much less dramatic for fetal $Na_V1.5$-delKPQ compared to delKPQ expressed in the adult isoform of the channel.

We also investigated whether repeated stimulation of mutant sodium channels would result in attenuated or enhanced loss of channel availability compared to WT channels. Cells were pulsed at frequencies of 1 or 2 Hz and sodium currents were normalized to the first pulse. It is important to note that the frequency of 2 Hz is similar to the fetal heart rate (~120 bpm) while a frequency of 1 Hz is similar to an adult heart rate (~60 bpm).[106,107] However these recording were performed at room temperature. $Na_V1.5$-A1330D and fetal $Na_V1.5$-A1330D both exhibited a significantly enhanced loss of channel availability at 1 and 2 Hz (Figure 28 & Figure 29). Furthermore, $Na_V1.5$-F1473C and fetal $Na_V1.5$-F1473C both exhibited a significantly enhanced loss of channel availability at 1 and 2 Hz (Figure 28 & 29). Typical onset mutation, delKPQ did not exhibit significant attenuation or enhanced loss of channel availability. This mutation exhibited effects more similar to WT channels upon frequent stimulation at 1 and 2 Hz. These results further suggest that early onset LQT3 mutations exhibit similar or more severe functional effects in the fetal splice variant compared to the adult $Na_V1.5$.

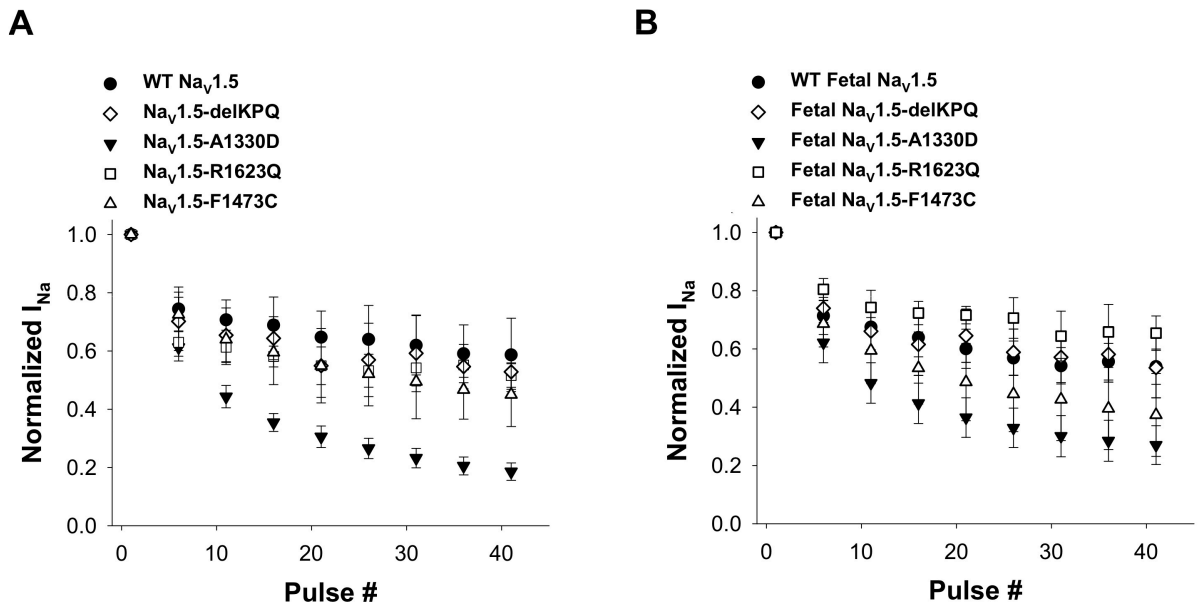

Figure 28: Pulse trains of WT and mutant Na$_V$1.5 channels at a frequency of 1 Hz.

(A) WT and mutant adult Na$_V$1.5 channels (n = 4-6). (B) WT and mutant fetal Na$_V$1.5 channels (n = 4-6). Statistical significance was assumed as $P < 0.05$ by Student's t-test.

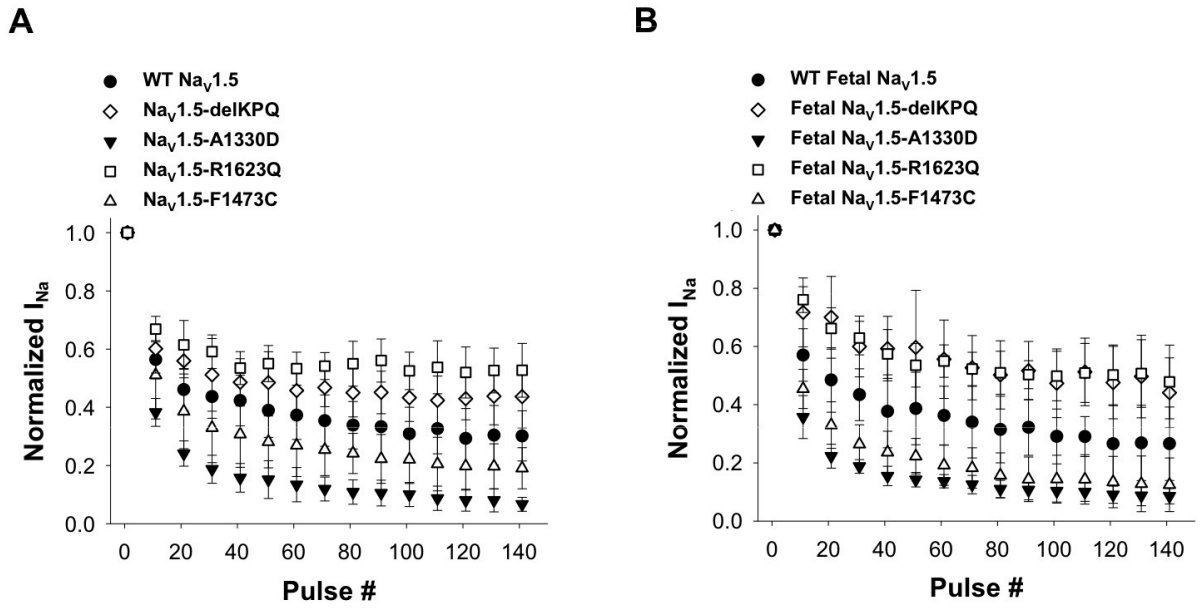

Figure 29: Pulse trains of WT and mutant Na$_V$1.5 channels at a frequency of 2 Hz.

(A) WT and mutant adult Na$_V$1.5 channels (n = 4-6). (B) WT and mutant fetal Na$_V$1.5 channels (n = 4-6). Statistical significance was assumed as $P < 0.05$ by Student's t-test.

Discussion

The three perinatal *SCN5A* mutations investigated encode dysfunctional cardiac sodium channels that exhibit persistent sodium current or impaired inactivation kinetics (R1623Q) but the degree of channel dysfunction determined in the context of the canonical adult $Na_V1.5$ splice product did not fully explain the unusual severity and early onset of LQTS in these cases. It has been reported that *SCN5A* undergoes developmentally-regulated alternative mRNA splicing to generate multiple isoforms of the protein.[88] Previously, we have shown that fetal $Na_V1.5$ is highly expressed in human fetal and neonatal hearts and that one *SCN5A* mutation associated with a severe fetal arrhythmia, L409P, exhibited more severe functional consequences in the context of fetal splice isoform of $Na_V1.5$ (Chapter II).[52]

Hence, we investigated the functional consequences of the three additional *SCN5A* mutations in the fetal $Na_V1.5$ splice isoform- A1330D, F1473C, and R1623Q. We also compared the functional effects of these early onset LQT3 mutations with that of a more typical onset LQT3 mutation, delKPQ. These experiments indicated that *SCN5A*-A1330D conferred much greater functional defects on fetal $Na_V1.5$ than when expressed in the adult $Na_V1.5$. Specifically, the proportion of persistent current was greater for fetal $Na_V1.5$-A1330D (1.7 ± 0.2%) compared to adult $Na_V1.5$-A1330D (0.9 ± 0.1%). This was accompanied with a significant increase in the late current density (Figure 20, Table 3). In addition, *SCN5A*-A1330D exhibited many other functional defects in the fetal $Na_V1.5$ such as a depolarized shift in the voltage-dependence of inactivation (Figure 21C), significantly slower inactivation kinetics (Figure 22), and an ultra-fast recovery from inactivation compared to WT channels (Figure 21D).

We also demonstrated that expression of F1473C and R1623Q in the fetal splice variant of $Na_V1.5$ mirrored the effects of the mutation in the adult background. Specifically, *SCN5A*-F1473C exhibited greater persistent sodium current in both the adult $Na_V1.5$ (1.5 ± 0.3%) and fetal $Na_V1.5$ (1.9 ± 0.6%) compared to WT channels (Figure 20, Table 3). Furthermore, F1473C exhibited ultra-fast recovery from inactivation (Figure 23D) that was also observed for *SCN5A*-L409P/R558 and *SCN5A*-A1330D, two other early onset LQTS mutations. Mutation *SCN5A*-R1623Q exhibited significantly slower inactivation kinetics in the adult and fetal $Na_V1.5$ compared to WT channels (Figure 22). The inactivation time constants for fetal $Na_V1.5$-R1623Q was slower than R1623Q expressed in the adult isoform. However, this was not statistically significant. Therefore, in the neonatal heart, where the expression ratio of fetal to adult mRNA is ~1:1,[52] mutant F1473C and R1623Q channels are severely dysfunctional in both backgrounds of the sodium channel.

In addition to these findings, we demonstrated that A1330D and F1473C channels exhibited an ultra-fast recovery from inactivation, a similar observation we made for L409P. Fetal $Na_V1.5$-A1330D exhibited an even faster recovery than A1330D in the adult background. However, pulse train experiments revealed that these mutations (A1330D and F1473C) result in an enhanced loss of channel availability following repeated stimulation. By contrast, R1623Q and delKPQ did not exhibit an ultra-fast recovery from inactivation when expressed in the fetal $Na_V1.5$ and had no significant effect on channel availability during pulse trains. We further investigated the recovery from inactivation at -140 and -90 mV to determine whether mutant channels were also dysfunctional at these extreme voltages. At -90 mV all mutant channels exhibited a significantly faster recovery from inactivation vs WT channels. However, the acceleration for delKPQ in the fetal splice variant was not as severe compared to adult $Na_V1.5$-

delKPQ (Figure 27, Table 5). We speculate that sodium channels with an ultra-rapid recovery mechanism that was observed for the early onset LQT3 mutations, may prime the cardiomyocyte for re-activation during ventricular repolarization in some cases. It is feasible that recovery from inactivation may be an important biophysical property in the immature heart especially under pathophysiological conditions such as re-entrant arrhythmias. However, further investigation of the molecular mechanism of mutant fetal $Na_V1.5$ in native cardiomyocytes or induced pluripotent cardiomyocytes (iPS-CMs) is required to determine if ultra-fast recovery from inactivation is pathological. Single channel recordings of fetal $Na_V1.5$-A1330D and fetal $Na_V1.5$-F1473C compared to WT channels may also provide further insight to the mechanism of enhanced loss of channel availability in addition to the ultra-fast recovery from inactivation observed for these mutations.

Here we have also compared the effects of *SCN5A*-delKPQ with that of the three early onset LQT3 mutations. Our rationale for investigating the effects of *SCN5A*-delKPQ in the fetal $Na_V1.5$ was that LQTS patients with *SCN5A*-delKPQ rarely present with an arrhythmia in early life (fetal – infancy) when expression of the fetal splice isoform is prominent.[115–117] Previous studies investigating the functional effects of delKPQ in tsA201 cells were performed using a different sodium channel background called hH1. The hH1 plasmid does not express the common variant arginine that is present at position 1027. Instead, hH1 expresses a glutamine that is considered to be a rare variant. In addition, the internal solutions used in the previous study contained 10 mM EGTA where our solution contained 2 mM EGTA.[118] This may change the concentration of free local calcium that has been shown to result in changes in the voltage-dependence of inactivation (also see Chapter IV). Therefore, these changes in the methods

may be responsible for the differences in the observed shifts in the voltage-dependence of activation and inactivation for $Na_V1.5$-delKPQ.

When we expressed delKPQ in the fetal $Na_V1.5$, there was an attenuated gain of function compared to adult $Na_V1.5$-delKPQ channels. Fetal $Na_V1.5$-delKPQ exhibited a significant reduction in current density (Figure 26A) and late current density (Figure 20, Table 3) compared to adult $Na_V1.5$-delKPQ. In this case, the functional effects of fetal $Na_V1.5$-delKPQ may be responsible for the later onset of cardiac events in patients with this mutation. In addition, adult or fetal $Na_V1.5$-delKPQ did not exhibit a significant change in channel availability during pulse trains compared with WT and early onset LQT3 mutations (L409P/R558, A1330D, and F1473C). Overall, the biophysical effects of *SCN5A* mutations expressed in the fetal $Na_V1.5$ may be a distinguishing factor in the timing of the onset and severity of LQTS.

CONCLUSIONS

In summary, we have shown that *SCN5A* mutations associated with some perinatal forms of LQTS (R1623Q, F1473C, and A1330D) exhibit more severe or similar functional consequences in the fetal $Na_V1.5$ compared to their expression in the canonical adult splice variant. By contrast, typical onset mutation, delKPQ demonstrated an attenuated gain of function in fetal $Na_V1.5$ but this was not observed when delKPQ was expressed in the canonical adult $Na_V1.5$. Our findings implicate dysfunction of a fetal-expressed sodium channel splice isoform as a distinguishing factor for early onset LQT3 compared to later onset arrhythmias. These studies are highly important for determining the molecular mechanism for severe arrhythmias that manifest in the earliest stages of development.

CHAPTER IV

Arrhythmogenic Calmodulin Mutations Disrupt Intracellular Cardiomyocyte Ca^{2+} Regulation by Distinct Mechanisms

INTRODUCTION

Congenital long QT syndrome (LQTS) and catecholaminergic polymorphic ventricular tachycardia (CPVT) are two forms of genetic disorders of heart rhythm that may present during childhood and cause life-threatening cardiac arrhythmias.[119] The molecular mechanisms underlying arrhythmia susceptibility have been inferred from studies of mutant gene products, which are largely ion channels or channel regulators. In LQTS, loss-of-function of potassium channels or gain-of-function in either sodium or calcium channels represent the major molecular mechanisms.[17] In contrast to disturbances in plasma membrane ion channel function, CPVT arises from disordered intracellular Ca^{2+} regulation most frequently because of mutation of the ryanodine receptor Ca^{2+}-release channel of the sarcoplasmic reticulum. These advances have improved our understanding of arrhythmogenesis and have revealed new therapeutic targets.

Recently, recurrent cardiac arrest in infants with a severe form of LQTS were discovered to have mutations in *CALM1* (D130G, F142L) or *CALM2* (D96V, D132E, and D134H), two genes encoding the ubiquitous Ca^{2+} signaling protein calmodulin (CaM).[92] Independently, two distinct CaM mutations (N54I, N98S) were discovered in subjects with a

CPVT-like syndrome although one of these mutations (N98S) has also been identified in a subject with LQTS.[120] In addition, another *CALM1* mutation, F90L, was identified in a family with idiopathic ventricular tachycardia and sudden death in adolescence.[121] There are three *CALM* genes (*CALM1, CALM2, CALM3*) that encode the same CaM protein.[92] However, the regulation of their expression is still being investigated. Most of the mutations described affect conserved amino acid residues that are known to participate in Ca^{2+} binding or in energetic coupling of ion binding to CaM activation (Figure 30). Biochemical studies revealed that most CaM mutations, except N54I, cause reduced Ca^{2+} binding affinity.[92,122] However, the cellular basis for arrhythmogenesis in the setting of CaM mutations has not been elucidated.

Calmodulin controls a large number of enzymes, ion channels and other proteins.[123,124] In cardiomyocytes, key CaM interacting proteins include those critically involved in beat-to-beat Ca^{2+} homeostasis. CaM interacts with the cardiac sodium channel via the C-terminal IQ domain or the D3/D4 linker.[123–125] Previous studies have shown that the binding interaction of CaM to the IQ of $Na_V1.5$ significantly enhances slow inactivation, a channel-gating process linked to life-threatening idiopathic ventricular arrhythmias.[126] In addition, CaM that is not bound to calcium, designated as apo-CaM, has been shown to interact with $Na_V1.5$ by nuclear magnetic resonance studies (NMR).[125] However the structural biology of the CaM-$Na_V1.5$ complex has not conclusively determined how CaM affects channel gating.

In addition to sodium channel effects, CaM is pre-bound to the cardiac L-type Ca^{2+} channel (LTCC) where it senses local Ca^{2+} influx and cytosolic Ca^{2+}. The complex of Ca^{2+}-CaM promotes a rapid inactivation of LTCC Ca^{2+} current (I_{CaL}).[127] This process, known as Ca^{2+}-dependent inactivation (CDI) is a major determinant of cardiac contractability.[128] Engineered CaM with carboxyl lobe (C-lobe) mutations abrogating Ca^{2+}-C-lobe binding

attenuated CDI and prolonged action potential (AP) duration.[128] The majority of the z-line CaM also binds to ryanodine receptor 2 (RyR2);[128] irrespective of Ca^{2+} concentrations, CaM inhibits RyR2 opening.[129,130] Disrupting the CaM-RyR2 complex has multiple effects including increased opening of RyR2, diminished I_{CaL}, and increased cytosolic Ca^{2+} at negative membrane potentials which creates a molecular substrate for arrhythmogenic triggers.[131] In this respect, CPVT and defective CaM-RyR2 function lead to a common endpoint. Whereas attenuated CDI evoked by engineered defective CaM prolongs action potential duration that could underpin QT interval prolongation.[32,33]

Here we investigated the effects of LQTS-associated CaM mutations on sodium and calcium channel currents to elucidate the molecular mechanisms underlying arrhythmia predisposition. We also show that CaM mutations had inconsistent effects on sodium channels but caused impaired CDI of I_{CaL} in cardiomyocytes. Our findings implicate different molecular substrates for arrhythmogenesis associated with CaM mutations.

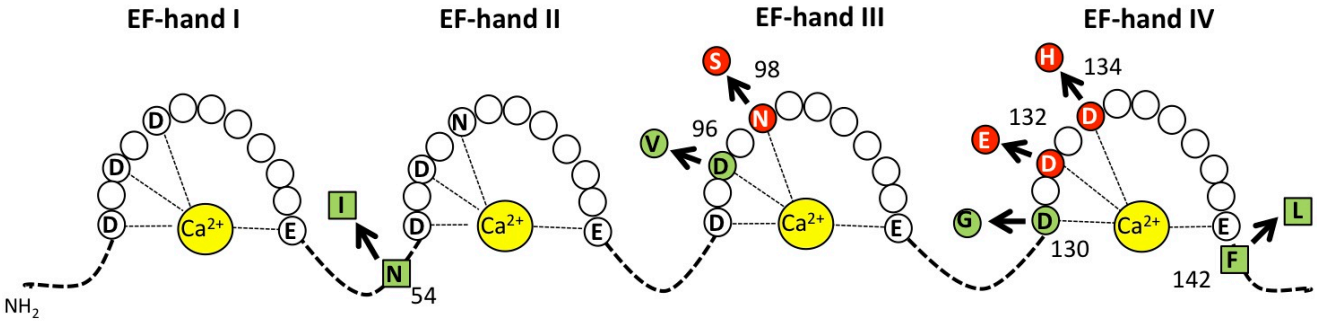

Figure 30: Calmodulin mutations associated with life-threatening cardiac arrhythmias.

CaM mutations associated with life-threatening cardiac arrhythmias affect conserved amino acid residues that are known to participate in Ca^{2+} binding or in energetic coupling of ion binding to CaM activation. Mutations associated with a LQTS phenotype include D96V, D130G, D132E, D134H, and F142L. Mutations associated with CPVT are N54I and N98S. The idiopathic VT mutation, F90L, (not shown) is located within the linker between EF hand II and EF hand III. Figure adapted from Makita et al. (2013).[120]

METHODS

Mutagenesis of calmodulin

The mutant calmodulin (CaM) was engineered by making one of the following amino acid substitutions: F90L, D96V, D130G, D132E, D134H, F142L. A mammalian expression plasmid was used to drive expression of wild-type (WT) or mutant CaM by the immediate early CMV promoter along with the coding region for either GFP or CD8 preceded by the IRES2 element as co-transfection markers.

Heterologous expression of human $Na_V1.5$ with calmodulin

Plasmids encoding recombinant human cardiac sodium channel isoforms ($Na_V1.5$) were described previously.[52] For studies of sodium channel function, wild-type (WT) cardiac sodium channel cDNA (0.5 μg) and WT or mutant CaM (F90L, D96V, D130G, D132E, D134H, F142L) cDNA (0.5 μg) were transiently transfected into tsA201 cells using FuGene HD (Roche Diagnostics, Indianapolis, IN), then incubated for 48 hours at 37°C prior to electrophysiological measurements. Cells selected for patch clamp recordings exhibited GFP or CD8 expression and were easily distinguishable from non-GFP or CD8 expressing cells.

In vitro electrophysiology of sodium channels

Sodium currents were recorded at room temperature using the whole-cell patch clamp technique as described previously.[52,132] The extracellular bath solution contained the following (in mmol/L): 140 NaCl, 4 KCl, 1.8 $CaCl_2$, 1 $MgCl_2$, 10 HEPES, and 10 glucose, pH 7.35 (adjusted with NaOH). The low calcium intracellular pipette solution contained the following (in

mmol/L): 10 NaF, 100 CsF, 20 CsCl, 20 BAPTA, 10 HEPES, 10 glucose, pH 7.35 (adjusted with CsOH). The high calcium (~1 μM free) intracellular pipette solution contained the following (in mmol/L): 10 NaF, 100 CsF, 20 CsCl, 1 BAPTA, 0.9 $CaCl_2$, 10 HEPES, 10 glucose, pH 7.35 (adjusted with CsOH).[124] Osmolarity was adjusted to 310 mOsm/l with sucrose for the bath solution and 300mOsm/l for pipette solution. Data were acquired with an Axopatch 200B patch-clamp amplifier and pClamp 10.2 software. Tetrodotoxin (TTX)-sensitive persistent current was determined with a 200-ms depolarization to -30 mV as the average current recorded between 190 and 200 ms and reported as a percentage of peak current following digital subtraction of currents recorded in the presence and absence of 30 μmol/L TTX (Tocris Biosciences, Ellisville, MO). Some experiments were performed in the presence of 10 μM KN-93, a small molecule inhibitor of CAMKII that was added into the intracellular pipette solution. All data were analyzed with pClamp 10.2 (Axon Instruments, Inc, Sunnyvale, CA) and plotted using Sigmaplot 10.0 (SPSS, Inc, Chicago, IL) software. Results are presented as mean ± SEM. For recovery from inactivation, amplitudes (A) are equal to 1.00 ± 0.1. Unless otherwise noted, statistical comparisons were made by using a one-way ANOVA and Bonferroni correction to WT $Na_V1.5$ co-expressed with WT CaM. Statistical significance was assumed for $P < 0.05$.

In vitro electrophysiology of L-type calcium channels and calcium transient measurements

All experimental procedures and protocols were approved by the Animal Care and Use Committee of the University of Kentucky, and conformed to the NIH Guide for Care and Use of Laboratory Animals. Isolated fetal ventricular mouse cardiomyocytes (FVM) were prepared as previously described.[33,133] L-type calcium current (I_{CaL}) was measured from FVM cells

expressing various CaM constructs in the whole-cell recording mode of the patch-clamp technique. This work was done by our collaborators in Jonathan Satin's laboratory at the University of Kentucky.

RESULTS

Functional effects of LQTS CaM mutants, *CALM1*-D130G, *CALM2*-D96V, and *CALM1*-F142L on cardiac sodium channels

Because calmodulin is known to regulate cardiac sodium channel inactivation and a specific defect in sodium channel inactivation (increased persistent sodium current) occurs in LQTS,[38] we investigated the effects of LQTS-CaM mutants on heterologously expressed $Na_V1.5$ as well as on native sodium current in FVMs. We performed heterologous co-expression of WT or mutant CaM with human $Na_V1.5$ in tsA201 cells and measured the electrophysiological properties of the expressed channels. When recording sodium current with a nominally Ca^{2+}-free intracellular solution (apo-CaM), we did not observe differences in the level of persistent sodium current (expressed as a % of peak current) for any of the CaM mutations compared to WT CaM. Therefore, we repeated these experiments with elevated intracellular calcium (~1 μM free Ca^{2+}) to provide a saturating concentration of calcium to promote binding of CaM to $Na_V1.5$.[92,124] Furthermore, because of the early age of onset of LQTS in the reported probands, we also tested the effects of CaM mutations on a fetal and neonatal expressed $Na_V1.5$ splice variant.[52]

Cells co-expressing CaM-D130G with fetal $Na_V1.5$ exhibited 7.5-fold larger persistent sodium current (1.5 ± 0.4%) compared to cells co-expressing the fetal splice variant with WT CaM (0.2 ± 0.1%; $p < 0.05$) when recordings were made with high intracellular calcium (Figure 31). This greater level of persistent current was not observed when CaM-D130G was co-expressed with the canonical (adult expressed) splice isoform of $Na_V1.5$ or with low

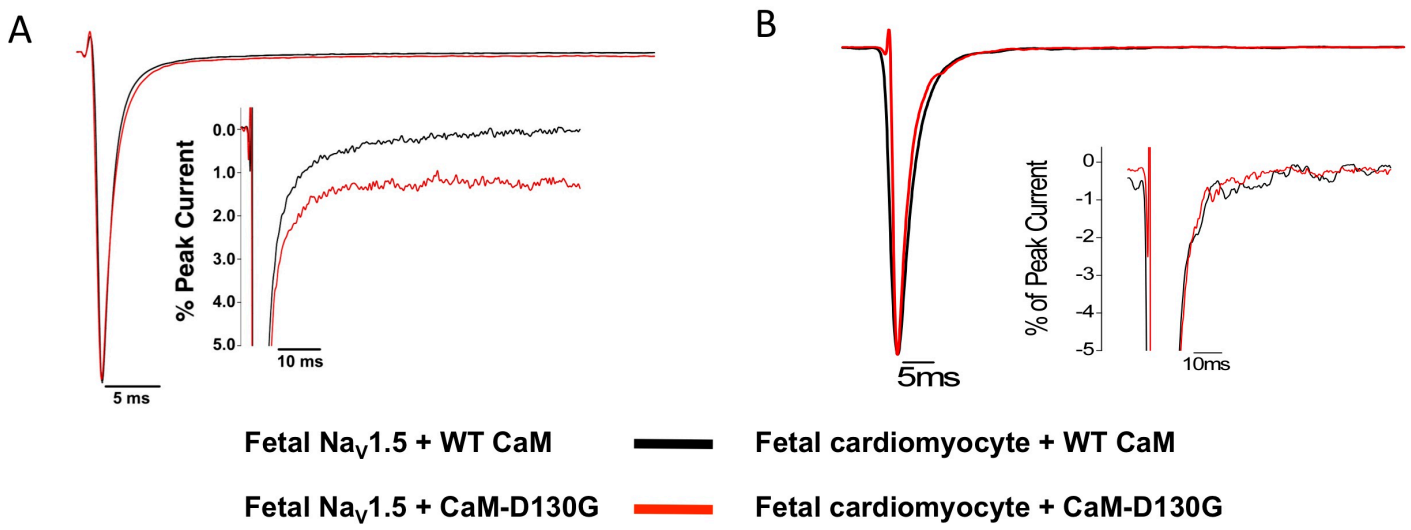

Figure 31: LQTS-CaM mutation effects on persistent sodium current of fetal Na$_V$1.5.

(A) CaM-D130G evoked increased persistent sodium current with fetal Na$_V$1.5. Averaged TTX-sensitive currents were normalized to the peak current measured at −30mV during a 200 ms depolarization recorded under high intracellular calcium concentration (see Methods). The inset represents the same data plotted on an expanded vertical scale. Summary data are provided in Table 6. (B) CaM-D130G has no significant effect on persistent sodium current in fetal ventricular cardiomyocytes (FVM). Tetrodotoxin (TTX)-sensitive currents were normalized to the peak current measured at −30mV during a 300 ms depolarization recorded under a high intracellular calcium concentration (see Methods). The inset represents the same data plotted on an expanded vertical scale.

intracellular calcium (Table 6). Electrophysiological recordings were also performed expressing β1 with $Na_V1.5$ and WT or mutant calmodulin. Fetal $Na_V1.5$ co-expressed with CaM-D130G and β1 evoked a greater persistent sodium current (1.4 ± 0.3%) compared to fetal channels co-expressed with WT CaM and β1 (0.3 ± 0.1%) under high calcium conditions. In contrast, cells co-expressing fetal or canonical $Na_V1.5$ splice isoforms with either CaM-D96V or CaM-F142L did not exhibit abnormal levels of persistent sodium current under high calcium conditions (Table 6).

Other sodium channel properties including the conductance-voltage relationship, voltage dependence of steady-state inactivation, inactivation kinetics, and recovery from inactivation were unaffected by CaM mutants (Figure 32, 33, & 34 Table 7). Furthermore, expression of CaM-D130G in fetal ventricular mouse cardiac myocytes (FVM) did not evoke detectable differences in the level of persistent sodium current compared with cells transfected with WT-CaM (Figure 31B). Given the inconsistent effect of CaM mutants on heterologous and native sodium current, we concluded that $Na_V1.5$ dysfunction was not the major cause for LQTS in the setting of CaM mutations.

Table 6: Persistent sodium current in cells expressing WT or mutant CaM.

	Persistent Current %	n
$Na_V1.5$ + apo-WT CaM	0.3 ± 0.2	4
$Na_V1.5$ + apo-CaM-D130G	0.2 ± 0.1	4
$Na_V1.5$ + WT CaM	0.3 ± 0.1	5
$Na_V1.5$ + CaM-D130G	0.2 ± 0.1	5
$Na_V1.5$ + CaM-D96V	0.2 ± 0.1	7
$Na_V1.5$ + CaM-F142L	0.1 ± 0.1	4
Fetal $Na_V1.5$ + apo-WT CaM	0.4 ± 0.1	6
Fetal $Na_V1.5$ + apo-CaM-D130G	0.6 ± 0.2	7
Fetal $Na_V1.5$ + WT CaM	0.2 ± 0.1	9
Fetal $Na_V1.5$ + CaM-D130G	1.5 ± 0.4*†‡	13
Fetal $Na_V1.5$ + WT CaM + KN93	0.1 ± 0.1	7
Fetal $Na_V1.5$ + CaM-D130G + KN93	0.8 ± 0.2‡	16
Fetal $Na_V1.5$ + CaM-D96V	0.4 ± 0.1	8
Fetal $Na_V1.5$ + CaM-F142L	0.6 ± 0.5	8

* $P < 0.05$ compared to $Na_V1.5$ + WT CaM
† $P < 0.05$ compared to fetal $Na_V1.5$ + WT CaM
‡ $P < 0.05$ compared to fetal $Na_V1.5$ + WT CaM with 10 μM KN-93

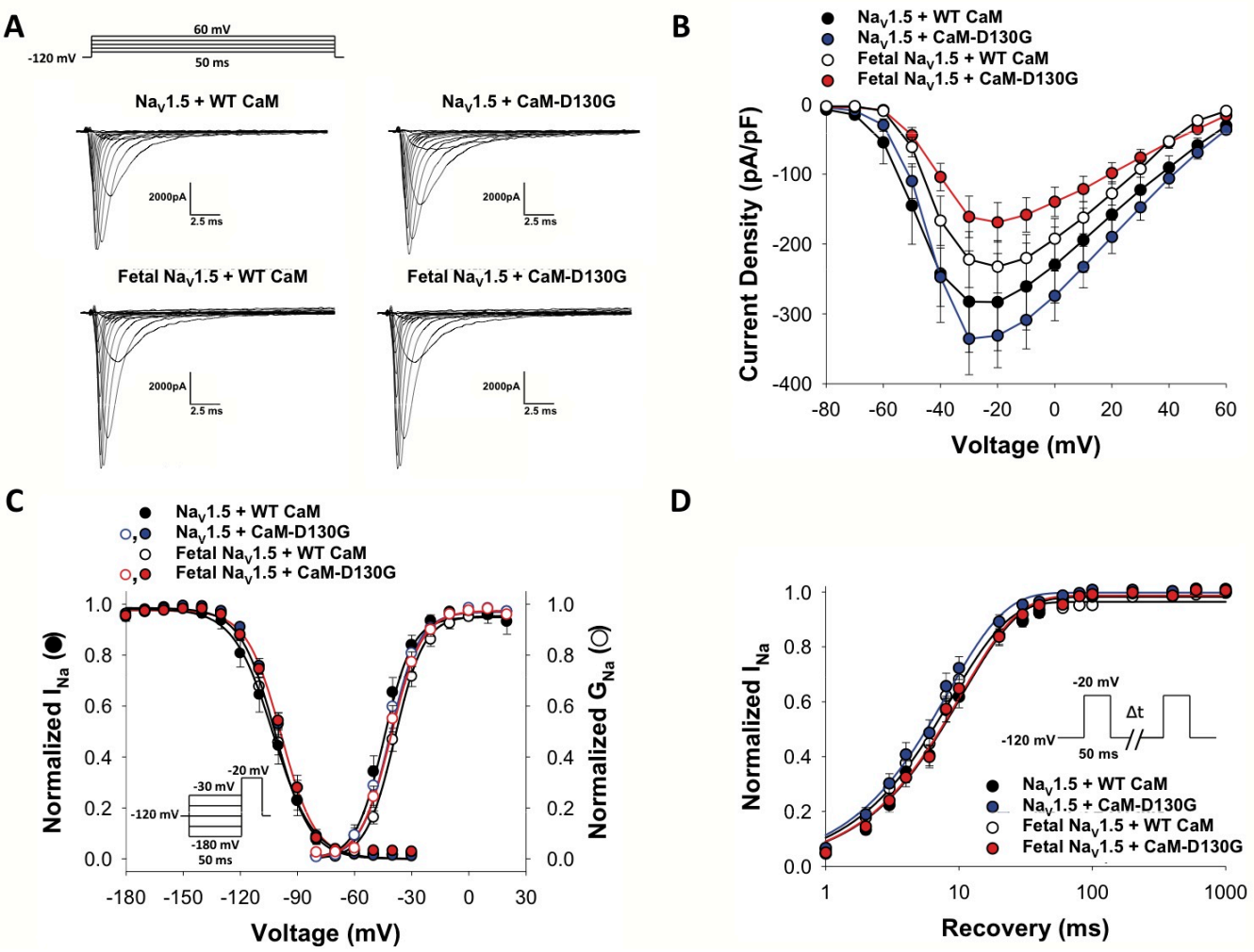

Figure 32: CaM-D130G does not have significant biophysical effects on peak sodium current.

(A) Representative traces of Na$_V$1.5 or fetal Na$_V$1.5 co-expressed with WT or CaM-D130G. (B) Current density-voltage relationships comparing WT and CaM-D130G effects on adult and fetal Na$_V$1.5 channels (n = 9-11). (C) Conductance-voltage and steady-state voltage dependence of inactivation relationships for adult and fetal Na$_V$1.5 co-expressed with WT or CaM-D130G (n = 9-11). Lines represent average fits of the data with Boltzmann functions. (D) Recovery from inactivation of Na$_V$1.5 or fetal Na$_V$1.5 co-expressed with WT or CaM-D130G (n = 6-10). Biophysical fit parameters for all experiments are provided in Table 7. All experiments were preformed under high calcium conditions.

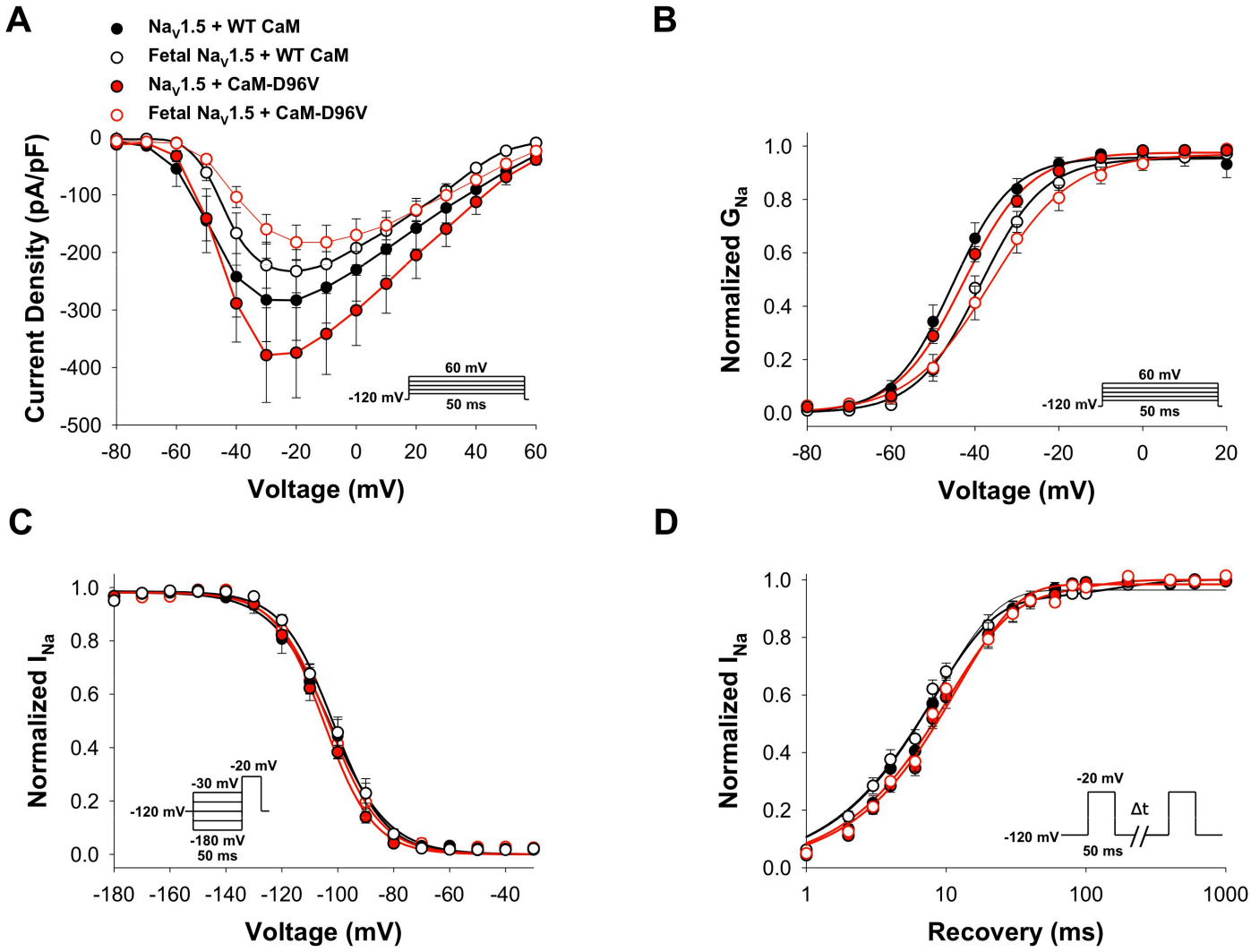

Figure 33: CaM-D96V does not have significant biophysical effects on peak sodium current.

(A) Representative traces of Na$_V$1.5 or fetal Na$_V$1.5 co-expressed with WT or CaM-D96V. (B) Current density-voltage relationships comparing WT and CaM-D96V effects on adult and fetal Na$_V$1.5 channels (n = 9-11). (C) Conductance-voltage and steady-state voltage dependence of inactivation relationships for adult and fetal Na$_V$1.5 co-expressed with WT or CaM-D96V (n = 9-11). Lines represent average fits of the data with Boltzmann functions. (D) Recovery from inactivation of Na$_V$1.5 or fetal Na$_V$1.5 co-expressed with WT or CaM-D96V (n = 6-10). Biophysical fit parameters for all experiments are provided in Table 7. All experiments were preformed under high calcium conditions.

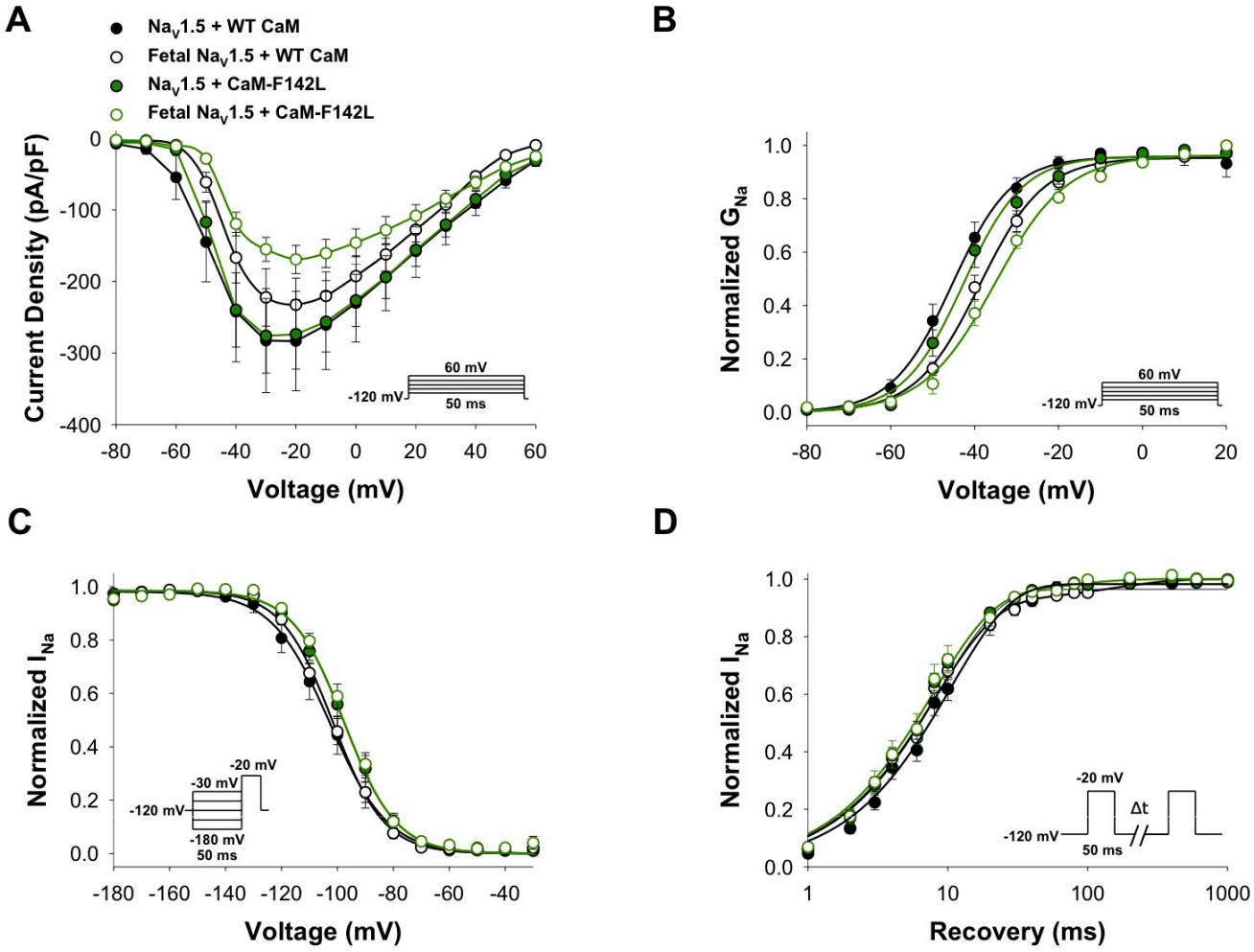

Figure 34: CaM-F142L does not have significant biophysical effects on peak sodium current.

(A) Representative traces of Na$_V$1.5 or fetal Na$_V$1.5 co-expressed with WT or CaM-F142L. (B) Current density-voltage relationships comparing WT and CaM-F142L effects on adult and fetal Na$_V$1.5 channels (n = 9-10). (C) Conductance-voltage and steady-state voltage dependence of inactivation relationships for adult and fetal Na$_V$1.5 co-expressed with WT or CaM-F142L (n = 9-10). Lines represent average fits of the data with Boltzmann functions. (D) Recovery from inactivation of Na$_V$1.5 or fetal Na$_V$1.5 co-expressed with WT or CaM-F142L (n = 6-10). Biophysical fit parameters for all experiments are provided in Table 7. All experiments were preformed under high calcium conditions.

Table 7: CaM mutants do not exhibit major biophysical effects on peak $I_{Na.}$

Biophysical Parameters								
	Voltage-Dependence of Activation			Steady-State Availability			Recovery From Inactivation	
	$V_{1/2}$ (mV)	k (mV)	n	$V_{1/2}$ (mV)	k (mV)	n	τ (msec)	n
$Na_V1.5$ + WT CaM	-45.0 ± 2.1	6.6 ± 0.5	9	-102.9 ± 3.2	-8.4 ± 0.2	10	10.9 ± 1.3	6
$Na_V1.5$ + CaM-D130G	-43.1 ± 2.3	6.6 ± 0.5	11	-98.5 ± 1.7	-8.1 ± 0.1	10	8.8 ± 1.1	8
$Na_V1.5$ + CaM-D96V	-42.6 ± 1.1	7.8 ± 0.3	10	-105.2 ± 1.0	-8.7 ± 0.4	13	11.2 ± 0.5	11
$Na_V1.5$ + CaM-F142L	-41.8 ± 2.0	6.7 ± 0.8	10	-96.4 ± 2.2	-8.5 ± 0.4	11	8.7 ± 0.6	10
Fetal $Na_V1.5$ + WT CaM	-38.4 ± 1.7	7.5 ± 0.5	11	-103.3 ± 2.2	-9.7± 1.0	9	9.1 ± 0.8	10
Fetal $Na_V1.5$ + CaM-D130G	-41.0 ± 1.7	7.2 ± 0.5	10	-98.6 ± 1.2	-8.9 ± 0.3	8	11.0 ± 1.3	9
Fetal $Na_V1.5$ + CaM-D96V	-35.2 ± 2.1*	9.4 ± 0.4‡	9	-99.1 ± 1.4	-13.1 ± 2.3†‡	9	12.1 ± 1.6	7
Fetal $Na_V1.5$ + CaM-F142L	-35.4 ± 1.7*	8.3 ± 0.6	6	-96.3 ± 1.7	-8.4 ± 0.3	7	8.9 ± 1.4	6

All recordings were performed with high intracellular calcium concentration
* $P < 0.05$ compared to $Na_V1.5$ + WT CaM
† $P < 0.05$ compared to fetal $Na_V1.5$ + WT CaM
‡ $P < 0.005$ compared to $Na_V1.5$ + WT CaM

Persistent current evoked by CaM-D130G on fetal $Na_V1.5$ is not due to CAMKII

Previous reports have shown that Ca^{2+}/calmodulin-dependent protein kinase II (CAMKII), a downstream effector of CaM, can also evoke persistent sodium currents.[123,134,135] Therefore, we investigated whether the persistent sodium current evoked by D130G was due to CAMKII activation by using a small molecule inhibitor of CAMKII, KN-93. In the presence of 10 μM KN-93, CaM-D130G still evoked an 8-fold increase in the level of persistent sodium current (Table 6). This suggests that the persistent sodium current evoked by CaM-D130G on fetal $Na_V1.5$ is not due to CAMKII.

Functional effects of *CALM2* mutants D132E and D134H on cardiac sodium channels

In addition to the three CaM mutations described, two other *CALM2* mutations, D132E and D134H were later discovered in two more neonatal LQTS cases. Mutation *CALM2*-D134H was identified in a girl who presented at age 19 months with syncope and a long QTc (579 ms) followed by several episodes of cardiac arrest. ECG features and treatment responses were consistent with LQT3. Mutation *CALM2*-D132E was discovered by targeted screening of *CALM1-3* in an adult female of European ancestry with a history of perinatal bradycardia and a diagnosis of neonatal LQTS who later exhibited clinical features consistent with CPVT at age 9 years.[120]

To investigate the functional effects of CaM-D132E and CaM-D134H on $Na_V1.5$, we heterologously expressed WT or mutant CaM with human $Na_V1.5$ in tsA201 cells and preformed electrophysiological recordings on the expressed channels (Figure 35). Neither mutation had a significant impact on the persistent sodium current of adult or fetal $Na_V1.5$, even under high calcium conditions (Table 9). However, CaM-D134H resulted in significant

effects on peak sodium current biophysical parameters such as the voltage-dependence of activation, inactivation, and recovery from inactivation under high calcium conditions (Figure 35 & 36, Table 8).

CaM-D134H resulted in a significant hyperpolarized shift in the voltage-dependence of activation of adult $Na_V1.5$ compared to expression with WT CaM (Figure 35B). Furthermore, CaM-D134H co-expressed with the fetal $Na_V1.5$ did not result in any changes in the voltage-dependence of activation (Figure 36B). Additionally, CaM-D134H shifted the voltage-dependence of inactivation of $Na_V1.5$ to more hyperpolarized potentials vs WT CaM (Figure 35C). By contrast, CaM-D134H expressed with fetal $Na_V1.5$ resulted in the opposite effect with a more depolarized inactivation compared to co-expression with the WT CaM (Figure 36C). Furthermore, co-expression of CaM-D134H with the adult $Na_V1.5$ resulted in significant slowing of the recovery from inactivation compared to WT CaM (Figure 35D). Interestingly, CaM-D134H resulted in a significantly faster recovery from inactivation of the fetal splice variant of $Na_V1.5$ (Figure 36D). These results highlight the differential effects of CaM-D134H on the adult and fetal isoforms of $Na_V1.5$ suggesting there may be subtle differences in the regulation of fetal sodium channels by calmodulin. No significant effects on sodium current density were observed (Figure 35A & 36A). Overall, CaM-D132E did not exhibit significant effects on either the adult or fetal $Na_V1.5$ peak current (Figure 35 & 36).

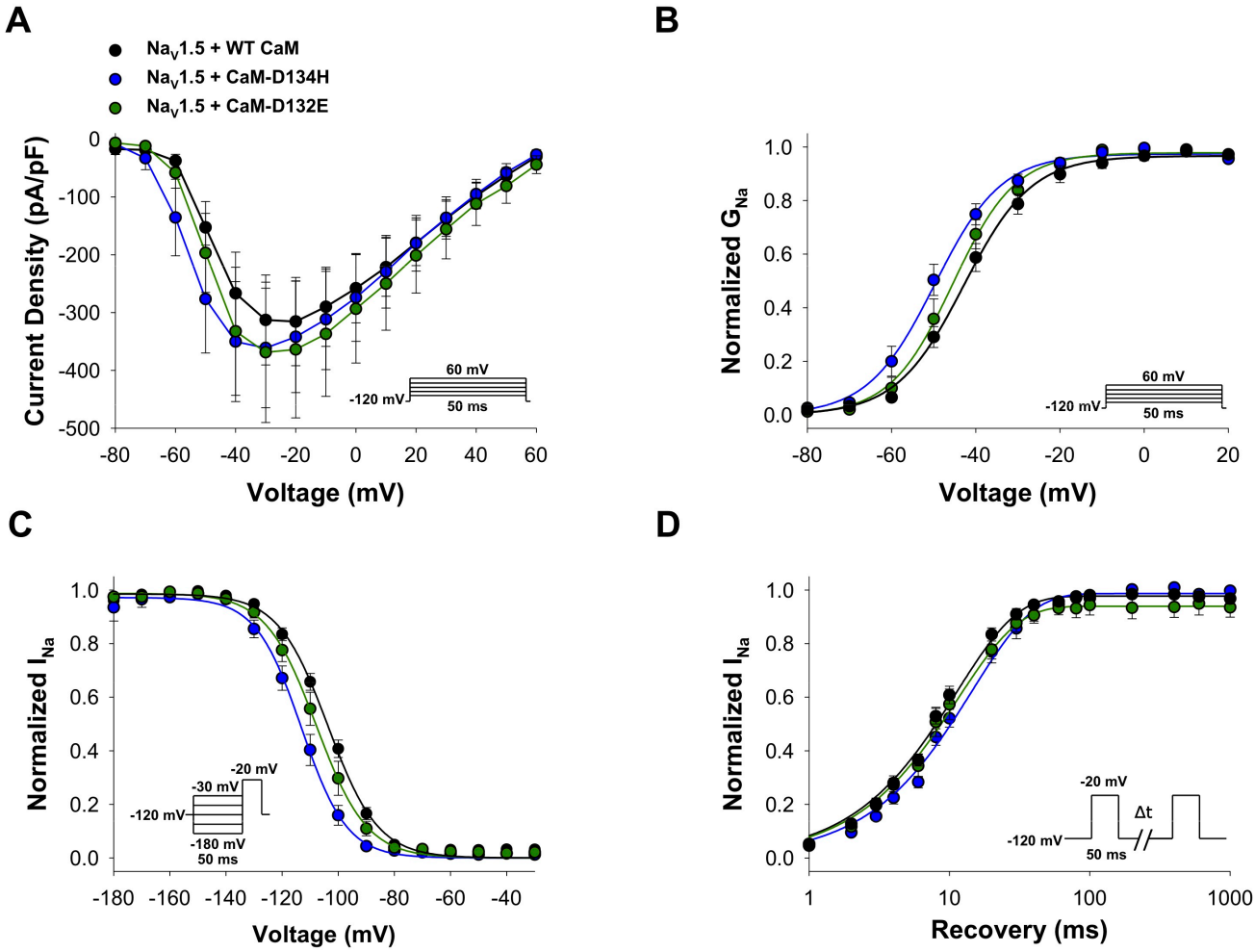

Figure 35: CaM-D134H results in significant effects on adult Na$_V$1.5 peak current.

(A) Current-voltage relationships for Na$_V$1.5 and WT CaM, Na$_V$1.5 and CaM-D134H, and Na$_V$1.5 and CaM-D132E (n = 6-7). Current was normalized to cell capacitance to give a measure of current density. (B) Conductance-voltage (right y-axis) relationships for sodium channels co-expressed with WT or mutant CaM. Lines represent average fits of the data with Boltzmann functions. (C) Superimposed curves representing the voltage-dependence of steady-state inactivation. (D) Time course of recovery from inactivation recorded using the illustrated voltage protocol. Biophysical fit parameters for all experiments are provided in Table 8.

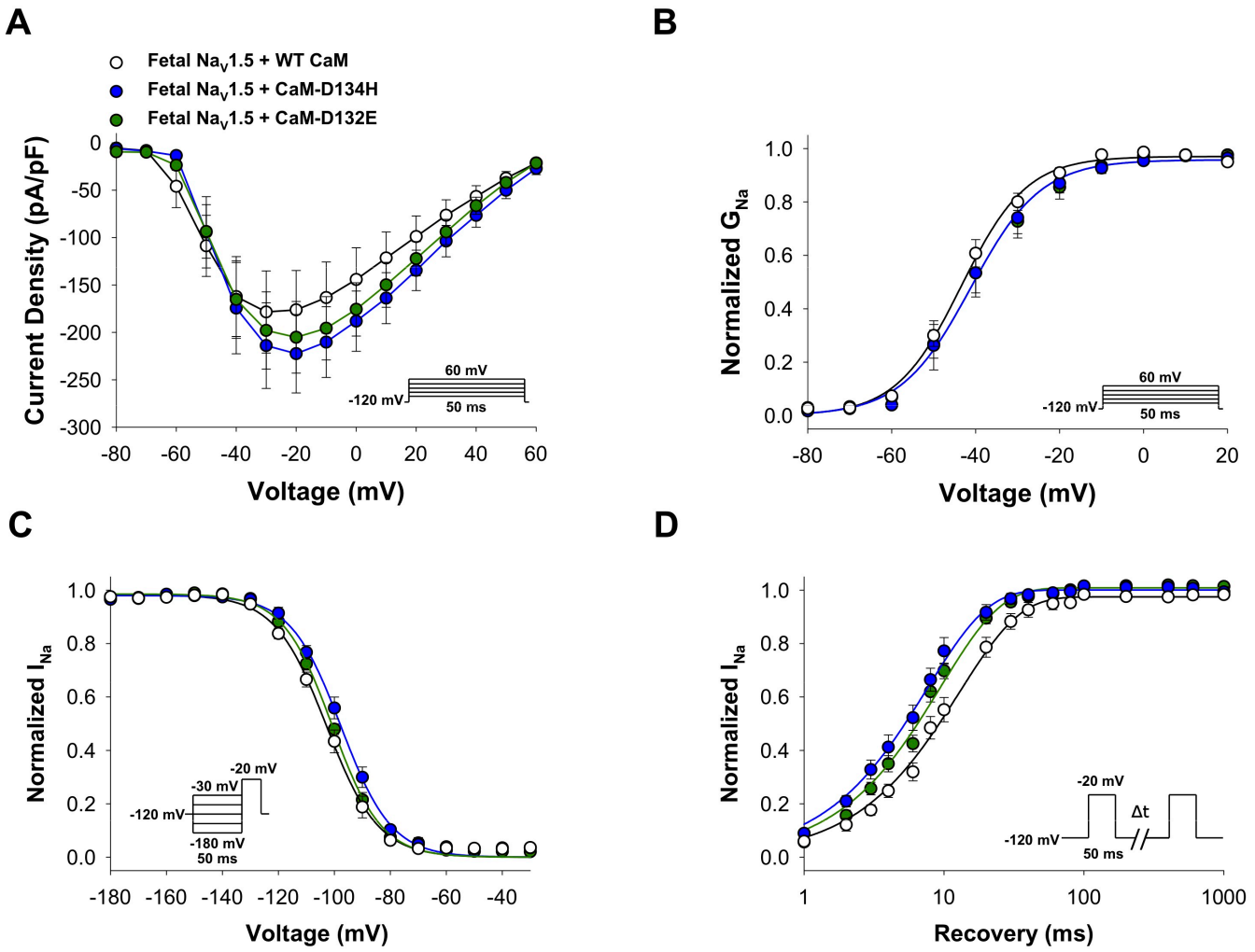

Figure 36: CaM-D134H results in significant effects on fetal Na$_V$1.5 peak current.

(A) Current-voltage relationships for fetal Na$_V$1.5 and WT CaM, fetal Na$_V$1.5 and CaM-D134H, and fetal Na$_V$1.5 and CaM-D132E (n = 6-7). Current was normalized to cell capacitance to give a measure of current density. (B) Conductance-voltage (right y-axis) relationships for fetal sodium channels co-expressed with WT or mutant CaM. Lines represent average fits of the data with Boltzmann functions. (C) Superimposed curves representing the voltage-dependence of steady-state inactivation. (D) Time course of recovery from inactivation recorded using the illustrated voltage protocol. Biophysical fit parameters for all experiments are provided in Table 8.

Table 8: CaM-D134H results in significant effects on $Na_V1.5$ peak current.

Biophysical Parameters								
	Voltage-Dependence of Activation			Steady-State Availability			Recovery From Inactivation	
	$V_{1/2}$ (mV)	k (mV)	n	$V_{1/2}$ (mV)	k (mV)	n	τ (msec)	n
$Na_V1.5$ + WT CAM	-42.4 ± 1.8	7.9 ± 0.5	7	-103.7 ± 1.2	-8.8 ± 0.4	7	11.5 ± 0.8	7
$Na_V1.5$ + D134H	-49.7 ± 2.1*	7.4 ± 0.4	7	-113.3 ± 2.0‡	-7.8 ± 0.4	7	14.9 ± 1.4*	6
$Na_V1.5$ + D132E	-45.4 ± 2.2	7.0 ± 0.5	6	-107.7 ± 2.3	8.3 ± 0.2	6	12.1 ± 1.5	6
Fetal $Na_V1.5$ + WT CAM	-43.3 ± 1.7	7.4 ± 0.3	7	-102.7 ± 1.7	-8.9 ± 0.3	8	13.8 ± 1.7	9
Fetal $Na_V1.5$ + D134H	-40.1 ± 2.9	7.3 ± 1.0	7	-97.6 ± 1.4*†	-9.0 ± 0.9	7	8.1 ± 1.0*†	7
Fetal $Na_V1.5$ + D132E	-39.9 ± 3.1	8.5 ± 0.9	7	-100.6 ± 1.1	-8.9 ± 0.5	8	9.7 ± 0.8	8

All recordings were performed with high intracellular calcium concentration
* P < 0.05 compared to $Na_V1.5$ + WT CAM ‡ P < 0.005 compared to $Na_V1.5$ + WT CAM
† P < 0.05 compared to Fetal $Na_V1.5$ + WT CAM

Table 9: There are no significant effects of CaM-D134H or CaM-D132E on persistent I_{Na}.

	Persistent Current %	n
$Na_V1.5$ + WT CaM	0.3 ± 0.1	9
$Na_V1.5$ + CaM-D134H	0.2 ± 0.1	5
$Na_V1.5$ + CaM-D132E	0.6 ±0.3	5
Fetal $Na_V1.5$ + WT CaM	0.4 ± 0.1	14
Fetal $Na_V1.5$ + CaM-D134H	0.5 ± 0.2	13
Fetal $Na_V1.5$ + CaM-D132E	0.5 ± 0.2	6

Functional effects of idiopathic VT mutation *CALM1*-F90L on cardiac sodium channels

We determined the functional consequences of CaM-F90L on cardiac sodium channel function by heterologously co-expressing WT CaM or mutant CaM-F90L with human $Na_V1.5$ in tsA201 cells and performed electrophysiological recordings (Figure 37A). Under usual conditions for recording sodium current in tsA201 cells, which involves a nominally calcium-free intracellular solution, we did not observe differences in the current density, voltage-dependence of activation, recovery from inactivation, or persistent sodium current of $Na_V1.5$ co-expressed with apo-CaM-F90L compared to apo-WT CaM (Table 10 & 11). However, apo-CaM-F90L shifted in the $V_{1/2}$ of the voltage-dependence of inactivation -5 mV (-115.0 ± 1.0 mV) compared to apo-WT CaM (-109.6 ± 1.1 mV) suggesting a loss of steady-state channel availability (Figure 37C).

To test the calcium-dependent effects of mutant CaM on $Na_V1.5$ function, we repeated these experiments with elevated intracellular calcium (~1 μM free Ca^{+2}) to provide a saturating concentration to promote binding of CaM to $Na_V1.5$.[92,124] Cells co-expressing CaM-F90L with $Na_V1.5$ exhibited a 2.2-fold increase in peak current density (-708.9 ± 137.1 pA/pF) compared to cells with WT CaM (-315.5 ± 76.4 pA/pF) or apo-WT CaM (-260.2 ± 60.6 pA/pF) (Figure 37B). The voltage-dependence of activation of $Na_V1.5$ significantly shifted the $V_{1/2}$ -7 mV by CaM-F90L (-49.7 ± 2.0 mV) compared to WT CaM (42.4 ± 1.8 mV) (Figure 37C). This suggests that CaM-F90L in the presence of elevated calcium levels results in a more depolarized activation of $Na_V1.5$. Also in the presence of elevated intracellular calcium, CaM-F90L still shifted $V_{1/2}$ of the voltage-dependence of inactivation -5 mV to more hyperpolarized potentials (-109.3 ± 2.1 mV) compared to WT CaM (-103.7 ± 1.2 mV) (Figure 37C). Mutant CaM-F90L also significantly slows the recovery from inactivation of $Na_V1.5$ (14.6 ± 2.3 msec)

compared to WT CaM (11.5 ± 0.8 msec) (Figure 37D). CaM-F90L also elicited similar effects on the fetal isoform of $Na_V1.5$ (Table 10). We did not observe any effects of CaM-F90L on persistent sodium current in high or low calcium (Table 11).

CDI is slowed by LQTS-CaM

(The following experiments were performed by researchers at the University of Kentucky in the laboratory of John Satin.)

We tested the hypothesis that LQTS-CaM mutations with impaired C-domain Ca^{2+} affinity will slow I_{CaL} decay in a native cardiomyocyte environment due to impaired CDI.[7] A slowing of CDI is one molecular mechanism of LQTS. Figure 38A illustrates representative current sweeps normalized to peak current for FVM expressing exogenous WT-CaM superimposed on traces from cells expressing each of the LQTS-CaM mutants. All LQTS-CaM mutants slow I_{CaL} decay to degrees that match the rank order of Ca^{2+}-CaM affinity (Figure 38B). Current density and voltage-dependence of current activation were not different between FVM expressing WT or LQTS-CaM mutants. These data suggest that attenuated CDI and resulting slower I_{CaL} decay contribute to mutant CaM-associated LQTS.

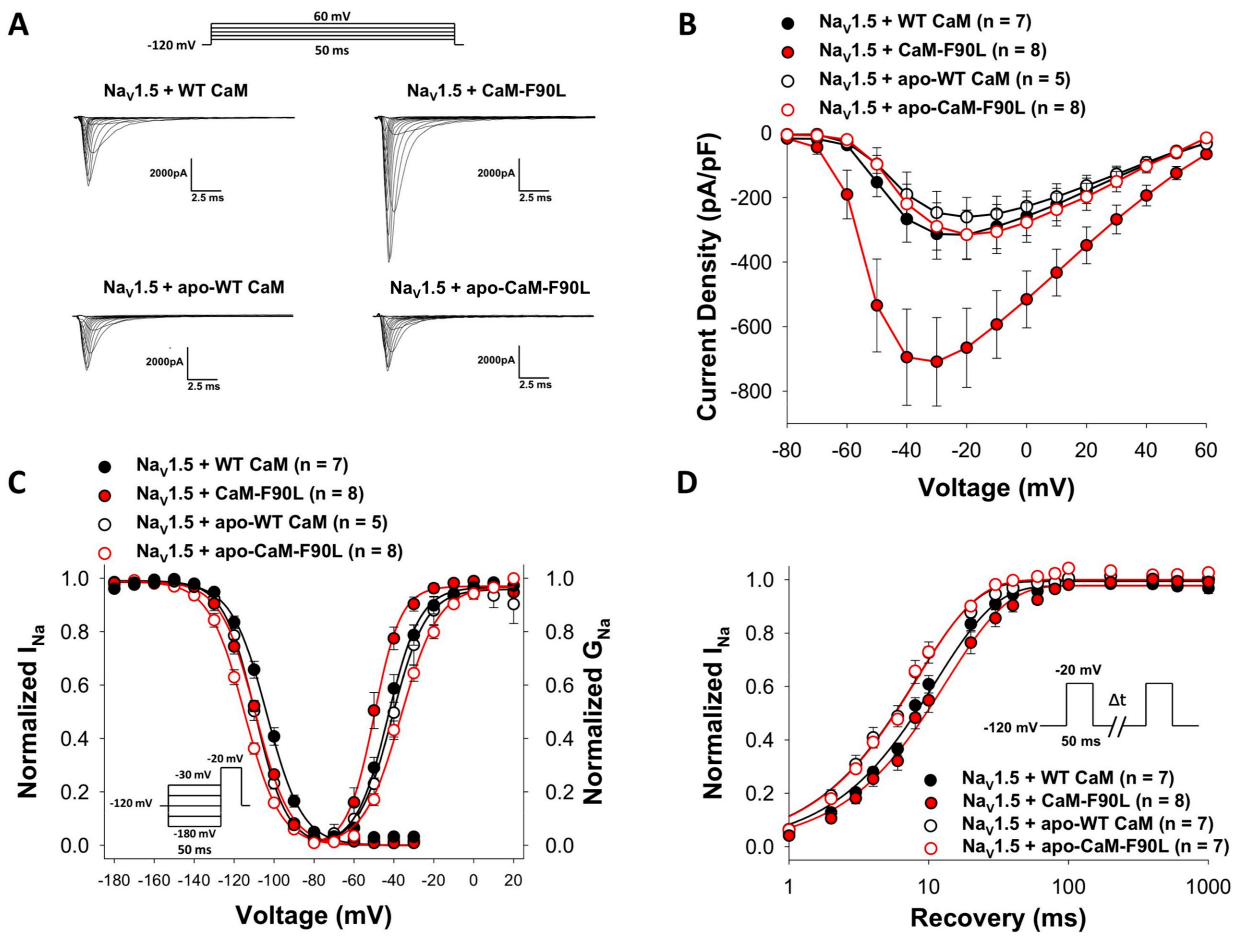

Figure 37: CaM-F90L increases current density, shifts voltage-dependence of activation, inactivation and slows the recovery from inactivation.

(A) Representative traces of Na$_V$1.5 co-expressed with WT CaM or CaM-F90L under conditions of nominal (apo) and elevated calcium. (B) Current density-voltage relationships comparing WT and CaM-F90L effects on Na$_V$1.5 channels (n = 5-8). (C) Conductance-voltage and steady-state voltage dependence of inactivation relationships for Na$_V$1.5 co-expressed with WT or CaM-F90L (n = 5-8). Lines represent average fits of the data with Boltzmann functions. (D) Recovery from inactivation of Na$_V$1.5 co-expressed with WT or CaM-F90L (n = 5-8). Biophysical fit parameters for all experiments are provided in Table 10.

Table 10: CaM-F90L increases current density, shifts voltage-dependence of activation, inactivation and slows the recovery from inactivation under high calcium conditions.

Biophysical Parameters										
	Current Density		Voltage-Dependence of Activation			Steady-State Availability			Recovery From Inactivation	
	Peak Current Density (pA/pF)	n	$V_{1/2}$ (mV)	k (mV)	n	$V_{1/2}$ (mV)	k (mV)	n	τ (msec)	n
$Na_V1.5$ + apo-WT CaM	-260.2 ± 60.6	5	-40.6 ± 3.7	8.0 ± 0.6	5	-109.6 ± 1.1	-7.9 ± 0.4	5	8.6 ± 0.9	7
$Na_V1.5$ + apo-CaM-F90L	-314.8 ± 75.6	8	-36.2 ± 1.3	9.2 ± 0.3	8	-115.0 ± 1.0 [c]	-9.0 ± 0.5	8	8.8 ± 0.4	7
$Na_V1.5$ + WT CaM	-315.5 ± 76.4	7	-42.4 ± 1.8	7.9 ± 0.5	7	-103.7 ± 1.2 [b]	-8.8 ± 0.4	7	11.5 ± 0.8	7
$Na_V1.5$ + CaM-F90L	-708.9 ± 137.1 [abc]	8	-49.7 ± 2.0 [ab]	6.2 ± 0.5‡	8	-109.3 ± 2.1 [bc]	-8.1 ± 0.2	8	14.6 ± 2.3 [ab]	8
Fetal $Na_V1.5$ + WT CaM	-178.4 ± 43.3	7	-43.3 ± 1.7	7.4 ± 0.3	7	-102.7 ± 1.7	-8.9 ± 0.3	8	13.8 ± 1.7	9
Fetal $Na_V1.5$ + F90L	-820.9 ± 164.9 [acd]	7	-50.0 ± 3.6	5.8 ± 0.4 [acd]	7	-107.8 ± 3.8	-8.5 ± 0.1	8	13.1 ± 3.0	7

[a] P < 0.05 compared to $Na_V1.5$ +apo-WT CaM
[b] P < 0.05 compared to $Na_V1.5$ + apo-CaM F90L
[c] P < 0.05 compared to $Na_V1.5$ + WT CaM
[d] < 0.05 compared to Fetal $Na_V1.5$ + WT CaM

Table 11: CaM-F90L does not have significant effects on persistent sodium $I_{Na.}$

	Persistent Current %	n
$Na_V1.5$ + WT CaM	0.3 ± 0.1	9
$Na_V1.5$ + CaM-F90L	0.3 ± 0.2	5
Fetal $Na_V1.5$ + WT CaM	0.4 ± 0.1	14
Fetal $Na_V1.5$ + CaM-F90L	0.2 ± 0.1	7

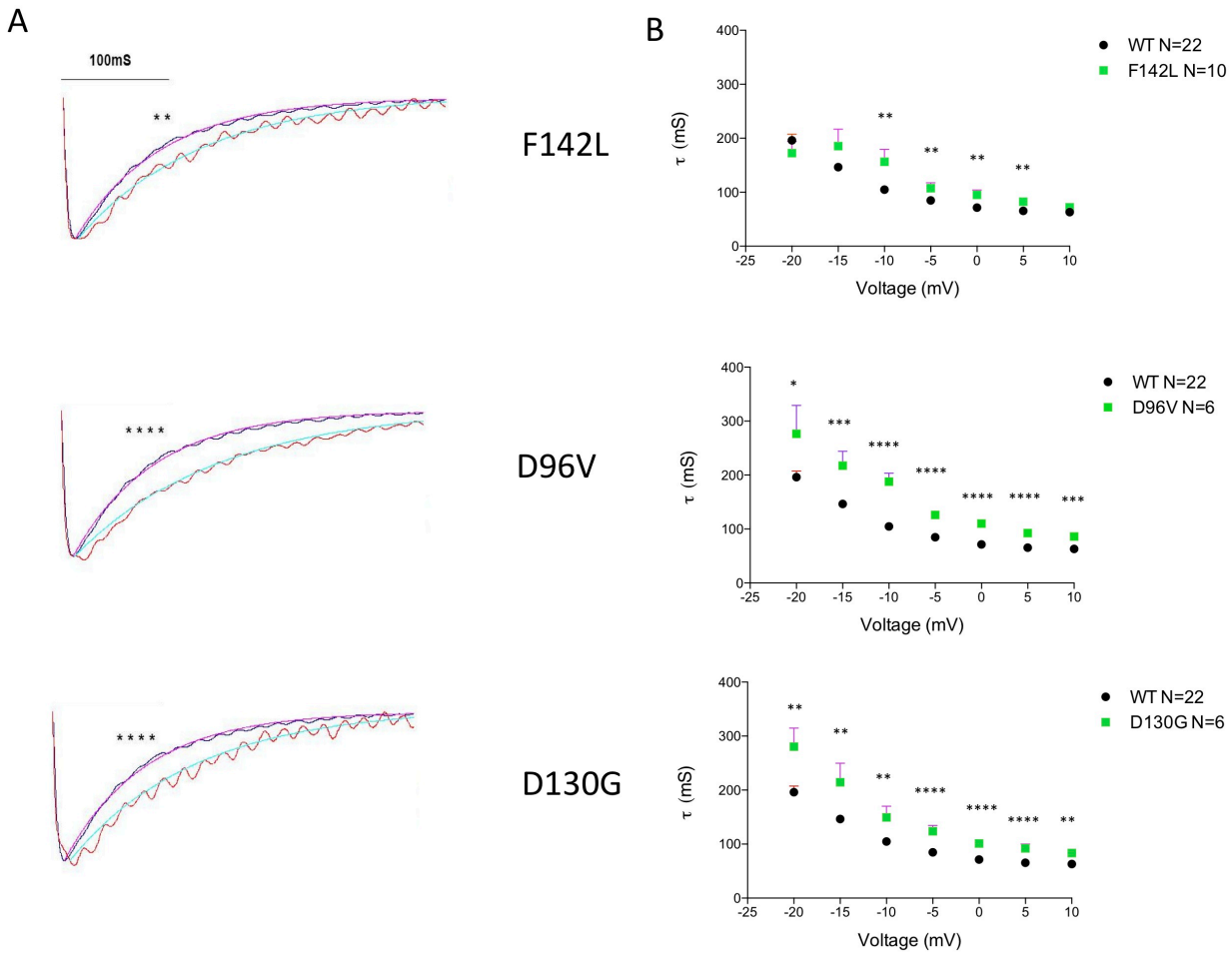

Figure 38: LQTS-CaM mutants slow CDI.

(A) Representative traces recorded during a depolarization to 0 mV. The single exponential fit of a representative WT-CaM current sweep (dotted line) is illustrated for reference. The smooth line through the current traces is a single exponential fit of the form: $I(t) = I_{peak} * e^{-t/t}$. (B) Inactivation time constant (t) plotted as a function of voltage. For clarity, the WT-CaM data are illustrated along with each LQTS-CaM mutation plot. **p<0.01; ****p<10^{-4}.

Discussion

The major new finding of this study is that CaM mutants associated with LQTS cause significantly slowed CDI of I_{CaL} that may alter Ca^{2+} homeostasis in fetal ventricular cardiomyocytes. We also excluded a major contribution of dysregulated sodium current caused by LQTS-CaM mutations. We can conclude that LQTS-CaM uses the novel mechanism of slowing of CDI to initiate the sequence of cellular physiological events leading to ventricular arrhythmia.

Fetal sodium channel dysfunction evoked by CaM-D130G under high calcium conditions suggests a unique interaction of mutant calmodulin with the fetal splice variant of $Na_V1.5$ that is calcium dependent. In addition, this effect is not due to CAMKII phosphorylation of $Na_V1.5$. However, there was not a persistent sodium current evoked by CaM-D130G in native fetal mouse cardiomyocytes that express fetal $Na_V1.5$ (Figure 31).[88] This may be an effect unique to the human fetal sodium channels or the expression of mouse fetal $Na_V1.5$ at that time in development. We cannot rule out speculation that under high calcium conditions that occur physiologically in the myocyte or under some pathological conditions,[136,137] there may be an aberrant interaction of mutant calmodulin with fetal $Na_V1.5$ that evokes persistent sodium currents in addition to the loss of CDI of L-type calcium channels. We speculate that the human fetal $Na_V1.5$ may also exhibit some allosteric effects on CaM-D130G that contribute to this unique effect. Further studies in human iPS-derived cardiomyocytes from these patients may provide further insight to the effects of CaM-D130G on human fetal $Na_V1.5$.

Although CaM mutations associated with LQTS did not have a consistent effect on sodium channel function, we show that a CaM mutant associated with idiopathic VT evokes a gain of function of $Na_V1.5$ under high calcium conditions (Figure 37). In addition, CaM-F90L

does not have any significant effects on the CDI of L-type calcium channels (data not shown). This suggests that $Na_V1.5$ may be involved in the molecular mechanisms of other arrhythmias associated with mutant CaMs. However, future studies in native cardiomyocytes will provide further insight on these effects.

The studies investigating mutant CaM effects on L-type calcium channel (LTCC) function show a rank-order relationship between Ca^{2+}-CaM affinity and the propensity for abnormal Ca^{2+} homeostasis. This relationship holds for the three tested LQTS-CaM mutants. LQTS is driven by a prolongation of the ventricular cellular action potential duration (APD), and APD is determined by the sum of ionic conductances, principally, net voltage-gated potassium channels and LTCC. CaM pre-bound to LTCC confers a direct relationship between CaM alterations of LTCC current and APD whereby increased Ca^{2+} influx prolongs APD.[4] The LQTS-CaM mutations studied occurred *de novo* within the carboxyl-terminus (C-lobe) of CaM.[92] The C-lobe of LTCC-bound CaM senses Ca^{2+}-entry through single LTCC channel openings and this occurs in a restricted space where local [Ca^{2+}] can reach levels as high as 60-100 μM.[138,139] The LQTS-CaM mutation F142L C-lobe Ca^{2+}-affinity K_d is 15 μM; well below the estimated local [Ca^{2+}] and thus may explain the relatively subtle effects observed with F142L. The D130G Ca^{2+} K_d is 150 μM that is consistent with a greater propensity to promote pathological Ca^{2+} transients among the LQTS-CaM mutants tested. Overall, LQTS-CaM slows Ca^{2+}-dependent inactivation of LTCCs (Figure 38) and further explains the pathogenesis of LQTS in these cases.

CONCLUSIONS

Here we conclude that the voltage-gated cardiac sodium channel is not consistently involved in the molecular mechanisms of LQTS associated with mutations in calmodulin. However, aberrant mutant CaM function that is calcium dependent may occur in some cases, such as in idiopathic VT, that results in sodium channel dysfunction. We also conclude that LQTS-CaM uses the novel mechanism of slowing of CDI to initiate the sequence of cellular physiological events leading to ventricular arrhythmia. In summary, LQTS-CaM mutations both disrupt calcium homeostasis in murine cardiomyocytes but there is a sharp dichotomy in pathways leading to pathological phenotypes. LQTS-CaM mutations occurring on the C-lobe of CaM reduce Ca^{2+}-affinity and consequently cause slowing of LTCC kinetics by attenuating CDI. These results suggest a potential proof-of-principle for genotype-specific treatment of “calmodulinopathies.”

CHAPTER V

Summary & Future Directions

SUMMARY

Mutations in *SCN5A* encoding the cardiac voltage-gated sodium channel ($Na_V1.5$) can result in severe life-threatening cardiac arrhythmias such as long QT syndrome (LQTS). However, the molecular basis for arrhythmia susceptibility in early developmental stages were previously unknown. Although many *SCN5A* mutations associated with SIDS or perinatal LQTS have been investigated in the canonical adult $Na_V1.5$, the molecular factors that predisposed to the early onset and severity of these arrhythmias were still unknown. Therefore we considered an alternative splicing mechanism of the cardiac sodium channel and proteins that interact with cardiac ion channels as molecular factors that may contribute to sudden death risk in early life.

Here we have presented the molecular mechanisms of *SCN5A* mutations and calmodulin mutations associated with perinatal LQTS in the context of a fetal-expressed splice variant of the voltage-gated cardiac sodium channel, fetal $Na_V1.5$. These studies are important for determining the molecular mechanism for severe arrhythmias that manifest in the earliest stages of development. We hypothesized that fetal $Na_V1.5$ would provide a sensitive background for mutations that have been associated with increased arrhythmia susceptibility

and sudden death during early life. Our findings demonstrate an important contribution of developmentally regulated alternative *SCN5A* splicing to the genetic risk for prenatal life-threatening cardiac arrhythmias. We have shown that the *SCN5A* mutations associated with perinatal forms of LQTS (L409P/R558, R1623Q, F1473C and A1330D) exhibit more severe or similar functional consequences in the fetal $Na_V1.5$ compared to their expression in the canonical adult sodium channel (Chapter II and III). In addition, we have shown that a more typical onset LQT3 mutation, delKPQ, exhibits an attenuated gain of function in the fetal $Na_V1.5$ compared to expression of the mutation in the adult $Na_V1.5$ (Chapter III). These results support the hypothesis that fetal $Na_V1.5$ may mask the effects of a typical onset LQT3 mutation. Therefore, fetal $Na_V1.5$ is a distinguishing factor in the presentation of LQT3 in these cases.

We also concluded that the voltage-gated cardiac sodium channel is not consistently involved in the molecular mechanisms of LQTS associated with mutations in calmodulin. Furthermore, it is the slowing of L-type calcium channel ($Ca_V1.2$) Ca^{2+}-dependent inactivation (CDI) that may promote arrythmogenesis in calmodulinopathies associated with LQTS (Chapter IV). These findings are important for the genotype-specific treatment of severe arrhythmias associated with calmodulin mutations.

Taken together we present a novel mechanism in the pathogenesis of cardiac arrhythmias associated with a severe and early onset of LQTS. This is also important for the appropriate treatment of these arrhythmias. Currently, fetal LQTS is treated by infusion of lidocaine, a sodium channel blocker. However, we have shown that lidocaine may be an ineffective treatment option in some cases of fetal LQTS such as for fetal $Na_V1.5$-L409P/R558

(Chapter II). Further experiments are required to determine whether the fetal $Na_V1.5$ exhibits an altered pharmacology in the presence of lidocaine compared to the adult $Na_V1.5$.

Further treatment options such as gene therapy or more selective channel blockers need to be explored for cases of fetal LQTS because treatment options are currently very limited. The majority of patients with neonatal LQTS are treated with implantable cardioverter defibrillators (ICD) after birth. ICDs use electrical pulses or shocks to treat life-threatening arrhythmias that occur in the ventricles. These devices have been shown to be beneficial in the long term for patients with severe forms of LQTS.[98,140,141] However, further research is required to determine the appropriate shock required to terminate fibrillation at the lowest energy to prevent severe tissue damage or inappropriate shocks.[142] It is very important to improve our understanding of the molecular mechanisms of cardiac arrhythmias so that patients can be treated appropriately.

FUTURE DIRECTIONS

The majority of the experiments shown in Chapters II-IV involve a heterologous expression system to express the fetal or adult $Na_V1.5$ in order to study specific functional effects of *SCN5A* or calmodulin mutations. While this is an appropriate method to elucidate the molecular mechanism of sodium channel dysfunction, further experiments are required to determine if these effects are pathological in the human heart. One simple approach would be to use a mathematical model with the persistent sodium currents measured from cells expressing WT or mutant sodium channels as an input to determine the effects on the human action potential. However, these models do not provide the concrete evidence needed to establish the mechanism of the arrhythmia.

It is more favorable to utilize an animal model such as the rabbit to determine if the persistent sodium currents evoked by *SCN5A* mutations result in abnormal action potential morphology compared to expression of WT channels. However, this approach poses a difficult technical problem of silencing or pharmacologically inhibiting the rabbit endogenous sodium currents while virally transducing the mutant or WT human sodium channels into isolated ventricular myocytes. Multiple approaches have been tested in our laboratory such as adenovirus, lentivirus, and biolistics but these approaches have been unsuccessful with sodium channel expression. Furthermore, there is heterogeneity of the ventricular action potential among animal models due to the variation in expression of ionic currents.[8,12,143,144]

Another approach to determine the effects of *SCN5A* mutations on action potential morphology would be to utilize human induced pluripotent stem cell derived-cardiomyocytes

(iPSC-CMs) to elucidate the molecular the mechanism of the arrhythmia.[21,145–147] However, this approach requires the consent of the patient or the patient's family to obtain the skin fibroblasts. Once the fibroblasts are obtained, they must be reprogrammed to a pluripotent state using viral vectors.[148,148,149] When the cells reach a state of pluripotency, they are coaxed to differentiate into cardiomyocytes.[146] The entire process can take up to several months.[145,150] The advantage of using these cells as a model is that they can recapitulate the disease phenotype of the patient such as prolonged action potentials from a patient with LQTS.[21,147]

Unfortunately, there are disadvantages to the use of iPSC-CMs because they are not mature cardiomyocytes. They cannot be differentiated into pure populations of ventricular or atrial cardiomyocytes.[145,146] It is still a technical challenge to sort iPSC-CMs based upon action potential morphology alone.[21,146] In addition, many factors may contribute to the variation and maturity of atrial, nodal, and ventricular-like action potentials including cardiomyocyte differentiation protocols, culture conditions of differentiated cardiomyocytes, and recording procedures.[146] Future work in the field is focused on investigating the molecular determinants involved in producing pure populations of cardiomyocytes and nodal cells.[151]

Our laboratory has demonstrated prominent expression of the alternatively spliced fetal $Na_V1.5$ mRNA transcript using RT-PCR in fetal and infant human heart.[52] We used the same assay to investigate the ratio of fetal to adult $Na_V1.5$ transcripts in iPSC-CMs 30 days post-induction. We observed that the fetal:adult ratio of mRNA transcript was 33.1 indicating predominant expression of the fetal splice variant in these cells. These data indicated that iPSC-CMs mainly express fetal $Na_V1.5$ at 30 days and 90 days post-induction. Further work was proposed to investigate the time-dependence of alternative splicing in iPSC-CMs and to establish correlations with channel function. However, a more mature population of cells is

required for these studies based on our preliminary findings that the fetal $Na_V1.5$ is primarily expressed in these cells.

In addition to changing the model to study the unique functional effects of fetal $Na_V1.5$, we must also consider that fetal $Na_V1.5$ may exhibit an altered pharmacology in response to sodium channel blockers such as lidocaine. Lidocaine is a class Ib anti-arrhythmic used in the treatment of ventricular arrhythmias. The mechanism of action of lidocaine on $Na_V1.5$ in the open and inactivated states promotes shortening of the cardiac action potential duration. Lidocaine has been administered to pregnant women whose fetuses exhibit ventricular rhythm disturbances and is a tolerable treatment at an early developmental stage.[152] In Chapter II we show that fetal $Na_V1.5$-L409P/R558 is resistant to lidocaine treatment suggesting this treatment may be ineffective in some cases of fetal LQTS.

Previous studies were preformed in our laboratory on the pharmacology of a splice variant of *SCN1A* (SCN1A-5N) which is the same conserved splicing event exhibited for fetal $Na_V1.5$.[84] The splice variant SCN1A-5N exhibited enhanced tonic block and use-dependent block by phenytoin and lamotrigine across a range of stimulation frequencies and concentrations as well as induced shifts in steady-state inactivation and recovery from fast inactivation. These data suggest that the splice variant is more sensitive to commonly used anti-epileptic drugs.[153] It is likely that the fetal splice variant of $Na_V1.5$ will also exhibit differential pharmacological responses to lidocaine or other sodium channel blockers when compared to the adult $Na_V1.5$. Another interesting candidate to study the pharmacological effects on the fetal $Na_V1.5$ is ranolazine because it has been shown to inhibit persistent sodium current.[132,154] These studies are required to evaluate the current methods of treatment of fetal and neonatal LQTS and to promote the development of new therapeutic strategies.

The remaining question beyond the studies presented in Chapters II-IV, is why the fetal heart requires an alternative splicing mechanism of $Na_V1.5$. We speculate that the depolarized activation of fetal $Na_V1.5$ may be a protective mechanism for the developmental changes in resting membrane potential of fetal cardiomyocytes from more depolarized potentials to hyperpolarized potentials. We conceive that this would result in a more depolarized threshold of sodium channel activation in the immature heart.[10,12,151,155]

It is also plausible that there is a functional role of fetal $Na_V1.5$ beyond membrane depolarization such as in the migration of fetal cardiomyocytes in the developing heart.[89] The disruption of the mouse cardiac sodium channel gene, *Scn5a*, causes intrauterine lethality in homozygotes with severe defects in ventricular morphogenesis whereas heterozygotes show normal survival.[156] Fetal $Na_V1.5$ has been shown to be required in the migration of human metastatic breast cancer cells (MDA-MB-231). Migrated MDA-MB-231 cells expressed more fetal $Na_V1.5$ protein at the plasma membrane than non-migrated cells.[89] To become motile and invasive, embryonic epithelial cells undergo a process of mesenchymal conversion known as epithelial-to-mesenchymal transition (EMT). Likewise, EMT can be seen in cancer cells as they leave the primary tumor and disseminate to other parts of the body to colonize distant organs and form metastases.[157,158] Therefore, the effects of fetal $Na_V1.5$ on MDA-MB-231 cells may also provide a similar mechanism in the developing heart.

To test whether fetal $Na_V1.5$ has a greater role in the developing heart, future work would require the development of a mouse model that only expressed either the adult or fetal $Na_V1.5$. For example, a fetal $Na_V1.5$ knockout mouse may reveal an abnormal phenotype that would result in further dissection of the function of fetal $Na_V1.5$ in embryonic development, cardiac conduction, or ventricular morphogenesis. However, the development of such a mouse

model would require further investigation into the mechanism of the alternative splicing event and required machinery involved. The mouse fetal $Na_V1.5$ has the same 7 amino acid substitutions found in the human fetal $Na_V1.5$ protein sequence (See Chapter I) but differs in the DNA sequence by 4 nucleotides, which may be either silent or regulatory. Therefore, a mouse model may be a useful experimental tool to investigate the molecular mechanisms of cardiac arrhythmias and cardiac development associated with fetal $Na_V1.5$ and provide further information on the regulation of the expression of the splice variant.[104,159,160]

In Chapter IV we show that the fetal $Na_V1.5$ is sensitive to a calmodulin mutation, CaM-D130G that evokes persistent sodium current under high calcium conditions. Although this effect was not recapitulated in mouse fetal cardiomyocytes, this suggests that human fetal $Na_V1.5$ may exhibit a unique interaction with calmodulin. Further studies investigating the calcium sensitivity of fetal $Na_V1.5$ may provide insight to the functional effects of CaM on the alternative splice variant compared to the adult isoform of the channel. These experiments could be modeled after previous work on the calcium sensitivity of canonical $Na_V1.5$.[124,161] Similar studies investigating the effect of pH changes on fetal $Na_V1.5$ may also provide insight to the adaptive electrophysiological response in fetal development.[162–166]

In summary, multiple approaches may be used to further investigate the molecular mechanisms of LQTS that manifest in the early stages of life. Future work to improve the differentiation of iPSC-CMs or to develop a mouse model to study the role of fetal $Na_V1.5$ in development would provide further insight to the mechanism of arrhythmogenesis of early onset LQT3. Furthermore, we have used our heterologous expression system (Chapter II-IV) to demonstrate an important contribution of developmentally regulated alternative *SCN5A* splicing to the genetic risk for perinatal life-threatening cardiac arrhythmias. These studies

were highly important to establish a molecular mechanism in the pathogenesis of LQT3 in the earliest stages of development.

REFERENCES

1. Roden, D. M., Balser, J. R., George, A. L., Jr & Anderson, M. E. Cardiac ion channels. *Annu. Rev. Physiol.* **64,** 431–475 (2002).

2. Dhamoon, A. S. & Jalife, J. The inward rectifier current (I_{K1}) controls cardiac excitability and is involved in arrhythmogenesis. *Heart Rhythm Journal* **2,** 316–324 (2005).

3. Kubo, Y. *et al.* International Union of Pharmacology. LIV. Nomenclature and molecular relationships of inwardly rectifying potassium channels. *Pharmacol. Rev.* **57,** 509–526 (2005).

4. Grant, A. O. Cardiac Ion Channels. *Circ. Arrhythm. Electrophysiol.* **2,** 185–194 (2009).

5. Antzelevitch, C. & Dumaine, R. *Handbook of Physiology: Electrical heterogeneity in the heart: physiological, pharmacological and clinical implications*. (Oxford University Press, 2002).

6. Watanabe, T., Delbridge, L. M., Bustamante, J. O. & McDonald, T. F. Heterogeneity of the action potential in isolated rat ventricular myocytes and tissue. *Circ. Res.* **52,** 280–290 (1983).

7. Boukens, B. J. D., Christoffels, V. M., Coronel, R. & Moorman, A. F. M. Developmental basis for electrophysiological heterogeneity in the ventricular and outflow tract myocardium as a substrate for life-threatening ventricular arrhythmias. *Circ. Res.* **104,** 19–31 (2009).

8. Felzen, B., Rubinstein, I., Lotan, R. & Binah, O. Developmental changes in ventricular action potential properties in guinea-pigs are modulated by age-related changes in the thyroid state. *J. Mol. Cell. Cardiol.* **23,** 787–794 (1991).

9. Kato, Y., Masumiya, H., Agata, N., Tanaka, H. & Shigenobu, K. Developmental changes in action potential and membrane currents in fetal, neonatal and adult guinea-pig ventricular myocytes. *J. Mol. Cell. Cardiol.* **28,** 1515–1522 (1996).

10. Abd Allah, E. *et al.* Changes in the expression of ion channels, connexins and Ca^{2+} handling proteins in the sinoatrial node during postnatal development. *Exp. Physiol.* (2011). doi:10.1113/expphysiol.2010.055780

11. Parilla, B. V. & Strasburger, J. F. Fetal Arrhythmias. *Glob. Libr. Womens Med.* (2009). doi:10.3843/GLOWM.10200

12. Cordeiro, J. M. *et al.* Developmental changes in expression and biophysics of ion channels in the canine ventricle. *J. Mol. Cell. Cardiol.* **64,** 79–89 (2013).

13. Kass, R. S. & Moss, A. J. Long QT syndrome: novel insights into the mechanisms of cardiac arrhythmias. *J. Clin. Invest.* **112,** 810–815 (2003).

14. Couch, J. R., West, T. C. & Hoff, H. E. Development of the Action Potential of the Prenatal Rat Heart. *Circ. Res.* **24,** 19–31 (1969).

15. Davies, M. P. *et al.* Developmental Changes in Ionic Channel Activity in the Embryonic Murine Heart. *Circ. Res.* **78,** 15–25 (1996).

16. Harrell, M. D., Harbi, S., Hoffman, J. F., Zavadil, J. & Coetzee, W. A. Large-scale analysis of ion channel gene expression in the mouse heart during perinatal development. *Physiol. Genomics* **28,** 273 (2007).

17. Crotti, L., Celano, G., Dagradi, F. & Schwartz, P. J. Congenital long QT syndrome. *Orphanet J. Rare Dis.* **3,** 18 (2008).

18. Cuneo, B. F. *et al.* Prenatal diagnosis and in utero treatment of torsades de pointes associated with congenital long QT syndrome. *Am. J. Cardiol.* **91,** 1395–1398 (2003).

19. Splawski, I. *et al.* Spectrum of Mutations in Long-QT Syndrome Genes K_V*LQT1*, *HERG, SCN5A*, *KCNE1*, and *KCNE2*. *Circulation* **102,** 1178–1185 (2000).

20. Moss, A. J. *et al.* Clinical Aspects of Type-1 Long-QT Syndrome by Location, Coding Type, and Biophysical Function of Mutations Involving the *KCNQ1* Gene. *Circulation* **115,** 2481–2489 (2007).

21. Itzhaki, I. *et al.* Modelling the long QT syndrome with induced pluripotent stem cells. *Nature* **471,** 225–229 (2011).

22. Takenaka, K. *et al.* Exercise stress test amplifies genotype-phenotype correlation in the LQT1 and LQT2 forms of the long-QT syndrome. *Circulation* **107,** 838–844 (2003).

23. Sy, R. W. *et al.* Repolarization dynamics during exercise discriminate between LQT1 and LQT2 genotypes. *J. Cardiovasc. Electrophysiol.* **21,** 1242–1246 (2010).

24. Kim, J. A. *et al.* Trigger-specific risk factors and response to therapy in long QT syndrome type 2. *Heart Rhythm Journal* **7,** 1797–1805 (2010).

25. Bianchi, L. *et al.* Cellular Dysfunction of LQT5-MinK Mutants: Abnormalities of I_{Ks}, I_{Kr} and Trafficking in Long QT Syndrome. *Hum. Mol. Genet.* **8,** 1499–1507 (1999).

26. Abbott, G. W. & Goldstein, S. A. Potassium channel subunits encoded by the KCNE gene family: physiology and pathophysiology of the MinK-related peptides (MiRPs). *Mol. Interv.* **1,** 95–107 (2001).

27. Um, S. Y. & McDonald, T. V. Differential Association between HERG and *KCNE1* or *KCNE2*. *PLoS ONE* **2,** (2007).

28. Schwartz, P. J., Ackerman, M. J., George, A. L., Jr & Wilde, A. A. M. Impact of genetics on the clinical management of channelopathies. *J. Am. Coll. Cardiol.* **62,** 169–180 (2013).

29. Yang-Feng, T. L. *et al.* Chromosomal organization of adrenergic receptor genes. *Proc. Natl. Acad. Sci. U. S. A.* **87,** 1516–1520 (1990).

30. Mohler, P. J., Davis, J. Q. & Bennett, V. Ankyrin-B Coordinates the Na/K ATPase, Na/Ca Exchanger, and InsP3 Receptor in a Cardiac T-Tubule/SR Microdomain. *PLoS Biol.* **3,** (2005).

31. Mohler, P. J. *et al.* Ankyrin-B mutation causes type 4 long-QT cardiac arrhythmia and sudden cardiac death. *Nature* **421,** 634–639 (2003).

32. Splawski, I. *et al.* Severe arrhythmia disorder caused by cardiac L-type calcium channel mutations. *Proc. Natl. Acad. Sci. U. S. A.* **102,** 8089–8096; discussion 8086–8088 (2005).

33. Crump, S. M., Andres, D. A., Sievert, G. & Satin, J. The cardiac L-type calcium channel distal carboxy terminus autoinhibition is regulated by calcium. *Am. J. Physiol. Heart Circ. Physiol.* **304,** H455–464 (2013).

34. Haack, J. A. & Rosenberg, R. L. Calcium-dependent inactivation of L-type calcium channels in planar lipid bilayers. *Biophys. J.* **66,** 1051–1060 (1994).

35. Tristani-Firouzi, M. *et al.* Functional and clinical characterization of *KCNJ2* mutations associated with LQT7 (Andersen syndrome). *J. Clin. Invest.* **110,** 381–388 (2002).

36. Hedley, P. L. *et al.* The role of CAV3 in long-QT syndrome: clinical and functional assessment of a caveolin-3/K_V11.1 double heterozygote versus caveolin-3 single heterozygote. *Circ. Cardiovasc. Genet.* **6,** 452–461 (2013).

37. Medeiros-Domingo, A. *et al.* SCN4B-encoded sodium channel beta4 subunit in congenital long-QT syndrome. *Circulation* **116,** 134–142 (2007).

38. George, A. L. Inherited disorders of voltage-gated sodium channels. *J. Clin. Invest.* **115,** 1990–1999 (2005).

39. Ruan, Y., Liu, N. & Priori, S. G. Sodium channel mutations and arrhythmias. *Nat Rev Cardiol* **6,** 337–348 (2009).

40. William A, C. From Ionic Currents to Molecular Mechanisms: The Structure and Function of Voltage-Gated Sodium Channels. *Neuron* **26,** 13–25 (2000).

41. Payandeh, J., Scheuer, T., Zheng, N. & Catterall, W. A. The crystal structure of a voltage-gated sodium channel. *Nature* **475,** 353–358 (2011).

42. Kuo, C.-C. & Bean, B. P. Na^+ channels must deactivate to recover from inactivation. *Neuron* **12,** 819–829 (1994).

43. Wilde, A. A. M. & Brugada, R. Phenotypical Manifestations of Mutations in the Genes Encoding Subunits of the Cardiac Sodium Channel. *Circ. Res.* **108,** 884 –897 (2011).

44. Huang, H., Priori, S. G., Napolitano, C., O'Leary, M. E. & Chahine, M. Y1767C, a novel *SCN5A* mutation, induces a persistent Na^+ current and potentiates ranolazine inhibition of $Na_V1.5$ channels. *Am. J. Physiol.-Heart Circ. Physiol.* **300,** H288 (2011).

45. Wedekind, H. *et al.* De Novo Mutation in the *SCN5A* Gene Associated With Early Onset of Sudden Infant Death. *Circulation* **104,** 1158 –1164 (2001).

46. Schwartz, P. J. Stillbirths, sudden infant deaths, and long-QT syndrome: puzzle or mosaic, the pieces of the Jigsaw are being fitted together. *Circulation* **109,** 2930–2932 (2004).

47. Wang, D. W. *et al.* Malignant Perinatal Variant of Long-QT Syndrome Caused by a Profoundly Dysfunctional Cardiac Sodium Channel / CLINICAL PERSPECTIVE. *Circ. Arrhythm. Electrophysiol.* **1,** 370 –378 (2008).

48. Bankston, J. R. *et al.* A Novel and Lethal De Novo LQT-3 Mutation in a Newborn with Distinct Molecular Pharmacology and Therapeutic Response. *PLoS ONE* **2,**

49. Yamagishi, H. *et al.* A de novo missense mutation (R1623Q) of the *SCN5A* gene in a Japanese girl with sporadic long QT sydrome. Mutations in brief no. 140. Online. *Hum. Mutat.* **11,** 481 (1998).

50. Chang, C. C. *et al.* A novel *SCN5A* mutation manifests as a malignant form of long QT syndrome with perinatal onset of tachycardia/bradycardia. *Cardiovasc. Res.* **64,** 268 –278 (2004).

51. Kehl, H. G. *et al.* Life-Threatening Neonatal Arrhythmia. *Circulation* **109,** e205 –e206 (2004).

52. Murphy, L. L. *et al.* Developmentally regulated *SCN5A* splice variant potentiates dysfunction of a novel mutation associated with severe fetal arrhythmia. *Heart Rhythm Journal* **9,** 590–597 (2012).

53. Miller, T. E. *et al.* Recurrent third-trimester fetal loss and maternal mosaicism for long-QT syndrome. *Circulation* **109,** 3029–3034 (2004).

54. Beinder, E. Fetal sinus bradycardia and the long QT syndrome. *Am. J. Obstet. Gynecol.* **185,** 743–747 (2001).

55. Byard, R. W. & Krous, H. F. Sudden Infant Death Syndrome: Overview and Update. *Pediatr. Dev. Pathol.* **6,** 112–127 (2003).

56. Schwartz, P. J. *et al.* Prevalence of the congenital long-QT syndrome. *Circulation* **120,** 1761–1767 (2009).

57. Schwartz, P. J. *et al.* Prolongation of the QT Interval and the Sudden Infant Death Syndrome. *N. Engl. J. Med*. **338,** 1709-1714 (1998).

58. Wang, D. W. *et al.* Cardiac Sodium Channel Dysfunction in Sudden Infant Death Syndrome. *Circulation* **115,** 368–376 (2007).

59. Arnestad, M. *et al.* Prevalence of Long-QT Syndrome Gene Variants in Sudden Infant Death Syndrome. *Circulation* **115,** 361–367 (2007).

60. Lilly, L. S. *Pathophysiology of Heart Disease*. (Lippincott Williams & Wilkins, 2007).

61. Wang, D. W., Viswanathan, P. C., Balser, J. R., George, A. L. & Benson, D. W. Clinical, Genetic, and Biophysical Characterization of *SCN5A* Mutations Associated With Atrioventricular Conduction Block. *Circulation* **105,** 341–346 (2002).

62. Besana, A., Wang, D. W., George, A. L., Jr & Schwartz, P. J. Nadolol block of $Na_V1.5$ does not explain its efficacy in the long QT syndrome. *J. Cardiovasc. Pharmacol.* **59,** 249–253 (2012).

63. Chandra, R., Starmer, C. F. & Grant, A. O. Multiple effects of KPQ deletion mutation on gating of human cardiac Na^+ channels expressed in mammalian cells. *Am. J. Physiol. - Heart Circ. Physiol.* **274,** H1643 –H1654 (1998).

64. Kambouris, N. G. *et al.* Phenotypic Characterization of a Novel Long-QT Syndrome Mutation (R1623Q) in the Cardiac Sodium Channel. *Circulation* **97,** 640–644 (1998).

65. Murphy, L. L. *et al.* Abstract 16964: *SCN5A* Splice Variant Potentiates Dysfunction of a Novel LQT3 Mutation Associated with Life-threatening Arrhythmia in a 19 Week Fetus. *Circulation.* **124**: A16964 (2011).

66. Gui, J., Wang, T., Trump, D., Zimmer, T. & Lei, M. Mutation-specific effects of polymorphism H558R in *SCN5A*-related sick sinus syndrome. *J. Cardiovasc. Electrophysiol.* **21,** 564–573 (2010).

67. Ackerman, M. J. *et al.* Spectrum and prevalence of cardiac sodium channel variants among black, white, Asian, and Hispanic individuals: implications for arrhythmogenic susceptibility and Brugada/long QT syndrome genetic testing. *Heart Rhythm Journal* **1,** 600–607 (2004).

68. Chen, L., Ballew, J., Herron, K., Rodeheffer, R. & Olson, T. A Common Polymorphism in *SCN5A* is Associated with Lone Atrial Fibrillation. *Clin. Pharmacol. Ther.* **81,** 35–41 (2007).

69. Makielski, J. C. *et al.* A Ubiquitous Splice Variant and a Common Polymorphism Affect Heterologous Expression of Recombinant Human *SCN5A* Heart Sodium Channels. *Circ. Res.* **93,** 821 –828 (2003).

70. Viswanathan, P. C., Benson, D. W. & Balser, J. R. A common *SCN5A* polymorphism modulates the biophysical effects of an *SCN5A* mutation. *J. Clin. Invest.* **111,** 341–346 (2003).

71. Tester, D. J. *et al.* Epidemiologic, molecular, and functional evidence suggest A572D-*SCN5A* should not be considered an independent LQT3-susceptibility mutation. *Heart Rhythm Journal* **7,** 912–919 (2010).

72. Chandra, R., Starmer, C. F. & Grant, A. O. Multiple effects of KPQ deletion mutation on gating of human cardiac Na^+ channels expressed in mammalian cells. *Am. J. Physiol.* **274,** H1643–1654 (1998).

73. Chandra, R., Chauhan, V. S., Starmer, C. F. & Grant, A. O. beta-Adrenergic action on wild-type and KPQ mutant human cardiac Na^+ channels: shift in gating but no change in Ca^{2+}:Na^+ selectivity. *Cardiovasc. Res.* **42,** 490–502 (1999).

74. Detta, N. *et al.* Novel deletion mutation in the cardiac sodium channel inactivation gate causes long QT syndrome. *Int. J. Cardiol.* **165,** 362–365 (2013).

75. Zipes, D. P. & Jalife, J. *Cardiac Electrophysiology: from Cell to Bedside: Expert Consult - Online and Print*. (Elsevier Health Sciences, 2013).

76. Antzelevitch, C. Genetic basis of Brugada syndrome. *Heart Rhythm Journal* **4,** 756–757 (2007).

77. Amin, A. S. *et al.* Facilitatory and inhibitory effects of *SCN5A* mutations on atrial fibrillation in Brugada syndrome. *Eur. Eur. Pacing Arrhythm. Card. Electrophysiol. J. Work. Groups Card.*

Pacing Arrhythm. Card. Cell. Electrophysiol. Eur. Soc. Cardiol. (2011). doi:10.1093/europace/eur011

78. Pandit, S. V. *et al.* Targeting atrioventricular differences in ion channel properties for terminating acute atrial fibrillation in pigs. *Cardiovasc. Res.* **89,** 843–851 (2011).

79. Nguyen, T. P., Wang, D. W., Rhodes, T. H. & George, A. L., Jr. Divergent biophysical defects caused by mutant sodium channels in dilated cardiomyopathy with arrhythmia. *Circ. Res.* **102,** 364–371 (2008).

80. Cheng, J. *et al. SCN5A* rare variants in familial dilated cardiomyopathy decrease peak sodium current depending on the common Polymorphism H558R and common splice variant Q1077del. *Clin. Transl. Sci.* **3,** 287–294 (2010).

81. Shi, R. *et al.* The cardiac sodium channel mutation delQKP 1507-1509 is associated with the expanding phenotypic spectrum of LQT3, conduction disorder, dilated cardiomyopathy, and high incidence of youth sudden death. *Europace* **10,** 1329–1335 (2008).

82. Makita, N. *et al.* The E1784K mutation in *SCN5A* is associated with mixed clinical phenotype of type 3 long QT syndrome. *J. Clin. Invest.* (2008). doi:10.1172/JCI34057

83. Black, D. L. Mechanisms of Alternative Pre-Messenger RNA Splicing. *Annu. Rev. Biochem.* **72,** 291–336 (2003).

84. Schroeter, A. *et al.* Structure and function of splice variants of the cardiac voltage-gated sodium channel $Na_V1.5$. *J. Mol. Cell. Cardiol.* **49,** 16–24 (2010).

85. Onkal, R. *et al.* Alternative splicing of $Na_V1.5$: An electrophysiological comparison of ‘neonatal’and ‘adult’isoforms and critical involvement of a lysine residue. *J. Cell. Physiol.* **216,** 716–726 (2008).

86. Shang, L. L. *et al.* Human Heart Failure Is Associated With Abnormal C-Terminal Splicing Variants in the Cardiac Sodium Channel. *Circ. Res.* **101,** 1146–1154 (2007).

87. Gao, G. & Dudley, S. C. *SCN5A* splicing variants and the possibility of predicting heart failure-associated arrhythmia. *Expert Rev. Cardiovasc. Ther.* **11,** 117–119 (2013).

88. Schroeter, A. *et al.* Structure and function of splice variants of the cardiac voltage-gated sodium channel $Na_V1.5$. *J. Mol. Cell. Cardiol.* (2010).

89. Brackenbury, W. J., Chioni, A. M., Diss, J. K. J. & Djamgoz, M. B. A. The neonatal splice variant of $Na_V1.5$ potentiates in vitro invasive behaviour of MDA-MB-231 human breast cancer cells. *Breast Cancer Res. Treat.* **101,** 149–160 (2006).

90. Chioni, A. M. *et al.* A novel polyclonal antibody specific for the $Na_V1.5$ voltage-gated Na^+ channel 'neonatal' splice form. *J. Neurosci. Methods* **147,** 88–98 (2005).

91. Plummer, N. W., McBurney, M. W. & Meisler, M. H. Alternative splicing of the sodium channel *SCN8A* predicts a truncated two-domain protein in fetal brain and non-neuronal cells. *J. Biol. Chem.* **272,** 24008–24015 (1997).

92. Crotti, L., Johnson, C.N., Graf, E., De Ferrari, G.M., Cuneo, B.F., Ovadia, M., Papagiannis, J., Feldkamp, M.D., Rathi, S.G., Kunic, J.D., Pedrazzini, M., Wieland, T., Lichtner, P., Beckmann, B., Clark, T., Shaffer, C., Benson, D.W., Kääb, S., Meitinger, T., Strom, T.M., Chazin, W.J., Schwartz, P.J., and George, A.L., Jr. Calmodulin Mutations Associated with Recurrent Cardiac Arrest in Infants. *Circulation* **In Press,** (2013).

93. Schwartz, P. J., Crotti, L., Zipes, D. & Jalife, J. *Cardiac Electrophysiology: From Cell to Bedside.* (Elsevier/Saunders, 2009).

94. Schulze-Bahr, E. *et al.* Long QT syndrome and life threatening arrhythmia in a newborn: molecular diagnosis and treatment response. *Heart Br. Card. Soc.* **90,** 13–16 (2004).

95. Hofbeck, M., Ulmer, H., Beinder, E., Sieber, E. & Singer, H. Prenatal findings in patients with prolonged QT interval in the neonatal period. *Heart Br. Card. Soc.* **77,** 198–204 (1997).

96. Ohkuchi, A. *et al.* Fetus with long QT syndrome manifested by tachyarrhythmia: a case report. *Prenat. Diagn.* **19,** 990–992 (1999).

97. Bankston, J. R. *et al.* A novel and lethal de novo LQT-3 mutation in a newborn with distinct molecular pharmacology and therapeutic response. *PloS One* **2,** e1258 (2007).

98. Ten Harkel, A. D. J. *et al.* Efficacy of an implantable cardioverter-defibrillator in a neonate with LQT3 associated arrhythmias. *Eur. Eur. Pacing Arrhythm. Card. Electrophysiol. J. Work. Groups Card. Pacing Arrhythm. Card. Cell. Electrophysiol. Eur. Soc. Cardiol.* **7,** 77–84 (2005).

99. Kehl, H. G. *et al.* Images in cardiovascular medicine. Life-threatening neonatal arrhythmia: successful treatment and confirmation of clinically suspected extreme long QT-syndrome-3. *Circulation* **109,** e205–206 (2004).

100. Gellens, M. E. *et al.* Primary structure and functional expression of the human cardiac tetrodotoxin-insensitive voltage-dependent sodium channel. *Proc. Natl. Acad. Sci. U. S. A.* **89,** 554–558 (1992).

101. Bennett, P. B., Yazawa, K., Makita, N. & George, A. L. Molecular mechanism for an inherited cardiac arrhythmia. *Nature* **376,** 683–685 (1995).

102. Watanabe, H. *et al.* Sodium channel β1 subunit mutations associated with Brugada syndrome and cardiac conduction disease in humans. *J. Clin. Invest.* **118,** 2260–2268 (2008).

103. Patino, G. A. & Isom, L. L. Electrophysiology and beyond: multiple roles of Na^+ channel β subunits in development and disease. *Neurosci. Lett.* **486,** 53–59 (2010).

104. Dhar Malhotra, J. *et al.* Characterization of sodium channel alpha- and beta-subunits in rat and mouse cardiac myocytes. *Circulation* **103,** 1303–1310 (2001).

105. Ou, S. W. *et al.* Tetrodotoxin-resistant Na^+ channels in human neuroblastoma cells are encoded by new variants of $Na_V1.5$/*SCN5A*. *Eur. J. Neurosci.* **22,** 793–801 (2005).

106. Pildner von Steinburg, S. *et al.* What is the 'normal' fetal heart rate? *PeerJ* **1,** e82 (2013).

107. Wilton, S. B. *et al.* Polymorphisms in multiple genes are associated with resting heart rate in a stepwise allele-dependent manner. *Heart Rhythm* **5,** 694–700 (2008).

108. Shinlapawittayatorn, K. *et al.* A common *SCN5A* polymorphism modulates the biophysical defects of *SCN5A* mutations. *Heart Rhythm* **8,** 455–462 (2011).

109. Shinlapawittayatorn, K. *et al.* A Novel Strategy Using Cardiac Sodium Channel Polymorphic Fragments To Rescue Trafficking-Deficient *SCN5A* Mutations. *Circ. Cardiovasc. Genet.* **4,** 500–509 (2011).

110. Berul. Neonatal long QT syndrome and sudden cardiac death. *Prog. Pediatr. Cardiol.* **11,** 47–54 (2000).

111. Crotti, L. *et al.* Long QT syndrome-associated mutations in intrauterine fetal death. *JAMA J. Am. Med. Assoc.* **309,** 1473–1482 (2013).

112. Chang, I. *et al.* Prenatal diagnosis and treatment of fetal long QT syndrome: a case report. *Prenat. Diagn.* **22,** 1209–1212 (2002).

113. Murphy, L. L., Kunic, J. D. & George, A. L. Abstract 14835: Ultra-Fast Recovery from Inactivation Distinguishes *SCN5A* Dysfunction in Fetal vs Later Onset Long-QT Syndrome. *Circulation* **126**:A14835 (2012).

114. Wang, Q. *et al.* Cardiac sodium channel mutations in patients with long QT syndrome, an inherited cardiac arrhythmia. *Hum. Mol. Genet.* **4,** 1603–1607 (1995).

115. Wang, Q. *et al. SCN5A* mutations associated with an inherited cardiac arrhythmia, long QT syndrome. *Cell* **80,** 805–811 (1995).

116. Ackerman, M. J. *et al.* Postmortem molecular analysis of *SCN5A* defects in sudden infant death syndrome. *JAMA J. Am. Med. Assoc.* **286,** 2264–2269 (2001).

117. Splawski, I. *et al.* Spectrum of Mutations in Long-QT Syndrome Genes K_VLQT1, HERG, *SCN5A*, *KCNE1*, and *KCNE2*. *Circulation* **102,** 1178–1185 (2000).

118. Wang, D. W., Yazawa, K., George, A. L. & Bennett, P. B. Characterization of human cardiac Na+ channel mutations in the congenital long QT syndrome. *Proc. Natl. Acad. Sci*. **93,** 13200–13205 (1996).

119. Napolitano, C., Bloise, R., Monteforte, N. & Priori, S. G. Sudden cardiac death and genetic ion channelopathies: long QT, Brugada, short QT, catecholaminergic polymorphic ventricular tachycardia, and idiopathic ventricular fibrillation. *Circulation* **125,** 2027–2034 (2012).

120. Naomasa Makita *et al.* 13371 - CALM2 Mutations Associated With Atypical Juvenile Long QT Syndrome. *Circulation* **128:A13371,** (2013).

121. Marsman, R. F. *et al.* A Mutation in CALM1 Encoding Calmodulin in Familial Idiopathic Ventricular Fibrillation in Childhood and Adolescence. *J. Am. Coll. Cardiol.* **63,** 259–266 (2014).

122. Nyegaard, M. *et al.* Mutations in calmodulin cause ventricular tachycardia and sudden cardiac death. *Am. J. Hum. Genet.* **91,** 703–712 (2012).

123. Aiba, T. *et al.* Na^+ channel regulation by Ca^{2+}/calmodulin and Ca^{2+}/calmodulin-dependent protein kinase II in guinea-pig ventricular myocytes. *Cardiovasc. Res.* **85,** 454 –463 (2010).

124. Potet, F. *et al.* Functional Interactions between Distinct Sodium Channel Cytoplasmic Domains through the Action of Calmodulin. *J. Biol. Chem.* **284,** 8846–8854 (2009).

125. Chagot, B. & Chazin, W. J. Solution NMR structure of Apo-calmodulin in complex with the IQ motif of human cardiac sodium channel $Na_V1.5$. *J. Mol. Biol.* **406,** 106–119 (2011).

126. Kim, J. *et al.* Calmodulin Mediates Ca^{2+} Sensitivity of Sodium Channels. *J. Biol. Chem.* **279,** 45004–45012 (2004).

127. Kim, J., Ghosh, S., Nunziato, D. A. & Pitt, G. S. Identification of the components controlling inactivation of voltage-gated Ca^{2+} channels. *Neuron* **41,** 745–754 (2004).

128. Alseikhan, B. A., DeMaria, C. D., Colecraft, H. M. & Yue, D. T. Engineered calmodulins reveal the unexpected eminence of Ca^{2+} channel inactivation in controlling heart excitation. *Proc. Natl. Acad. Sci. U. S. A.* **99,** 17185–17190 (2002).

129. Yamaguchi, N., Takahashi, N., Xu, L., Smithies, O. & Meissner, G. Early cardiac hypertrophy in mice with impaired calmodulin regulation of cardiac muscle Ca release channel. *J. Clin. Invest.* **117,** 1344–1353 (2007).

130. Yamaguchi, N., Xu, L., Pasek, D. A., Evans, K. E. & Meissner, G. Molecular basis of calmodulin binding to cardiac muscle $Ca(^{2+})$ release channel (ryanodine receptor). *J. Biol. Chem.* **278,** 23480–23486 (2003).

131. Arnáiz-Cot, J. J. *et al.* Cardiac calcium signaling pathologies associated with defective calmodulin regulation of type 2 ryanodine receptor. *J. Physiol.* (2013). doi:10.1113/jphysiol.2013.256123

132. Kahlig, K. M., Lepist, I., Leung, K., Rajamani, S. & George, A. L. Ranolazine selectively blocks persistent current evoked by epilepsy-associated $Na_V1.1$ mutations. *Br. J. Pharmacol.* **161,** 1414–1426 (2010).

133. Lester, W. C. *et al.* Steady-state coupling of plasma membrane calcium entry to extrusion revealed by novel L-type calcium channel block. *Cell Calcium* **44,** 353–362 (2008).

134. Ashpole, N. M. *et al.* Ca^{2+}/calmodulin-dependent protein kinase II (CaMKII) regulates cardiac sodium channel $Na_V1.5$ gating by multiple phosphorylation sites. *J. Biol. Chem.* (2012). doi:10.1074/jbc.M111.322537

135. Wagner, S. *et al.* Ca^{2+}/calmodulin-dependent protein kinase II regulates cardiac Na^+ channels. *J. Clin. Invest.* **116,** 3127–3138 (2006).

136. Bers, D. M. Calcium Fluxes Involved in Control of Cardiac Myocyte Contraction. *Circ. Res.* **87,** 275–281 (2000).

137. Bers, D. M. in *Compr. Physiol.* (John Wiley & Sons, Inc., 2011). at <http://onlinelibrary.wiley.com/doi/10.1002/cphy.cp020109/abstract>

138. Neher, E. Vesicle pools and Ca^{2+} microdomains: new tools for understanding their roles in neurotransmitter release. *Neuron* **20,** 389–399 (1998).

139. Tay, L. H. *et al.* Nanodomain Ca^{2+} of Ca^{2+} channels detected by a tethered genetically encoded Ca^{2+} sensor. *Nat. Commun.* **3,** 778 (2012).

140. Horner, J. M. *et al.* Implantable cardioverter defibrillator therapy for congenital long QT syndrome: a single-center experience. *Heart Rhythm Journal* **7,** 1616–1622 (2010).

141. Mönnig, G. *et al.* Implantable cardioverter-defibrillator therapy in patients with congenital long-QT syndrome: a long-term follow-up. *Heart Rhythm Journal* **2,** 497–504 (2005).

142. Bragard, J. *et al.* Shock-induced termination of reentrant cardiac arrhythmias: comparing monophasic and biphasic shock protocols. *Chaos Woodbury N* **23,** 043119 (2013).

143. Liu, G. X. *et al.* Differential conditions for early after-depolarizations and triggered activity in cardiomyocytes derived from transgenic LQT1 and LQT2 rabbits. *J. Physiol.* **590,** 1171–1180 (2012).

144. Pinz, I., Zhu, M., Mende, U. & Ingwall, J. S. An Improved Isolation Procedure for Adult Mouse Cardiomyocytes. *Cell Biochem. Biophys.* **61,** 93–101 (2011).

145. Amabile, G. & Meissner, A. Induced pluripotent stem cells: current progress and potential for regenerative medicine. *Trends Mol. Med.* **15,** 59–68 (2009).

146. Ma, J. *et al.* High purity human-induced pluripotent stem cell-derived cardiomyocytes: electrophysiological properties of action potentials and ionic currents. *Am. J. Physiol. - Heart Circ. Physiol.* **301,** H2006–H2017 (2011).

147. Malan, D., Friedrichs, S., Fleischmann, B. K. & Sasse, P. Cardiomyocytes obtained from induced pluripotent stem cells with long-QT syndrome 3 recapitulate typical disease-specific features in vitro. *Circ. Res.* **109,** 841–847 (2011).

148. Okita, K., Ichisaka, T. & Yamanaka, S. Generation of germline-competent induced pluripotent stem cells. *Nature* **448,** 313–317 (2007).

149. Park, I. H. *et al.* Disease-specific induced pluripotent stem cells. *Cell* **134,** 877–886 (2008).

150. Dick, E., Matsa, E., Young, L. E., Darling, D. & Denning, C. Faster generation of hiPSCs by coupling high-titer lentivirus and column-based positive selection. *Nat. Protoc.* **6,** 701–714 (2011).

151. Doss, M. X. *et al.* Maximum Diastolic Potential of Human Induced Pluripotent Stem Cell-Derived Cardiomyocytes Depends Critically on IKr. *PLoS ONE* **7,** (2012).

152. Trappe, H. J. Acute Therapy of Maternal and Fetal Arrhythmias During Pregnancy. *J. Intensive Care Med.* **21,** 305 –315 (2006).

153. Thompson, C. H., Kahlig, K. M. & George, A. L., Jr. *SCN1A* splice variants exhibit divergent sensitivity to commonly used antiepileptic drugs. *Epilepsia* **52,** 1000–1009 (2011).

154. Yeung, E., Krantz, M. J., Schuller, J. L., Dale, R. A. & Haigney, M. C. Ranolazine for the Suppression of Ventricular Arrhythmia: A Case Series. *Ann. Noninvasive Electrocardiol. Off. J. Int. Soc. Holter Noninvasive Electrocardiol. Inc* (2014). doi:10.1111/anec.12137

155. Wahler, G. M. Developmental increases in the inwardly rectifying potassium current of rat ventricular myocytes. *Am. J. Physiol.- Cell Physiol.* **262,** C1266 (1992).

156. Papadatos, G. A. *et al.* Slowed conduction and ventricular tachycardia after targeted disruption of the cardiac sodium channel gene *SCN5A*. *Proc. Natl. Acad. Sci.* **99,** 6210–6215 (2002).

157. Nieto, M. A. Epithelial plasticity: a common theme in embryonic and cancer cells. *Science* **342,** 1234850 (2013).

158. Human embryonic genes re-expressed in cancer cells. *Publ. Online 06 Dec. 2001 Doi101038sjonc1205088* **20,** (2001).

159. Watanabe, H. *et al.* Striking In Vivo Phenotype of a Disease-Associated Human *SCN5A* Mutation Producing Minimal Changes in Vitro / Clinical Perspective. *Circulation* **124,** 1001 – 1011 (2011).

160. Rentschler, S. *et al.* Myocardial Notch signaling reprograms cardiomyocytes to a conduction-like phenotype. *Circulation* **126,** 1058–1066 (2012).

161. Wingo, T. L. *et al.* An EF-hand in the sodium channel couples intracellular calcium to cardiac excitability. *Nat. Struct. Mol. Biol.* **11,** 219–225 (2004).

162. Phillips, K. P., Léveillé, M. C., Claman, P. & Baltz, J. M. Intracellular pH regulation in human preimplantation embryos. *Hum. Reprod.* **15,** 896–904 (2000).

163. Gillespie, J. & McHanwell, S. Measurement of intra-embryonic pH during the early stages of development in the chick embryo. *Cell Tissue Res.* **247,** 445–451 (1987).

164. Williams, K. P. & Galerneau, F. Intrapartum fetal heart rate patterns in the prediction of neonatal acidemia. *Am. J. Obstet. Gynecol.* **188,** 820–823 (2003).

165. Wei, J. *et al.* Congenital long-QT syndrome caused by a novel mutation in a conserved acidic domain of the cardiac Na^+ channel. *Circulation* **99,** 3165–3171 (1999).

166. Cheng, J. *et al.* The common African American polymorphism *SCN5A*-S1103Y interacts with mutation *SCN5A*-R680H to increase late Na current. *Physiol. Genomics* **43,** 461 –466 (2011).